AD-A076 907 GRUMMAN AEROSPACE CORP BETHPAGE N Y RESEARCH DEPT F/G 18/2
THE JET MEMBRANE PROCESS FOR URANIUM SEPARATION AND ENRICHMENT.(U)
SEP 79 J W BROOK , V CALIA
UNCLASSIFIED RE-586 NL

1 OF 2
AD A076907

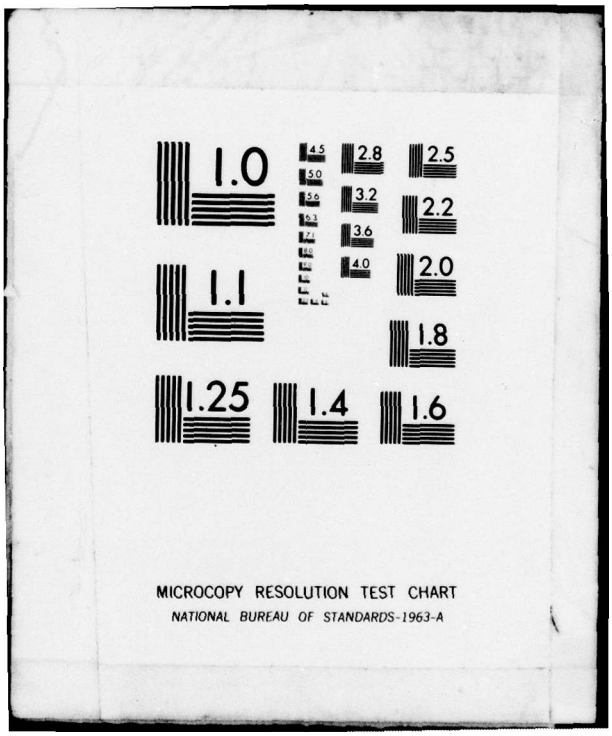
1.0
1.1
1.25
1.4
1.6
1.8
2.0
2.2
2.5
2.8
3.2
3.6
4.0
4.5
5.0
5.6
6.3
MICROCOPY RESOLUTION TEST CHART
NATIONAL BUREAU OF STANDARDS-1963-A

RE-586

THE JET MEMBRANE PROCESS FOR URANIUM SEPARATION AND ENRICHMENT

September 1979

RESEARCH DEPARTMENT

GRUMMAN AEROSPACE CORPORATION
BETHPAGE NEW YORK

UNCLASSIFIED

SECURITY CLASSIFICATION OF THIS PAGE *(When Data Entered)*

REPORT DOCUMENTATION PAGE		READ INSTRUCTIONS BEFORE COMPLETING FORM
1. REPORT NUMBER RE-586	2. GOVT ACCESSION NO.	3. RECIPIENT'S CATALOG NUMBER
4. TITLE *(and Subtitle)* THE JET MEMBRANE PROCESS FOR URANIUM SEPARATION AND ENRICHMENT		5. TYPE OF REPORT & PERIOD COVERED
		6. PERFORMING ORG. REPORT NUMBER RE-586
7. AUTHOR(s)		8. CONTRACT OR GRANT NUMBER(s)
9. PERFORMING ORGANIZATION NAME AND ADDRESS Grumman Aerospace Corporation Bethpage, N.Y., 11714		10. PROGRAM ELEMENT, PROJECT, TASK AREA & WORK UNIT NUMBERS
11. CONTROLLING OFFICE NAME AND ADDRESS		12. REPORT DATE September 1979
		13. NUMBER OF PAGES 77
14. MONITORING AGENCY NAME & ADDRESS*(if different from Controlling Office)*		15. SECURITY CLASS. *(of this report)* Unclassified
		15a. DECLASSIFICATION/DOWNGRADING SCHEDULE

16. DISTRIBUTION STATEMENT *(of this Report)*

Approved for public release; distribution unlimited.

17. DISTRIBUTION STATEMENT *(of the abstract entered in Block 20, if different from Report)*

18. SUPPLEMENTARY NOTES

19. KEY WORDS *(Continue on reverse side if necessary and identify by block number)*

Uranium Enrichment

Jet Membrane

Aerodynamic Separation

20. ABSTRACT *(Continue on reverse side if necessary and identify by block number)*

The jet membrane is a new aerodynamic separation concept for enriching uranium. The project described in this report had two objectives: 1) to demonstrate experimentally that uranium isotopes can be separated using the jet membrane concept, and 2) to make an assessment of the economic viability of the jet membrane in relation to competing processes. To address the first objective a laboratory suitable for handling UF_6 was outfitted, a jet membrane apparatus compatible with UF_6 was constructed, and a mass spectro-

DD FORM 1 JAN 73 1473 EDITION OF 1 NOV 65 IS OBSOLETE
S/N 0102-014-6601 |

UNCLASSIFIED

SECURITY CLASSIFICATION OF THIS PAGE *(When Data Entered)*

meter capable of providing the necessary precision for UF_6 isotope measurements was purchased. Isotopic enrichment of both SF_6 and UF_6 was successfully demonstrated in our laboratory using the jet membrane apparatus. To aid in addressing the second objective two separate laboratory facilities were constructed. Program supporting experiments were conducted in these laboratories, using a variety of gas combinations, to investigate those system parameters that were identified in our economics analysis as major capital and energy cost drivers. In addition, a theoretical study was conducted to aid in analyzing data and to provide scaling laws. Our cost analysis, based upon the measured UF_6 results and the supporting experiments, indicates that the jet membrane is a viable concept for enriching uranium industrially.

(14)

Grumman Research Department Report RE-586

(6)

THE JET MEMBRANE PROCESS FOR URANIUM SEPARATION AND ENRICHMENT.

by (9) Final rept. on Phase 2,

(10) John W. Brook
Vincent Calia

Fluid Dynamics

(11) September 1979 (12) 147

Approved by: Richard A. Scheuing
Richard A. Scheuing
Director of Research

FOREWORD

This document was prepared by the Grumman Aerospace Corporation Research Department as the final report on Phase II of the Jet Membrane Project. Funding for this contract was supplied both by the Electric Power Research Institute (EPRI) under Program RP 506-4 and the Grumman Aerospace Corporation.

Mr. Mel Lapides of EPRI was the contract monitor. Dr. Robert Madey of Grumman Energy Systems was the program manager. Dr. John Brook and Mr. Vincent Calia of the Grumman Aerospace Corporation Research Department were the principal investigators. Significant portions of the work were also carried out by the General Energy Associates, Inc. (GEA) under contract to Grumman.

The gaseous jet experiments were performed under Grumman funding by GEA by Drs. E. P. Muntz, P. Scott, and T. Deglow. The FC-43 condensible jet experiments were carried out under EPRI funding by Mr. Calia and Mr. J. DeCarlo. The theoretical work was performed under EPRI funding by Drs. Brook and B. B. Hamel of GEA. The cost analyses were carried out under Grumman funding by Drs. Hamel and Brook.

ABSTRACT

The jet membrane is a new aerodynamic separation concept for enriching uranium. The project described in this report had two objectives: 1) to demonstrate experimentally that uranium isotopes can be separated using the jet membrane concept, and 2) to make an assessment of the economic viability of the jet membrane in relation to competing processes. To address the first objective a laboratory suitable for handling UF_6 was outfitted, a jet membrane apparatus compatible with UF_6 was constructed, and a mass spectrometer capable of providing the necessary precision for UF_6 isotope measurements was purchased. Isotopic enrichment of both SF_6 and UF_6 was successfully demonstrated in our laboratory using the jet membrane apparatus. To aid in addressing the second objective two separate laboratory facilities were constructed. Program supporting experiments were conducted in these laboratories, using a variety of gas combinations, to investigate those system parameters that were identified in our economics analysis as major capital and energy cost drivers. In addition, a theoretical study was conducted to aid in analyzing data and to provide scaling laws. Our cost analysis, based upon the measured UF_6 results and the supporting experiments, indicates that the jet membrane is a viable concept for enriching uranium industrially.

CONTENTS

ILLUSTRATIONS

TABLES

NOMENCLATURE

The nomenclature used in this report is listed below. Also indicated with some terms is the Section in which the nomenclature is first used and in those instances where it is defined elsewhere, the location of the definition. For example (Fig. 2-1; Ref.2) means that the symbol is first used in Fig. 2-1 and is defined in Ref. 2. To aid the reader, Refs. 1 and 2 are attached to this report as Appendices A and B.

A	Area
a	width of lamina, large collector probe model (Sec. 5.2.1)
a_i^*	coefficients used in economy of scale analysis (Table 2-4; Ref.2)
C	specific cost ($/SWU/yr) (Table 2-3; Ref. 2)
C/A	cost ($)/unit area of stages (Table 2-3; Ref. 2)
C_D	discharge coefficient (Table 2-5; Ref. 2)
CECI	cost multiplier-engineering, contingency, and interest during construction (Table 2-3; Ref. 2)
C/E	cost ($)/unit of energy (Table 2-5; Ref. 2)
$\bar{c}$	mean molecular random speed = $\sqrt{8kT/\pi m}$ (Sec. 5.1.2)
c_{eff}	constant related to effective velocity at probe face (Sec. 7.3)
D	diameter or width (two dimensions)
$\mathcal{D}$	diffusion coefficient (Sec. 5.1.3)
e	enrichment factor, α-1 (or β-1) (Sec. 5.1.2)
G	function used in large collector probe model (Sec. 5.2.1)
H	energy/mole (Table 2-5; Ref. 2); mole ratio (mass spectrometer standard) (Sec. 7.1.3)
H_v	energy of vaporization/mole (Table 2-5; Ref. 2)
i^+	ion current (Sec. 7.3)
Kn	Knudsen number (Sec. 4.5)
k	Boltzmann's constant
L	molar flux/stage or per probe (Fig. 2-1; Ref. 2); length of lamina in large probe model (Sec. 5.2.1)
M	molecular weight (Table 2-5)
m	molecular mass

$\dot{m}$	mass flow
n	number density
P	power costs ($/SWU) (Table 2-5; Ref. 2)
p	pressure
R	gas constant
R_p, R_∞	length scales in rarefied model (Sec. 5.1.2; Ref. 1)
R'_p	experimentally determined value of R_p (Sec. 5.1.5)
$\bar{R}$	ion ratio (mass spectrometer)(Sec. 7.1.3)
S	plant size or capacity (SWU/yr) (Table 2-4; Ref. 2)
SWU	separative work units (summary: Ref. 5)
s	distance along lamina in large collector probe model (Sec. 5.2.1)
$\bar{s}$	parameter in rarefied and continuum models (Sec. 5.1.2)
T	temperature
t	transmission coefficient (Table 2-3; Ref. 2); time
V,v	velocity
$\bar{V}$	relative velocity (Sec. 5.1.4; Ref. 1)
w	width of orifice plate (Sec. 4.1; Sec. 6.1.1)
x	mole fraction of light species in tails (Sec. 7.3; Ref. 2)
x_o	shift in origin, large collector probe data (Sec. 5.2.2)
x_p	collector probe position (Sec. 4.1; Sec. 6.1.1)
y	mole fraction of light species in heads (Sec. 7.3; Ref. 2)
α	stage separation factor (heads to tails; used also to mean separation in general)(Sec. 2.3.1)
α_{GD}	theoretical effusive separation factor (heads to tails) (Sec. 2.3.1)
β	stage separation factor (heads to feed) (Sec. 2.3.1)
γ	ratio of specific heats (Table 2-5; Ref.2)
ΔH_{CB}	energy to raise jet fluid from condenser temperature to boiler temperature
δ	fraction of stage area open to flow (Table 2-3; Ref. 2)
ϵ	rarefaction parameter (Sec. 5.1.1; Ref. 1)
η	coefficient of viscosity (Sec. 7.3)
$\bar{\eta}$	mixture viscosity (Sec. 7.3)
λ	mean free path (Sec. 4.5)
ξ	relative enrichment (Table 2-3; Sec. 2.3.1)
Ω	collision cross-section (Sec. 4.5)

Subscripts

b	background (Fig. 2-1; Ref. 2)
c	collector probe (Fig. 2-1; Sec. 6.1.1) or collector chamber (Sec. 4.4; see also Fig. 6.4)
eff	effective conditions at the face of the collector probe (Sec. 7.3)
GD	gaseous diffusion (Table 2-3; Ref. 2)
H	heavy (molecule) (Sec. 5.1.2)
h	high (pressure) (Fig. 2-1; Ref. 2)
I	instrumentation (Table 2-3; Ref. 2)
J	jet (in economic analysis) (Fig. 2-1; Ref. 2)
j	jet (Sec. 2.3.3)
JM	jet membrane (Table 2-3; Ref. 2)
JO	jet off (Sec. 4.4)
L	light (molecule) (Sec. 5.1.2)
ℓ	low (pressure) (Fig. 2-1; Ref. 2)
m	measured (transmission)(Sec. 4)
max	maximum (adiabatic velocity) (Sec. 5.1.2)
o	open (area) (Fig. 2-1; Sec. 2.3.3)
P	pumping (Table 2-3; Ref. 2)
PB	process building (Table 2-3; Ref. 2)
PG	process gas (Fig. 2-1; Ref. 2)
p	plant (enrichment) (Table 2-3; Sec. 2.3.1) or collector probe (outside diameter) (Sec. 2.3.3; Sec. 6.1.1)
S	support (Table 2-3; Ref. 2)
s	stagnation or source (Fig. 2-1; Ref. 2)
ST	stage (Table 2-3; Ref. 2)
T	total (static pressure) (Sec. 7.3)
x	unknown (mass spectrometer) (Sec. 7.1.3)
*	sonic (velocity) (Sec. 5.1.4)

SUMMARY

The jet membrane project has as its objective the demonstration and development of a new gas dynamic technique for enriching uranium. The final report on this two year program, sponsored by the Electric Power Research Institute (EPRI) and the Grumman Aerospace Corporation, provides answers to two basic questions:

1. Can uranium be enriched by the jet membrane process?
2. Is the jet membrane process economically viable vis-a-vis competing schemes?

In answer to the first question, the enrichment of $^{235}UF_6$ was demonstrated experimentally using the jet membrane apparatus developed during the EPRI supported program*. The measured amount of separation is within the expected theoretical bounds and correlates appropriately with our earlier experiments in benign gases.

In answer to the second questions, based on our econometric model, the measured UF_6 enrichment results, and supporting theoretical and experimental work, we believe the process to have favorable economics vis-a-vis competing enrichment technologies.

In Table S-1, the jet membrane is compared with both gaseous diffusion and the centrifuge for a large (3,000,000 SWU/yr) enrichment plant. As can be seen, the jet membrane compares favorably with both processes from the point of view of capital required, electrical energy required, and final cost of enriched uranium. This size plant is, however, close to the upper bound possible for the jet membrane due to limitations on the thermal energy requirements.

In Table S-2, the jet membrane is compared to gaseous diffusion and the centrifuge for a small (300,000 SWU/yr) enrichment plant. As can be seen, all jet membrane costs and the energy requirements are significantly lower than those corresponding to gaseous diffusion. Compared to the centrifuge the jet membrane costs are

*All materials and equipment used during this program were procured using Grumman funds.

lower while the electrical energy requirements are approximately the same. More important, however, is the fact that the cost of enriched uranium for a small jet membrane plant is comparable to the costs associated with large gaseous diffusion and centrifuge plants while the capital investment required is only approximately 9-13%. This will allow following the demand for enriched uranium more closely than is possible with the larger plants, but at the same cost of enriched uranium. In addition, the energy requirements of jet membrane small enrichment plants suggest the possibility of co-locating them with power plants.

TABLE S-1

PROJECTED CAPITAL AND ENERGY REQUIREMENTS FOR A 3,000,000 SWU/YR ENRICHMENT PLANT (1974 Dollars)

	Jet Membrane	Gaseous Diffusion*	Centrifuge
Relative Enrichment	3.0	1.0	--
Capital Cost	$385M	$1.64B	$1.13B**
Cost of Enriched Uranium/SWU	$30	$99	$70**
Electrical Power Cost Relative to Gaseous Diffusion	0.102	1.0	0.10†
Electrical Power (MWe)	91	891	89.1
Thermal Power Cost Relative to Gaseous Diffusion Electrical Cost	0.255	--	--
Thermal Power (MW)	*2600††*	--	--
Total Power Cost Relative to Gaseous Diffusion	0.357	1.0	0.10

*Data scaled as in Sec. 2.2.2

**Ref. 12

†Ref. 13

††For plants larger than 3,000,000 SWU/yr; size of the available thermal source will likely be limiting for the jet membrane.

TABLE S-2

PROJECTED CAPITAL AND ENERGY REQUIREMENTS FOR A 300,000 SWU/YR ENRICHMENT PLANT (1974 DOLLARS)

	Jet Membrane	Gaseous Diffusion*	Centrifuge
Relative Enrichment	3.0	1.0	--
Capital Cost	$145M	$493M	$235M**
Cost of Enriched Uranium/SWU	$72	$208	$171**
Electrical Power Cost Relative to Gaseous Diffusion	0.102	1.0	0.10†
Electrical Power (MWe)	9.1	89.1	8.9
Thermal Power Cost Relative to Gaseous Diffusion Electrical Cost	0.255	--	--
Thermal Power (MW)	261	--	--
Total Power Cost Relative to Gaseous Diffusion	0.357	1.0	0.10

*Data scaled as in Sec. 2.2.2

**Ref. 12

†Ref. 13

SECTION 1

INTRODUCTION

The projected increase in the production of electrical power by means of nuclear reactors will require an increase in the supply of enriched uranium to fuel these reactors. In the past this enrichment has been carried out by the gaseous diffusion process, a method that requires large capital investment and one that consumes large amounts of electrical energy. Recently, attention has shifted to alternative means of enriching uranium in order to reduce the capital and power costs required. Among the processes which have undergone some degree of development are the centrifuge, Becker nozzle (Germany), and various laser schemes. In addition to these schemes, various other concepts have been suggested as possessing economic merit, but very little specific information concerning them is available. One of these alternative schemes is the jet membrane process. This report summarizes a two year program sponsored by the Electric Power Research Institute (EPRI) and the Grumman Aerospace Corporation to investigate this process.

The jet membrane is a gas dynamic (or aerodynamic) scheme for enriching uranium. The components of the basic unit process are described in Section 2. Briefly, the major feature of the jet membrane from an economic point of view is the fact that the working fluid, or carrier fluid, in this process is a condensible vapor. Therefore, in contrast to most other aerodynamic enrichment schemes, the working fluid can be thermally rather than mechanically pumped. The energy supply can be waste heat or solar energy, rather than electrical energy. Another feature of the concept which makes the process economically attractive is that no new high technology item needs to be developed, i.e., the technology is similar to existing gaseous diffusion plant technology.

The work reported on herein consists of Phase II of the jet membrane project. In what follows, we present an outline of the earlier work leading up to Phase II and the objectives and development of the Phase II program to achieve these objectives. Details of the process and the results achieved are found in succeeding Sections of this report.

During the earlier Phase I of the jet membrane project, experiments were performed to demonstrate the jet membrane separation effect in various benign gases. These experiments employed nitrogen as a jet and backgrounds consisting of mixtures of argon and carbon dioxide, helium and neon and neon isotopes. At the same time, a theoretical study of the jet membrane was undertaken in the regime of parameters in which the experiments were performed. This study was directed at obtaining an understanding of the basic physics underlying the jet membrane and also at providing similarity laws for the physical parameters involved, such as pressure levels, molecular weights and cross sections, etc. Subsequently, a preliminary systems analysis of the jet membrane, as applied to uranium enrichment, was carried out.

Based on the systems analysis, in conjunction with the experimental data and the theoretical scaling laws, it was possible to show that the jet membrane is indeed a viable candidate for economical uranium enrichment. Furthermore, the analysis also established some of the critical parameters affecting the economics of the jet membrane. Further details on these parameters and definitions of other terms may be found in the Nomenclature and Section 2 of this report.

However, even though the experimental data and the available scaling laws indicated that the jet membrane would work using UF_6 as the process gas, sooner or later this presumption had to be demonstrated in the laboratory. Phase II of the project was then developed and structured to provide answers to two basic questions:

- Can uranium be enriched by the jet membrane process?
- Is the process economically attractive vis-a-vis competing schemes?

To answer the first question, the fundamental task performed under Phase II was to demonstrate uranium enrichment by the jet membrane in a UF_6/FC-43 (perfluorotributylamine) system. As part of this task it was necessary to carry out several preliminary tasks:

- Prepare a special laboratory to safely handle UF_6
- Design and construct an experimental apparatus (apparatus No. 3)* compatible with UF_6

*Throughout this report reference will be made to apparatus Nos. 1, 2, and 3. Experiments were conducted in three separate apparatus. Basically, apparatus No. 1 was used to investigate separation of benign mixtures using a gaseous jet; apparatus no. 2 was used to investigate separation of benign mixtures using a condensible jet; apparatus no. 3 was designed to investigate separation of UF_6 isotopes using a condensible jet, but was also used to investigate separation of SF_6 isotopes.

- Prepare specifications and procure a UF_6 qualified mass spectrometer for in situ measurements of isotopic abundance.

During the period that these preparations were underway a separate apparatus (apparatus no. 2) was constructed to carry out the following tasks:

- Investigate the FC-43 thermal cycle and jet properties
- Investigate separation of Neon isotopes using FC-43 to provide a data base with a condensible jet and to provide an overlap with previous gaseous jet experiments
- Investigate separation of sulfur hexafluoride (SF_6) isotopes using FC-43 to provide the first heavy isotope separation data and to establish baseline data for apparatus no. 3. These experiments were conducted in a separate laboratory using a magnetic and a quadrupole spectrometer that were available at that time.

Finally, in the new laboratory, and using the UF_6 apparatus no. 3 and the UF_6 qualified mass spectrometer, the following tasks were performed:

- Repeat of FC-43/SF_6 experiment to check out the new apparatus and to establish experimental procedures
- Separation of UF_6 isotopes using FC-43 over as wide a range of parameters as possible.

The results of the experiments outlined above are presented in Section 3 and 5 of this report. Descriptions of the UF_6 laboratory, experimental apparatus, UF_6 mass spectrometer and experimental procedures are presented in Sections 6 and 7.

The remainder of the Phase II program was designed to answer the second part of the program objectives stated above, namely those concerning economic viability. To achieve this, the following tasks were set forth:

- Supporting experiments in apparatus no. 2 using FC-43 as the carrier fluid (jet)
- Supporting experiments in a gaseous jet apparatus (apparatus no. 1)
- Theoretical program
- Econometric analysis of jet membrane
- Comparative analysis with competing processes.

The primary objective of the supporting experiments was to obtain data on the effect of various geometrical and physical parameters on jet membrane performance (Section 2) so that the effects of these parameters could be reflected in the econometric analysis. These experiments were performed using benign gas systems,

not only for ease of handling and making the measurements, but also because the exploratory nature of these experiments required the ability to make changes in the apparatus more quickly. The specific areas of investigation studied during these experiments were:

- Collector probe/orifice geometry
- System pressures and pressure limits
- Jet fluid mass flows.

The results of these program supporting experiments are presented in Sections 4 and 5.

Concurrent with the experimental program, a theoretical program was conducted. The objectives of the theoretical program were:

- To analyze the unit process with the aim of developing an understanding of the physics of the jet membrane
- To provide a framework for analyzing data and directing further experimental and theoretical work
- To aid in developing scaling laws.

Jet membrane theoretical considerations are presented in Section 5. Further details on jet membrane theories may be found in Ref. 1.(Ref. 1 is also attached as Appendix A)

The basis of our economic predictions lies with our own econometric analysis which was developed during Phase I of the jet membrane project and improved and coded for a digital computer during the early part of Phase II. The features of this analysis are:

- Basic capital cost categories of the jet membrane are comparable to gaseous diffusion, with the exception of jet handling equipment, for which capital cost data are published
- Parametric models of the capital costs are used to scale gaseous diffusion costs to the jet membrane
- Parametric models of the energy costs are used to scale gaseous diffusion costs to the jet membrane
- Effects of varying plant size (SWU/yr) are scaled for both gaseous diffusion and the jet membrane using published gaseous diffusion data for two plant sizes.

The econometric model is outlined in Section 2; further details may be found in Ref. 2. (Ref. 2 is attached as Appendix B.) Our analysis of thermal energy cost is attached as Appendix C.

Finally, the comparative analysis had as its objective the comparison of jet membrane economics with those of other competing processes, where data were available. For the most part, the available data are restricted to the gaseous diffusion process and the centrifuge. The results of our comparisons are presented in Section 2, along with a discussion of the assumptions that were used as input for the jet membrane.

A visual summary of the Phase II program of the jet membrane project is presented in Fig. 1-1. To recapitulate where the various tasks (dashed boxes in Fig. 1-1) are discussed in this report, we have the following:

- Experimental A-1 — Sections 3, 5, 6, 7
- Experimental A-2 — Sections 4, 5, 6, 7
- Theoretical B — Section 5
- Econometric Analysis C — Section 2
- Comparative Analysis D — Section 2

The remainder of this report has been organized to reflect the two program objectives stated above, in particular as they affect jet membrane economics. Thus, Section 2 is an overview of the process that contains:

- Description of the unit process
- The economic model, including an identification of the critical parameters
- Discussion of the process variables and a summary of the numerical values used as input to the economic model
- Results of cost analysis (economics).

Section 3 contains the results of the UF_6 and related (Ne and SF_6) isotope experiments. The primary emphasis of this section is experimental demonstration of uranium enrichment. Section 4 contains the results of the program supporting experiments. These results and the UF_6 measurements provide the primary justification for the process variable inputs used in Section 2. Sections 3 and 4 contain only the final results. The details of the measurement technique, apparatus, etc., may be found in Sections 6 and 7 so that the reader is not encumbered at this point by unnecessary detail.

Section 5 contains a discussion of some of the theoretical aspects of the jet membrane including details that are beyond what is necessary as input to the economics model. In this section is included:

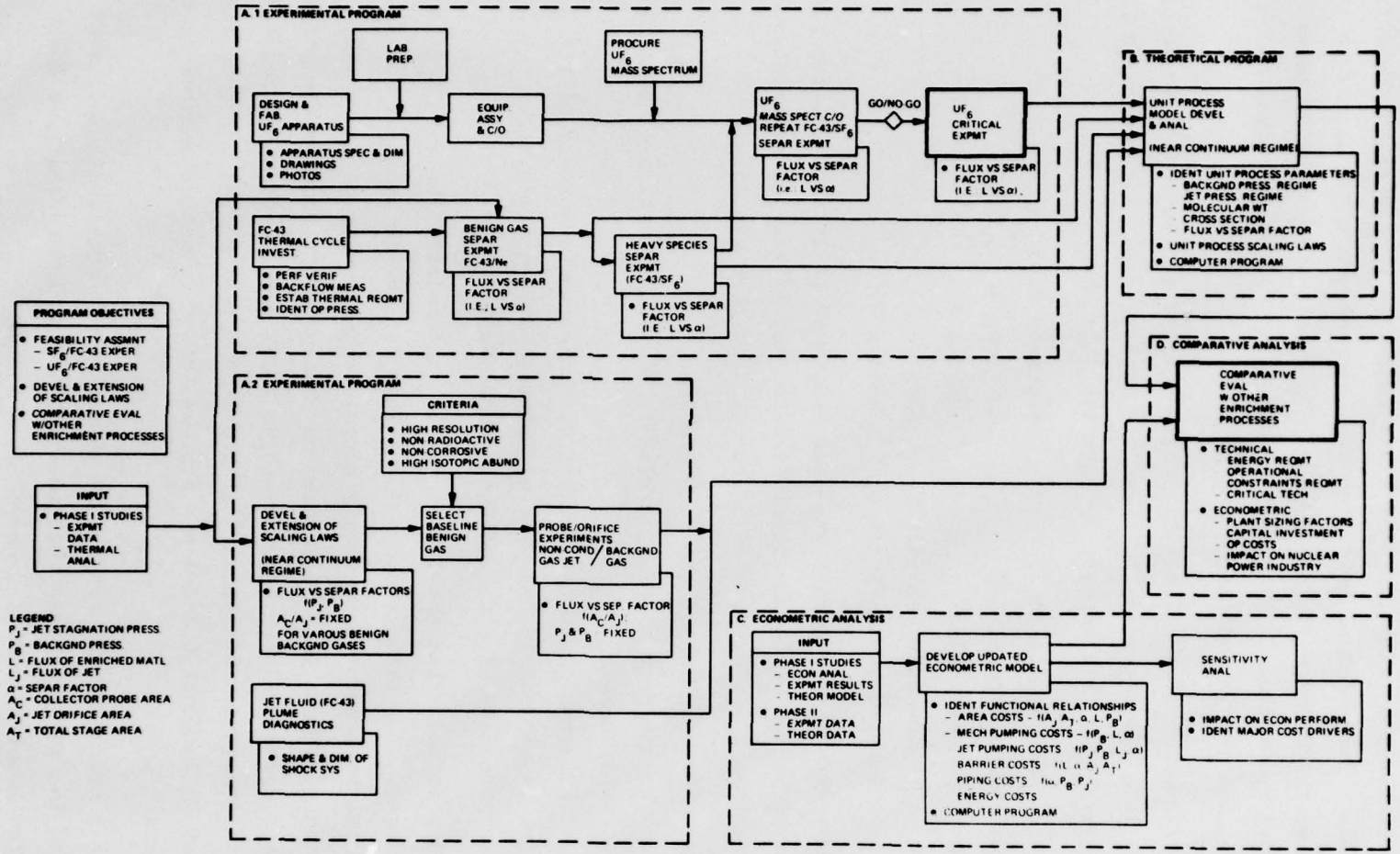

Figure 1-1. Phase II Program Flow Plan

- Theoretical modeling
- Comparison of predicted and experimental performance (input to economics)
- Comparison of predicted and experimental attenuation and enrichment vs collector probe position.

In Section 6, a detailed description of the various experimental apparatus, the UF_6 separation laboratory, and the Nuclide 12-90-CG UF_6 qualified mass spectrometer are presented; in Section 7 a description of the experimental techniques and interpretation of data are presented. Finally, Section 8 contains our conclusions as to the present status of the jet membrane process and our recommendations for future work.

SECTION 2

PROCESS OVERVIEW

The name jet membrane arises from the analogy with the gaseous diffusion process where the barrier, or membrane, is a physical one. In this section we provide an overview of the jet membrane and our method of making projections as to the economic viability of this process for enriching uranium.

This section starts with a description of the basic unit process and its unique features. The economic model is then outlined showing the method of estimating capital costs, effects of plant size, energy costs, and the cost of enriching uranium. Most of the details of our economic model, which is based upon a scale up of published gaseous diffusion data, may be found in Ref. 2. Only an outline is presented here. Following this, the different groups of variables which are needed as input to the economic model are discussed. Three major groups are identified: gaseous diffusion parameters, engineering and design variables, and process parameters. The first group includes, in addition to the cost data, the operating parameters of a gaseous diffusion plant, such as pressures, enrichment factor, etc. The second group contains variables which will be influenced by the details of plant design, such as interstage connections, stage design, condenser design, etc. With the exception of the choice of jet fluid, most of these variables have not been considered in any detail. The final group, the process parameters, contains the primary operating parameters of a jet membrane plant. The values of these parameters that we have used in our economic projection are set forth and the manner in which they were determined is indicated. For the most part, the process parameters are based on the experimental and theoretical results presented in Sections 3, 4, and 5.

Finally, we present our projections of jet membrane economics. The projections indicate that the jet membrane offers economic advantages over the gaseous diffusion and centrifuge processes for plant sizes up to about 3×10^6 SWU/Yr. For small plants in the neighborhood of 3×10^5 SWU/Yr the jet membrane economics are significantly better than these competing processes. Three comparisons are shown:

- Costs and energy requirements of jet membrane vs gaseous diffusion and centrifuge for a 3,000,000 SWU/yr enrichment plant

- Costs and energy requirements of jet membrane vs gaseous diffusion and centrifuge for a 300,000 SWU/yr enrichment plant
- Costs of jet membrane vs gaseous diffusion and centrifuge for varying enrichment plant capacity between 300,000 and 8,750,000 SWU/yr.

It should be noted that virtually all of the jet membrane process parameters used as input to these calculations have been achieved experimentally in some gas system.

2.1 DESCRIPTION OF PROCESS

The jet membrane is a gas dynamic scheme for enriching uranium. The major features of a basic unit process are depicted in Fig. 2-1. Also shown in Fig. 2-1 are the major process parameters of the jet membrane. Natural uranium (the process gas) is introduced as a uranium hexafluoride (UF_6) feed (background) into a chamber into which a free jet of a heavy condensible gas (the jet) flows. Due to preferential penetration of the UF_6 into the jet, the lighter species, $^{235}UF_6$ is enriched relative to the heavy species, $^{238}UF_6$. The enriched UF_6 (upflow or heads) is collected by a probe facing downstream in the jet and is passed to another unit for further enrichment (the cascade) or to a mass spectrometer for analysis. In contrast to other aerodynamic schemes using light carrier gases that must be pumped mechanically, in the jet membrane the jet is thermally pumped. The boiler can be operated on low grade heat (e.g., waste heat or solar); the jet gas is collected at the condenser as a liquid and recycled to the boiler for further use. The depleted UF_6, which has a lower fraction of $^{235}UF_6$ than the feed gas, is passed to another unit in the cascade, or removed from the system.

As opposed to gaseous diffusion, in the jet membrane the degree of separation obtained can be varied and depends upon the position in the jet at which the heads are collected. This is controlled by the position of the collector probe. However, an increasing separation also leads to a decreasing heads flux (throughput). Since separative capacity depends upon both the separation factor and the throughput, the probe position becomes a factor in analyzing and optimizing jet membrane economics, in addition to the other process parameters.

The variation of throughput with separation, or in dimensionless form transmission vs relative enrichment, is referred to as the performance of the jet membrane. For isotopes, the shape of a performance curve, for all other process parameters constant, has been shown both theoretically and experimentally, to be exponential (see sketch).

p_b = BACKGND PRESS.
p_h = SYS HIGH PRESS.
p_ℓ = SYS LOW PRESS.
p_s = STAGNATION PRESS.
T_b = BACKGND TEMP
T_s = STAGNATION TEMP
L_{PG} = ENRICHED PROCESS GAS FLUX
A_C = COLLECTOR PROBE AREA
L_J = JET FLUX
A_O = JET OPEN AREA

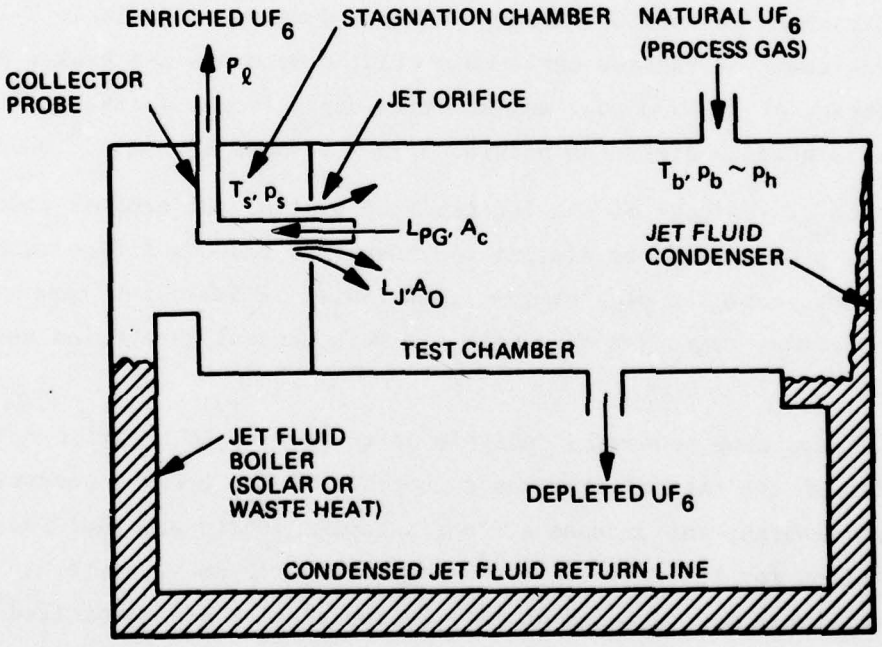

Figure 2-1. Jet Membrane Unit Process: Schematic

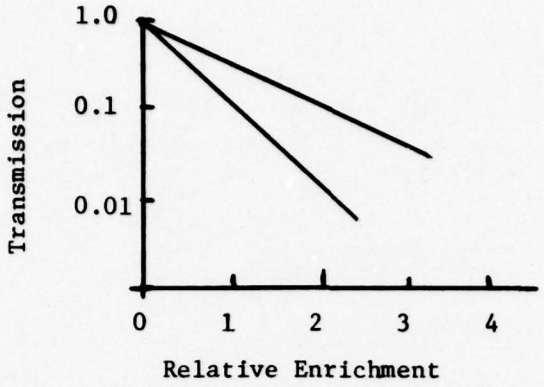

Basically then, a quantitative measure of jet membrane performance is the slope of the performance curve. Improved performance is related to a decrease in the slope of the performance curve. In Sections 3, 4, and 5 we shall be concerned primarily with how the process parameters affect jet membrane performance.

2.2 THE ECONOMIC MODEL

2.2.1 Capital Costs

The basic gaseous diffusion capital costs that we have used in our scale-up economics are presented in Ref. 3. These costs are summarized in Table 2-1 where the capital costs of various enrichment plant components are broken down into both percentage of capital cost and specific capital cost ($/SWU/yr) for two different size gaseous diffusion plants, 8.75×10^6 and 17.5×10^6 SWU/yr.

With the exception of the cost of the jet handling system, the capital costs of a jet membrane plant should be similar to those of a gaseous diffusion plant. However, rather than consider each of the items listed in Table 2-1 separately, for convenience we have regrouped them into the more general categories shown in Table 2-2.

The thrust of our scale-up economics analysis is to provide an analytic model for the variation of the capital costs as a function of the process parameters. The ratio of jet membrane and gaseous diffusion capital costs are then found from analytic expressions for the ratio of the appropriate process parameters. The details of the analysis may be found in Ref. 2; the results are summarized in Table 2-3 (definitions of the variables may be found under Nomenclature).

TABLE 2-1 ESTIMATED PLANT CAPITAL COST BREAKDOWNS BY PROCESS STAGE COMPONENTS FOR NEW GASEOUS DIFFUSION PLANTS LOCATED IN THE UNITED STATES (1970 TECHNOLOGY) (REF. 3)+

Total Plant Capital Costs 10^9	1.2		1.9	
Separative Capacity 10^6 SWU/Yr	8.75		17.5	
	% Capital Cost	Specific Capital Investment $/SWU/Yr	% Capital Cost	Specific Capital Investment $/SWU/Yr
Direct Pumping Costs	45.5	62.4	46.7	50.7
Gas Compressors	12.5	17.1	13.7	14.9
Compressor Drive Motors	7.6	10.4	11.4	12.4
Electrical System	13.1	18.0	11.2	12.2
Heat Removal System	4.4	6.0	4.7	5.1
Process Piping & Valves	7.9	10.8	5.7	6.2
Gas Diffusers (Stage)	8.9	12.2	10.8	11.7
Process Buildings & Enclosures	7.1	9.7	7.5	8.1
Instrumentation	2.3	3.2	1.5	1.6
Support	11.8	16.2	9.1	9.9
Miscellaneous Systems*	2.9	4.0	2.2	2.4
Process Support Facilities**	8.0	11.0	6.3	6.8
Plant Startup & Support	0.9	1.2	0.6	0.7
Engineering	3.4	4.7	3.4	3.7
Contingency	11.8	16.2	11.8	12.8
Interest During Construction	9.2	12.6	9.2	10.0
Grand Total	100.0	137.1	100.0	108.6

* Includes process ventilation, fire protection, sanitary water and sewage.

**Includes such facilities as administration building, technical services building, maintenance building, shops, cleaning and decontamination, purge and produce building and site preparation.

+ Costs shown are in 1971 dollars.

TABLE 2-2

JET MEMBRANE CAPITAL COST CATEGORIES

- DIRECT PUMPING
- STAGE (GAS DIFFUSERS)
- PROCESS BUILDING
- INSTRUMENTATION
- SUPPORTING FACILITIES
- JET GAS SYSTEM (NOT NEEDED IN GASEOUS DIFFUSION PLANTS)
- ENGINEERING, CONTINGENCY, & INTEREST DURING CONSTRUCTION

Table 2-3 contains two changes that were not in the original analysis:

1. The effect of pressure ratio on the capital costs of mechanical pumping has been added as an option. This addition is based on the assumption that the number of stages of a compressor depends upon the logarithm of the pressure ratio.

2. The capital cost of the jet handling system has been modeled. The constant multiplier is based on information received from the Garrett Corporation (Ref. 4).

As can be seen from Table 2-1, direct pumping costs are the major capital cost driver in a gaseous diffusion plant; this will undoubtedly be true for a jet membrane plant. From Table 2-3, we see that the two major factors controlling this cost in a jet membrane plant are the relative enrichment and suction pressure. The factors which affect the latter have been a major concern of this program.

2.2.2 Economy of Scale of Capital Costs

Economy of scale arises from the fact that the specific cost of equipment generally decreases as the size increases. Here we apply this to calculating how the specific capital costs of the categories defined above vary with the size, or

TABLE 2-3

JET MEMBRANE CAPITAL COSTS: ANALYTICAL EXPRESSIONS

- DIRECT PUMPING (GAS COMPRESSORS, COMPRESSOR DRIVE MOTORS, ELECTRICAL SYSTEM, HEAT REMOVAL SYSTEM, PROCESS PIPING, VALVES)

$$\frac{(C_P)_{JM}}{(C_P)_{GD}} = \frac{1}{\xi_\rho}\left[\frac{(p_\ell)_{GD}}{(p_\ell)_{JM}}\,\frac{\log (P_h/P_\ell)_{JM}}{\log (P_h/P_\ell)_{GD}}\,\frac{1}{\xi_P}\right]^{.7}$$

- STAGE (GAS DIFFUSERS) AREA

$$\frac{(C_{ST})_{JM}}{(C_{ST})_{GD}} = \frac{(C/A)_{JM}}{(C/A)_{GD}}\,\frac{1}{\xi_P^2}\,\frac{(p_h)_{GD}}{(p_h)_{JM}}\,\frac{\delta_{GD}}{\delta_{JM}}\,\frac{t_{GD}}{t_{JM}}$$

- PROCESS BUILDING

$$\frac{(C_{PB})_{JM}}{(C_{PB})_{GD}} \sim [0(1)/\xi_P]^{.74}$$

- INSTRUMENTATION AND SUPPORTING FACILITIES

$$\frac{(C_I)_{JM}}{(C_I)_{GD}} = \frac{1}{\xi_P}\,;\,\frac{(C_s)_{JM}}{(C_s)_{GD}} = \frac{1}{\xi_P}$$

- JET GAS HANDLING SYSTEM

$$(C_J)_{JM} = 6.28\,\frac{(L_J)_{JM}}{L_{JM}}\,\frac{1}{\xi_P^2} \quad (\$/SWU/YR)$$

- ENGINEERING, CONTINGENCY & INTEREST DURING CONSTRUCTION. TOTAL CAPITAL = CECI X (ALL OTHER CAPITAL). CECI DEPENDS PRIMARILY ON CONTINGENCY FACTOR.

capacity, of the enrichment plant in SWU/yr. The details of the calculation may be found in Ref. 2. The results of the analysis are presented in Table 2-4. The method shown in Table 2-4 has been used to scale both the jet membrane and gaseous diffusion plant capital costs with plant size.

2.2.3 Energy Costs

Jet membrane energy costs basically fall into two categories: the energy required to mechanically pump the UF_6 and the energy required to pump the jet gas. The process gas energy will be electrical and the jet gas energy will be thermal. The method of calculating the energy is outlined in Table 2-5; the details are in Ref. 2.

From Table 2-5, we see that the major jet membrane energy cost drivers are the level of enrichment and the ratio of the total jet flux to the flux of enriched process gas. It can also be seen that for a given enrichment and throughput the dominant factor in the latter ratio is the open area of the jet, A_o, relative to the collector area, A_c, i.e., the geometry of the collector probe/orifice configuration. The effect of probe/orifice configuration on jet membrane performance has also been a major concern in this program (see Section 4).

2.2.4 Cost of Enriching Uranium

The cost of enriching uranium is computed simply according to the following expression:

$$\text{Cost (\$/SWU)} = \text{Specific Energy Cost} + \text{Capital Charge X Specific Capital Cost} \qquad (2\text{-}1)$$

Energy costs have been assumed to scale linearly with plant size, i.e., specific energy costs are assumed constant.

2.3 PROCESS VARIABLES

The jet membrane process variables, i.e., all of those that are used to estimate jet membrane costs, fall into three groups: gaseous diffusion variables, engineering and design variables, and process parameters. The gaseous diffusion variables are those which have been identified above in the analytical modeling of the scale-up economics. These include, e.g., the plant separation factor,

TABLE 2-4

ECONOMY OF SCALE: CAPITAL COSTS

$$C_{JM} = CECI \left[(C_P)_{JM} \left(\frac{S_o}{S}\right)^{a_1^*} + (C_{ST})_{JM} \left(\frac{S_o}{S}\right)^{a_2^*} + (C_{PB})_{JM} \left(\frac{S_o}{S}\right)^{a_3^*} + (C_I)_{JM} \left(\frac{S_o}{S}\right)^{a_4^*} + (C_S)_{JM} \left(\frac{S_o}{S}\right)^{a_5^*} + (C_J)_{JM} \left(\frac{S_o}{S}\right)^{a_6^*} \right] \quad (8\text{-}1)$$

C_{JM} = SPECIFIC CAPITAL COST OF A PLANT OF CAPACITY S SWU/YR

$(C\ )_{JM}$ = SPECIFIC CAPITAL COSTS OF VARIOUS CATEGORIES FOR A PLANT OF CAPACITY S_o SWU/YR

CECI = FACTOR ACCOUNTING FOR ENGINEERING, CONTINGENCY AND INTEREST DURING CONSTRUCTION

S_o = REFERENCE SIZE = 8.75×10^6 SWU/YR

$a_1^* = .3$ $\quad a_4^* = 1$

$a_2^* = 0$ $\quad a_5^* = .710$

$a_3^* = .26$ $\quad a_6^* = .7$

TABLE 2-5

JET MEMBRANE ENERGY COSTS

- ELECTRICAL

$$\frac{(P_{PG})_{JM}}{(P_{PG})_{GD}} = \frac{\log (p_h/p_\ell)_{JM}}{\log (p_h/p_\ell)_{GD}} \frac{1}{\xi^2}$$

- THERMAL

$$\frac{(P_J)_{JM}}{(P_{PG})_{JM}} = \frac{(L_J)_{JM}}{L_{JM}} \frac{(H_J)_{JM}}{(H_{PG})_{JM}} \frac{(C_J/E)_{JM}}{(C_{PG}/E)_{JM}}$$

$$\frac{(L_J)_{JM}}{L_{JM}} = \sqrt{2\pi\gamma_J} \left(\frac{2}{\gamma_J + 1}\right)^{\frac{\gamma_J + 1}{2(\gamma_J - 1)}} \frac{A_o}{A_c} \frac{p_s}{p_b} \sqrt{\frac{T_b}{T_s}} \sqrt{\frac{M_{PG}}{M_J}} \frac{C_D}{t_{JM}}$$

$$(H_J)_{JM} = H_v + \Delta H_{CB}$$

$$(H_{PG})_{JM} = RT_b \log (p_h/p_\ell)_{JM}$$

- TOTAL

$$\frac{P_{JM}}{P_{GD}} = \frac{(P_{PG})_{JM}}{(P_{PG})_{GD}} \left[1 + \frac{(P_J)_{JM}}{(P_{PG})_{JM}}\right]$$

pressure levels, etc. The engineering and design variables are those which relate to the details of plant design, such as condenser design, interstage connections, effects of solubility, etc. The final group, the process parameters, contains those which have a direct influence on jet membrane performance, and the major capital and energy cost drivers, the suction pressure and jet flux. In the following subsections and, in particular, the subsection dealing with process parameters, we briefly indicate the numerical values of the primary parameters that were used to make our economics projections and how these parameters were generated.

2.3.1 Gaseous Diffusion Parameters

Most of the data required here, e.g., pressure levels, are classified, hence, unavailable in the open literature. In these cases, we have made estimates based on foreign information (Ref. 5). The value of the gaseous diffusion plant separation factor, however, may be calculated from data presented in Ref. 6 for the Paducah gaseous diffusion enrichment plant.

In Ref. 6 (p. 13) the total number of stages of the Paducah plant is given as 1812, capable of producing 5% ^{235}U before incurring a sharp drop in capacity. If we assume a tails assay of 0.3% ^{235}U (Ref. 6, p. 15), then, from the equations for an ideal cascade (Ref. 7) we find for the heads-to-tails separation factor $(\alpha_{GD})_p = 1.00316$. However, in our experiments, we have used the feed mole ratio as the reference. In order to make the proper comparison, it is necessary to compute the gaseous diffusion plant heads to feed separation factor $(\beta_{GD})_p$. From Ref. 8

$$\beta = \sqrt{\alpha} \tag{2-2}$$

hence, the gaseous diffusicn plant heads to feed separation factor $(\beta_{GD})_p = 1.00158$. This is to be compared with the theoretical effusive separation factor $\alpha_{GD} = 1.004289$. Therefore, in the cost analysis we shall compare the measured jet membrane heads-to-feed point separation factor to the gaseous diffusion heads-to-feed stage separation factor. The plant relative enrichment, ξ_p, is then given by

$$\xi_p = \frac{\beta_{JM}-1}{(\beta_{GD})_p-1} = \frac{\beta_{JM}-1}{0.00158} \tag{2-3}$$

For convenience, however, the experimental data that are presented later have been compared to the theoretical effusive separation factor α_{GD} which is known unambiguously. The experimental values of relative enrichment are then computed from

$$\xi = \frac{\beta_{JM}-1}{\alpha_{GD}-1} = \frac{\beta_{JM}-1}{0.00429} \qquad (2\text{-}4)$$

2.3.2 Engineering and Design Variables

For the most part, such items as condenser design, interstage connections, piping losses, and the effect on costs of various design philosphies have been considered as beyond the scope of our economic analysis. A more basic question, which depends upon the results of an engineering analysis is the choice of jet fluid. We have used FC-43 (Ref. 9) (Molecular weight = 671)* in our experiments because it is known to be compatible with UF_6 (Ref. 10). Another potential jet fluid that has suitable vapor pressure properties is FC-75 (molecular weight, M = 420). The final choice of jet fluid will depend on the entire system design, including distillation requirements, condenser properties, etc. We have carried out a simplified analysis of the thermal requirements and, assuming no difference in performance between FC-43 and FC-75, concluded that FC-75 would be more suitable as a jet fluid. Based on the simplified thermal analysis, we have assumed that the relative energy requirement (jet thermal/process gas electrical) shown in Table 2-5 is 16. The relative cost/unit of energy of thermal to electrical energy has been taken as 0.087, based upon thermal energy supplied from a dual purpose power plant. The analysis upon which this value is based may be found in Appendix C.

The capital cost of jet handling equipment (boilers, condensers, etc.) that we have used is an estimate based on preliminary information supplied by the Garrett Corporation (Ref. 4). The numerical value of the coefficient shown in Table 2-3 is based on their initial estimate of these costs for a point design. The dependence of this cost on the jet flux and relative enrichment is our estimate as to how these quantities will influence the cost.

*One of a class of "Fluorinert" liquids produced by the 3M company

2.3.3 Process Parameters

The four categories of jet membrane variables we address in this subsection are jet membrane unit process size, pressure levels, jet flux, and performance. Here we specify the particular process parameters which show the greatest effect on these categories. The section in the remainder of this report that provides the basis for selecting the numerical values of these parameters is also noted.

- Size: based on results of Section 4.3 and Becker nozzle technology (Ref. 11)
  - Nozzle width, D_j = 0.01 cm
  - Collector probe width, D_c = 0.009 cm = D_p (collector probe is assumed to have zero thickness)
  - Two-dimensional nozzle/probe configuration
- Pressures
  - Source (stagnation) pressure, p_s = 420 torr: based on sizes above and the scaling parameter derived in Section 4.5
  - Background pressure, p_b = 280 torr: based on p_s and the jet pressure ratio p_s/p_b = 1.5 (Sections 4.2 and 5.2.2)
  - Suction pressure, p_ℓ = 70 torr: based on p_b and the pumping pressure ratio p_b/p_ℓ = 4.0 obtained from the conical probe configuration with partial pressure condensation pumping (Section 4.6)
- Jet Flux - calculation is based on Table 2-5 and the following:
  - Specific heat ratio, γ_j = 1.05: typical for heavy molecules like FC-43
  - Jet to probe area ratio, A_o/A_c = 1/9: based on sizes above
  - Orifice pressure ratio, p_s/p_b = 1.5: based on Sections 4.2 and 5.2.2
  - Orifice temperature ratio, T_s/T_b = 1.0: typical value; results are insensitive to this ratio
  - Orifice discharge coefficient, C_D = 0.8: typical upper bound; values of $C_D \sim 0.15$ have been measured with the conical probe configuration and an SF_6 jet
  - UF_6/FC-75 mass ratio, m_{PG}/m_j = 0.831
  - Transmission, t_{JM}, depends upon the performance results and the relative enrichment. Relative enrichment is the independent variable in each optimization study.

- Performance
  - The performance curve used is the exponential curve fit to the small probe FC-43/UF_6 experimental data, referred to the gaseous diffusion plant separation factor, as discussed in Section 2.3.1. This curve is shown in Fig. 2-2 along with the FC-43/UF_6 experimental data. Also shown are all of the FC-43/SF_6 experimental data (small and large probe) scaled to the gaseous diffusion plant separation factor. The enlargement of the data base for UF_6 is confirmed by all of the results (Sections 3, 4, and 5) which indicate that SF_6 data are transferable to UF_6.

2.4 RESULTS OF COST ANALYSIS

Based on the parameters cited previously we have carried out a series of calculations using our jet membrane economics analysis and compared these results with available gaseous diffusion plant (GDP) and gas centrifuge plant (GCP) data. In the jet membrane results to be presented below we have assumed a plant relative enrichment factor $\xi_p = 3$. Although our calculations indicate that these results are not optimum, we have used this value since it corresponds to a UF_6 separation factor that we have achieved experimentally to date. As mentioned earlier, it should be noted that virtually all of the other process parameters have also been achieved experimentally, in some gas system.

In order to provide a comparison between a jet membrane plant, GDP and GCP having the same time base, we have made use of 1974 data, for both gaseous diffusion and the centrifuge, that may be found in Ref. 12. In particular, the capital investment for a nominal 9 million SWU/yr gaseous diffusion plant is cited as $3.16 billion. This value is different than the $1.2 billion quoted in Ref. 3. Therefore, all of the specific capital costs for an 8.75 million SWU/yr GDP shown in Table 2-1 have been multiplied by the ratio 3.16/1.2 = 2.63 in order to reflect the increase in capital costs between 1970 and 1974. The jet membrane specific capital costs have then been calculated as discussed in Section 2.2.1 and the variation of capital costs with plant size for both the jet membrane and gaseous diffusion have been calculated as shown in Section 2.2.2. A 15% contingency has been applied to the jet membrane, the same as quoted in Ref. 3 for the GDP and in Ref. 12 for the GCP.

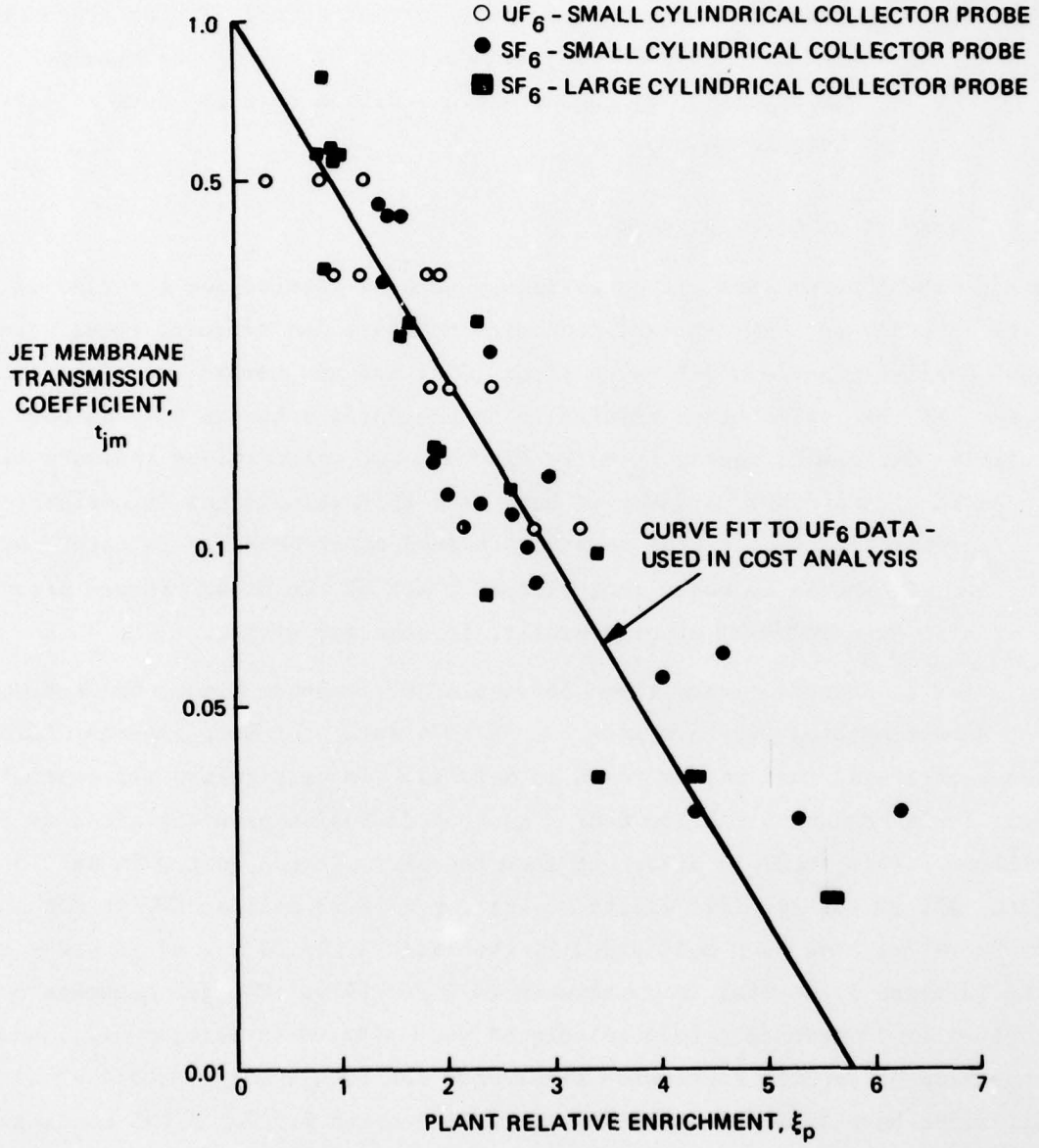

Figure 2-2. Summary of UF_6 and SF_6 Performance Referred to Gaseous Diffusion Plant Separation Factor

The 1974 operating costs of the 8.75 million SWU/yr GDP are given in Ref. 12 at $44/SWU. We have assumed that the bulk of this cost is electrical energy and used this value to calculate the energy cost of the jet membrane, as discussed in Section 2.2.3.

The cost of enriched uranium has been calculated for the jet membrane and GDP as in Section 2.2.4. A 10% capital charge has been applied to the gaseous diffusion capital cost (Ref. 12) and an 11.7% capital charge to the jet membrane, the same value as assigned the centrifuge in Ref. 12.

Comparisons of a jet membrane plant, GDP, and GCP are shown in Tables 2-6 through 2-8. Table 2-6 presents a cost and energy summary for a large (3,000,000 SWU/yr) enrichment plant; Table 2-7 is a cost and energy comparison for a small (300,000 SWU/yr) enrichment plant; and Table 2-8 is a cost comparison vs plant size. Based on these Tables, we conclude:

- For a 3×10^6 SWU/yr plant, the cost of enriched uranium using the jet membrane is projected to be approximately 30% of the gaseous diffusion cost and 43% of the centrifuge cost
- The total capital investment required for a 3×10^6 SWU/yr jet membrane plant is projected to be 23% of gaseous diffusion and 34% of centrifuge for plants of the same size
- For jet membrane plants larger than 3×10^6 SWU/yr the size of available thermal sources is likely to be a limiting factor.
- For a small (3×10^5 SWU/yr) plant the capital investment for a jet membrane plant is projected to be 29% of gaseous diffusion and 62% of centrifuge capital investments. The relative costs of enriched uranium are 35% and 42%, respectively
- The cost of enriched uranium for a 3×10^5 SWU/yr jet membrane plant is comparable (91%) to the cost for an 8.75×10^6 gaseous diffusion plant whereas the capital investment required is only 4.5%. Compared to a 3×10^6 SWU/yr centrifuge plant, the equivalent percentages are 103% and 13%, respectively
- The jet membrane thus holds promise as a load follower, i.e., the cost of enriched uranium for a 3×10^5 SWU/yr jet membrane plant is projected to be similar to present day (i.e., 1974) costs but the capital investment required is projected to be

TABLE 2-6

PROJECTED CAPITAL AND ENERGY REQUIREMENTS FOR A 3,000,000 SWU/YR ENRICHMENT PLANT (1974 Dollars)

	Jet Membrane	Gaseous Diffusion*	Centrifuge
Relative Enrichment	3.0	1.0	--
Capital Cost	$385M	$1.64B	$1.13B**
Cost of Enriched Uranium/SWU	$30	$99	$70**
Electrical Power Cost Relative to Gaseous Diffusion	0.102	1.0	0.10†
Electrical Power (MWe)	91	891	89.1
Thermal Power Cost Relative to Gaseous Diffusion Electrical Cost	0.255	--	--
Thermal Power (MW)	2600††	--	----
Total Power Cost Relative to Gaseous Diffusion	0.357	1.0	0.10

*Data scaled as in Sec. 2.2.2

**Ref. 12

†Ref. 13

††For plants larger than 3,000,000 SWU/yr; size of the available thermal source will likely be limiting for the jet membrane.

TABLE 2-7

PROJECTED CAPITAL AND ENERGY REQUIREMENTS FOR A 300,000 SWU/YR ENRICHMENT PLANT (1974 DOLLARS)

	Jet Membrane	Gaseous Diffusion*	Centrifuge
Relative Enrichment	3.0	1.0	---
Capital Cost	$145M	$493M	$235M**
Cost of Enriched Uranium/SWU	$72	$208	$171**
Electrical Power Cost Relative to Gaseous Diffusion	0.102	1.0	0.10†
Electrical Power (MWe)	9.1	89.1	8.9
Thermal Power Cost Relative to Gaseous Diffusion Electrical Cost	0.255	---	---
Thermal Power (MW)	261	---	---
Total Power Cost Relative to Gaseous Diffusion	0.357	1.0	0.10

*Data scaled as in Sec. 2.2.2

**Ref. 12

†Ref. 13

TABLE 2-8

PROJECTED CAPITAL COST AND COST OF ENRICHED URANIUM VS PLANT SIZE (1974 DOLLARS)

Plant Size SWU/Yr		Jet Membrane ($\xi_p = 3$)	Gaseous Diffusion*	Centrifuge**
8.75×10^6	Capital Cost	$681M	$3.16B	$2.56B
	Cost of Enriched Uranium/SWU	$24	$79	$58
3.0×10^6	Capital Cost	$385M	$1.64B	$1.13B
	Cost of Enriched Uranium/SWU	$30	$99	$70
1.0×10^6	Capital Cost	$231M	$880M	$492M
	Cost of Enriched Uranium/SWU	$42	$132	$95
0.3×10^5	Capital Cost	$145M	$493M	$235M
	Cost of Enriched Uranium/SWU	$72	$208	$171

*Cost calculated as in Sec. 2.2.2

**Ref. 12

significantly lower than for present day processes. Therefore, changes in demand for enrichment services can be financed more readily using small jet membrane plants.

SECTION 3

UF_6 AND RELATED ISOTOPE SEPARATION EXPERIMENTS

Measurements are presented in this section that demonstrate the jet membrane separation effect in several isotopic systems, leading up to and including UF_6. The experiments employed a heavy condensible fluorocarbon vapor jet (FC-43) and process gas backgrounds of Ne, SF_6 and UF_6; i.e., of increasingly heavy isotopes. For comparison, to show the effect of a different jet gas, separation of Ne isotopes by an N_2 jet is also shown. In all of these experiments the enriched upflow is collected by a small cylindrical tube located on the centerline of the jet. The separation factor and corresponding upflow vary as this tube is moved relative to the plane of the jet orifice.

The details of the experimental technique may be found in Section 7. Briefly, however, the measurements of separation factor and upflow were made separately, as a function of probe position. The separation factor was measured directly using a mass spectrometer. Absolute measurements of the upflow material flow rate were not made; instead the ion current in the mass spectrometer, which is proportional to the upflow of enriched material, was the measured quantity. The data obtained were made dimensionless and the probe position eliminated by cross-plotting to obtain jet membrane performance, as defined in Section 2 (measured transmission, t_m, vs. relative enrichment, ξ).

The dimensionless quantities, measured transmission and relative enrichment, are defined as follows: measured transmission is the ratio of the ion current at some probe position to the ion current with the jet off. Relative enrichment is the measured enrichment (separation factor -1) divided by the ideal effusive enrichment ($\sqrt{M_H/M_L}-1$). Both of these quantities reflect the effect of both the jet and the collector probe on jet membrane performance. However, since the collector probe used in these experiments is simply a diagnostic tool, and is not representative of a configuration that would be considered in an enrichment plant, the question arises as to how this probe affects the results. This question is discussed in detail in Section 7. To summarize the results obtained there, we conclude that the method of presenting the data, measured transmission vs. relative enrichment, accurately represents the jet membrane separation effect,

i.e., the effect of the jet is isolated from the effect of the collector probe. Furthermore, we conclude that the measured transmission t_m is virtually the same as the defined jet membrane transmission coefficient t_{JM} that is used in the economic analysis (Ref. 2).

These important conclusions allow us to use the measured uranium enrichment data presented in this section, in conjunction with the experiments to be described in Section 4, to make economic predictions for an enrichment plant.

In this section measured results are only presented. The data are presented as measured transmission t_m vs relative enrichment as described above (e.g., the performance plane). Comparisons of measured performance with theoretical predictions is discussed in Section 5. The experimental apparatus are discussed in Section 6.

3.1 SMALL CYLINDRICAL COLLECTOR PROBE EXPERIMENTS

In Fig. 3-1, performance data for neon isotopes in a jet membrane unit process are shown. The measurements were made in the gaseous jet apparatus (apparatus no. 1) using a nitrogen jet gas. The data envelope indicated is representative of a large number of experiments that were conducted over a wide range of process pressures. The circles represent the calculated average value of separation from all of the experiments.

Based on these results we conclude that:

- Isotopic separation by the jet membrane process has been demonstrated
- Performance is unchanged well into the continuum flow regime as indicated by the range of the rarefaction parameter, ε (see Section 5)
- Nozzle pressure ratio effects on performance are small; e.g., all of the measurements lie in the range indicated.
- Process gas upflow rate decreases exponentially with increasing enrichment. This observation is consistent with both rarefied and continuum model predictions (see Section 5).

Separation data for neon isotopes in a heavy molecule (FC-43) condensible jet are shown in Fig. 3-2. The measurements were initially made in the benign gas condensible jet apparatus (apparatus no. 2) using a 2 in. radius mass

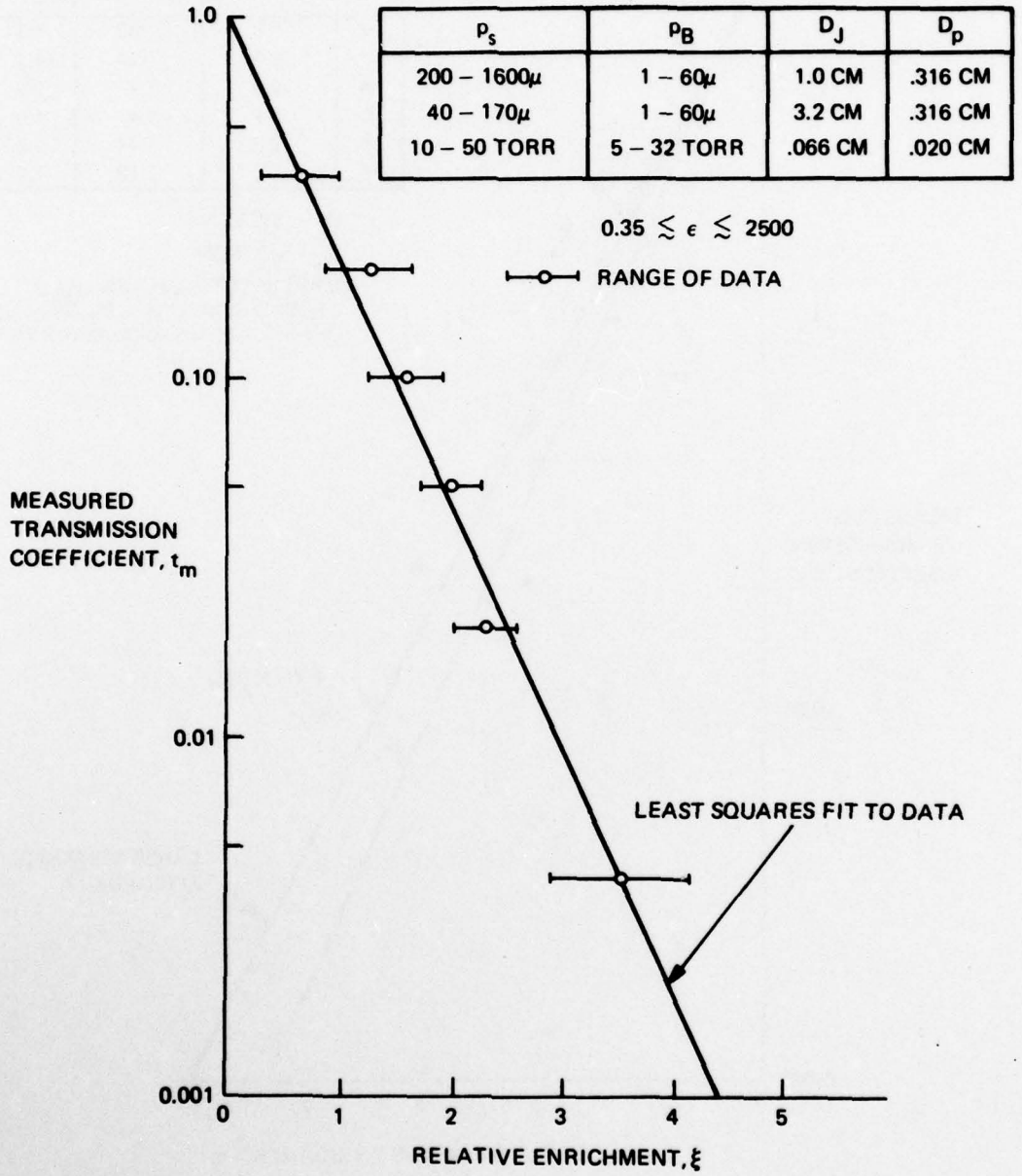

Figure 3-1. Separation of $^{20}Ne/^{22}Ne$: N_2 Jet: Small Cylindrical Collector Probe

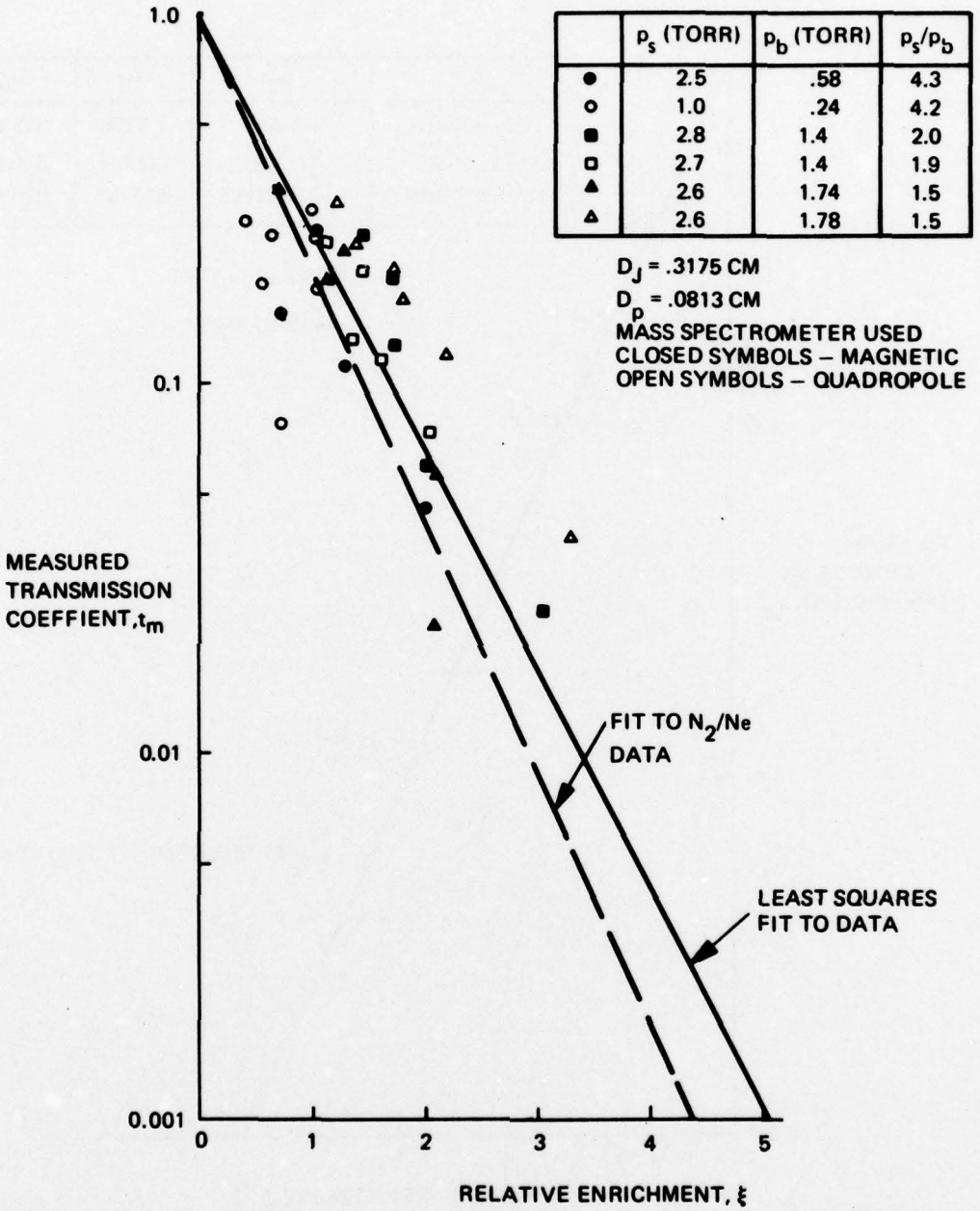

	p_s (TORR)	p_b (TORR)	p_s/p_b
●	2.5	.58	4.3
○	1.0	.24	4.2
■	2.8	1.4	2.0
□	2.7	1.4	1.9
▲	2.6	1.74	1.5
△	2.6	1.78	1.5

Figure 3-2. Separation of $^{20}Ne/^{22}Ne$: FC-43 Jet: Small Cylindrical Collector Probe

spectrometer. Several months into the program a quadrupole instrument became available and the measurements were repeated. Data quality is only fair as can be seen by comparing the open and closed symbols for fixed process conditions. From these data we conclude that:

- The results are in good agreement with those obtained using a nitrogen jet gas
- Jet membrane performance is relatively insensitive to the size of the jet gas molecule
- Jet pressure ratios as low as 1.5 can be employed without noticeably degrading performance.

Measurements of SF_6 separation in an FC-43 jet are shown in Fig. 3-3. The experiments were performed in apparatus no. 2 using the 2 in. radius magnetic spectrometer and the quadrupole instrument. Although neither instrument was capable of providing high precision isotopic ratio measurements in SF_6, we can still conclude from these preliminary data that

- It is possible to obtain separation of heavy isotopes using the jet membrane
- Upflow rate decreases exponentially with increasing relative enrichment as with N_2/Ne and FC-43/Ne.

Improved SF_6 separation measurements taken in the UF_6 apparatus (apparatus no. 3) with the Nuclide 12-90-CG 12 in. radius mass spectrometer are presented in Fig. 3-4. The Nuclide instrument is specifically designed for isotopic ratio measurements. Details of this instrument are described in Section 6.3. The results show that

- Isotopic separation in SF_6 is achieved
- Performance data again displays an exponential character
- Performance is unaffected by changes in nozzle pressure ratio in the range $2 \leq p_s/p_b \leq 5$
- Good baseline data has been established for comparison with UF_6 results; theory (Section 5) predicts that the separation performance for SF_6 and UF_6 isotopes should be virtually identical
- Measurement precision is good

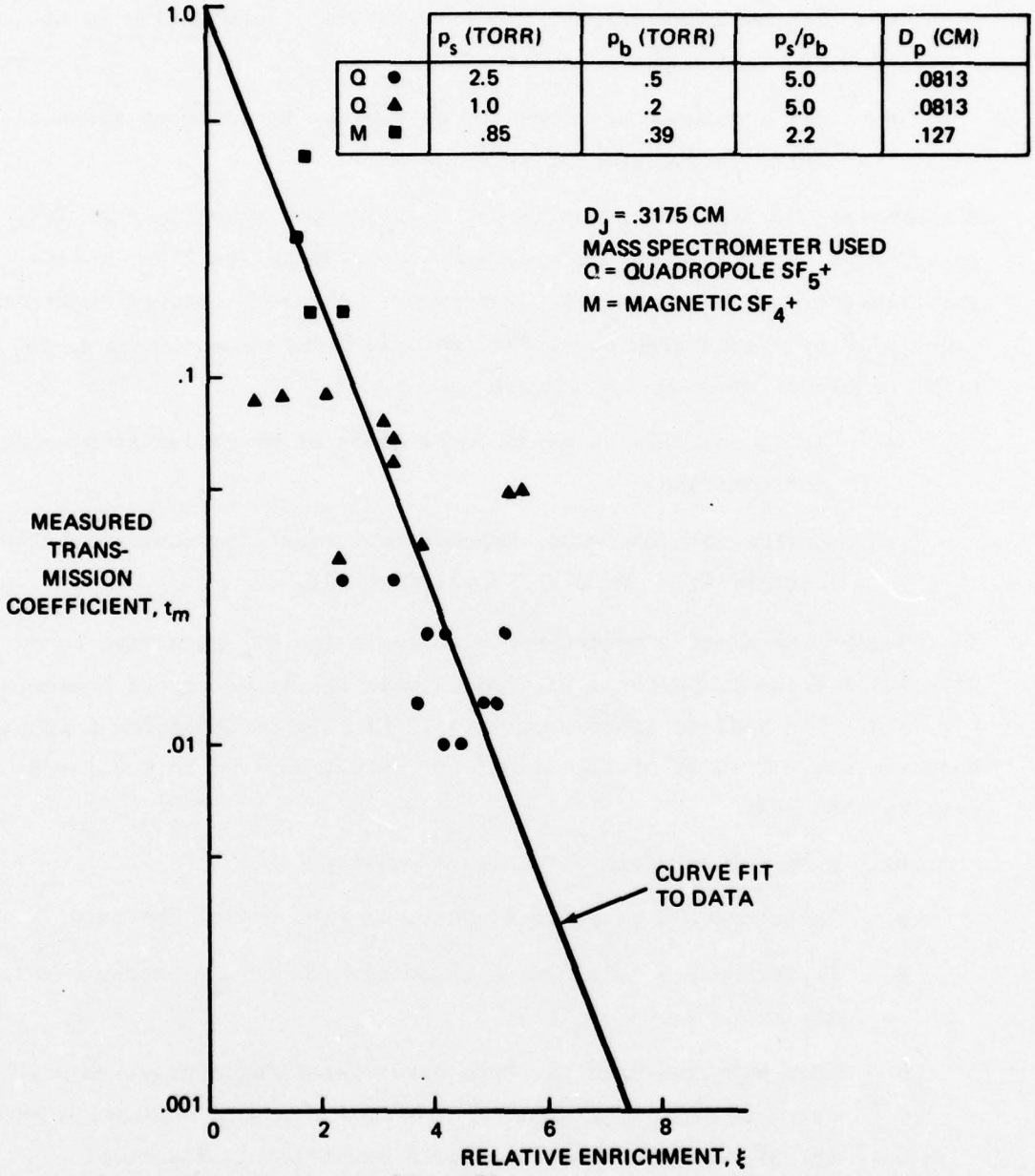

	p_s (TORR)	p_b (TORR)	p_s/p_b	D_p (CM)
Q ●	2.5	.5	5.0	.0813
Q ▲	1.0	.2	5.0	.0813
M ■	.85	.39	2.2	.127

Figure 3-3. Separation of $^{32}SF_6/^{34}SF_6$: FC-43 Jet: Small Cylindrical Collector Probe: Preliminary Data with Low Precision Mass Spectrometer

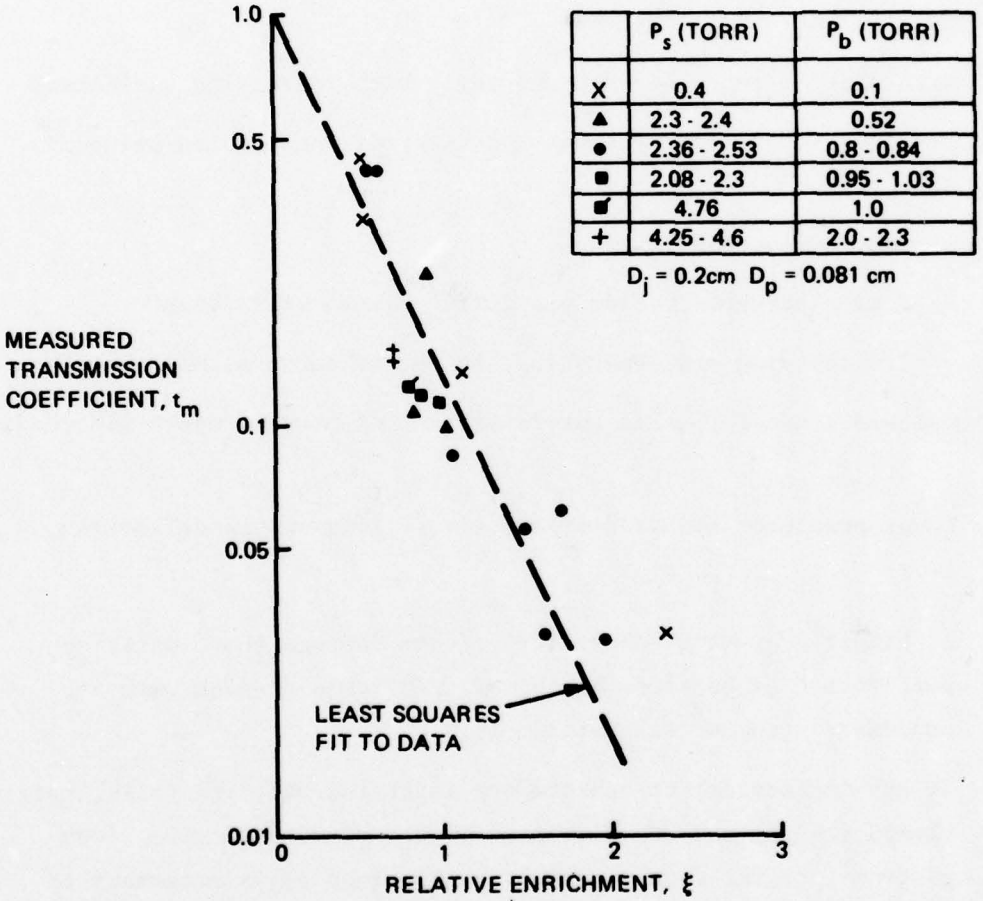

Figure 3-4. Separation of $^{32}SF_6/^{34}SF_6$: FC-43 Jet: Small Cylindrical Collector Probe

- Relative standard deviation of better than 0.1% was attained for all single point measurements
- Scatter in the measurements is greatly reduced; e.g., compare repeated runs, at the same relative flux level, for fixed operating conditions.

Repeated measurements of UF_6 separation, at several relative flux levels, are shown in Fig. 3-5. To obtain reasonable precision in the measurement, process gas upflow samples were collected in a liquid nitrogen cooled trap. Sample collection time was about 20 hours at a relative flux level of 0.1. The jet membrane operating pressures indicated in the figure are average values based upon a time series of pressure measurements taken before and after sample collection. The results indicate that

- UF_6 separation is achieved
- Transmission decreases exponentially with increasing enrichment
- Data quality is fair; measurement imprecision results primarily from
  - Sample size limitations
  - Source pressure variations during sample collection
  - Transmission and separation are not measured simultaneously.

The data base was limited to this particular set of process operating conditions because

- Lower pressures required prohibitively long sample collection times
- At higher pressures solubility effects depress the separation performance by backflow mixing of unenriched uranium with the processed uranium (see Section 5).
- It was impractical to operate the apparatus with the boiler return closed (to prevent UF_6 dissolved in the FC-43 condensate from getting into the source vapor) for the long times necessary to collect upflow samples.

In Fig. 3-6 we compare UF_6 and SF_6 performance. As can be seen

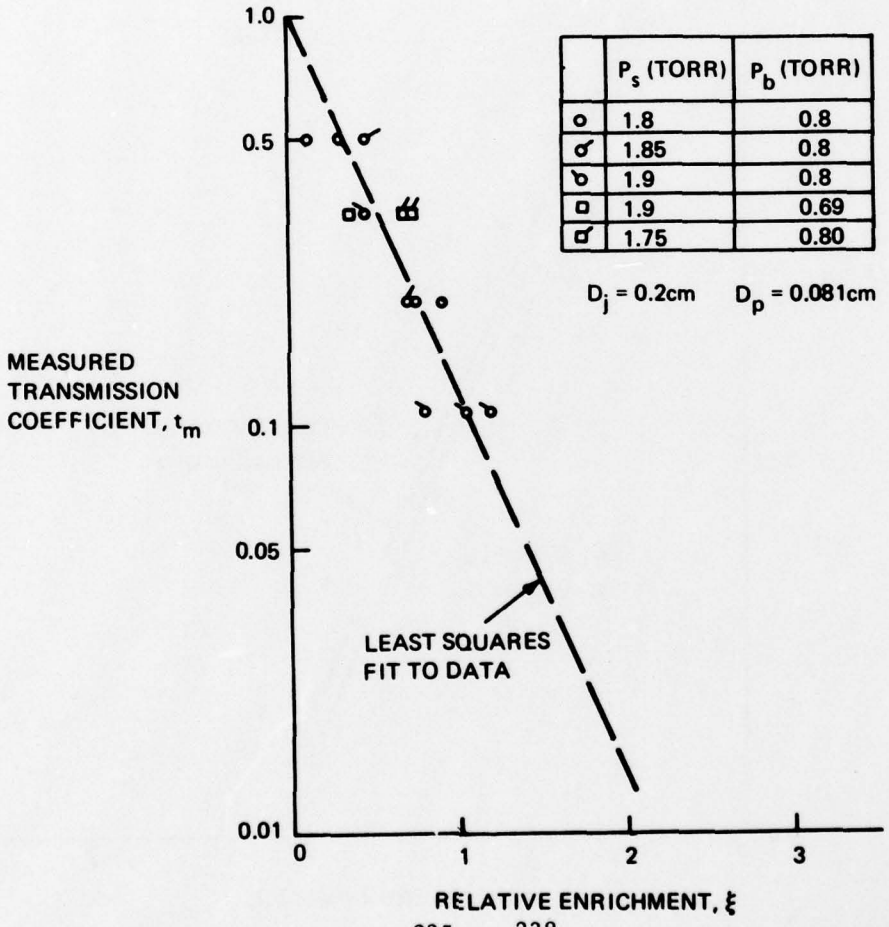

	P_s (TORR)	P_b (TORR)
o	1.8	0.8
♂	1.85	0.8
♁	1.9	0.8
□	1.9	0.69
♂	1.75	0.80

Figure 3-5. Separation of $^{235}UF_6/^{238}UF_6$: FC-43 Jet: Small Cylindrical Collector Probe

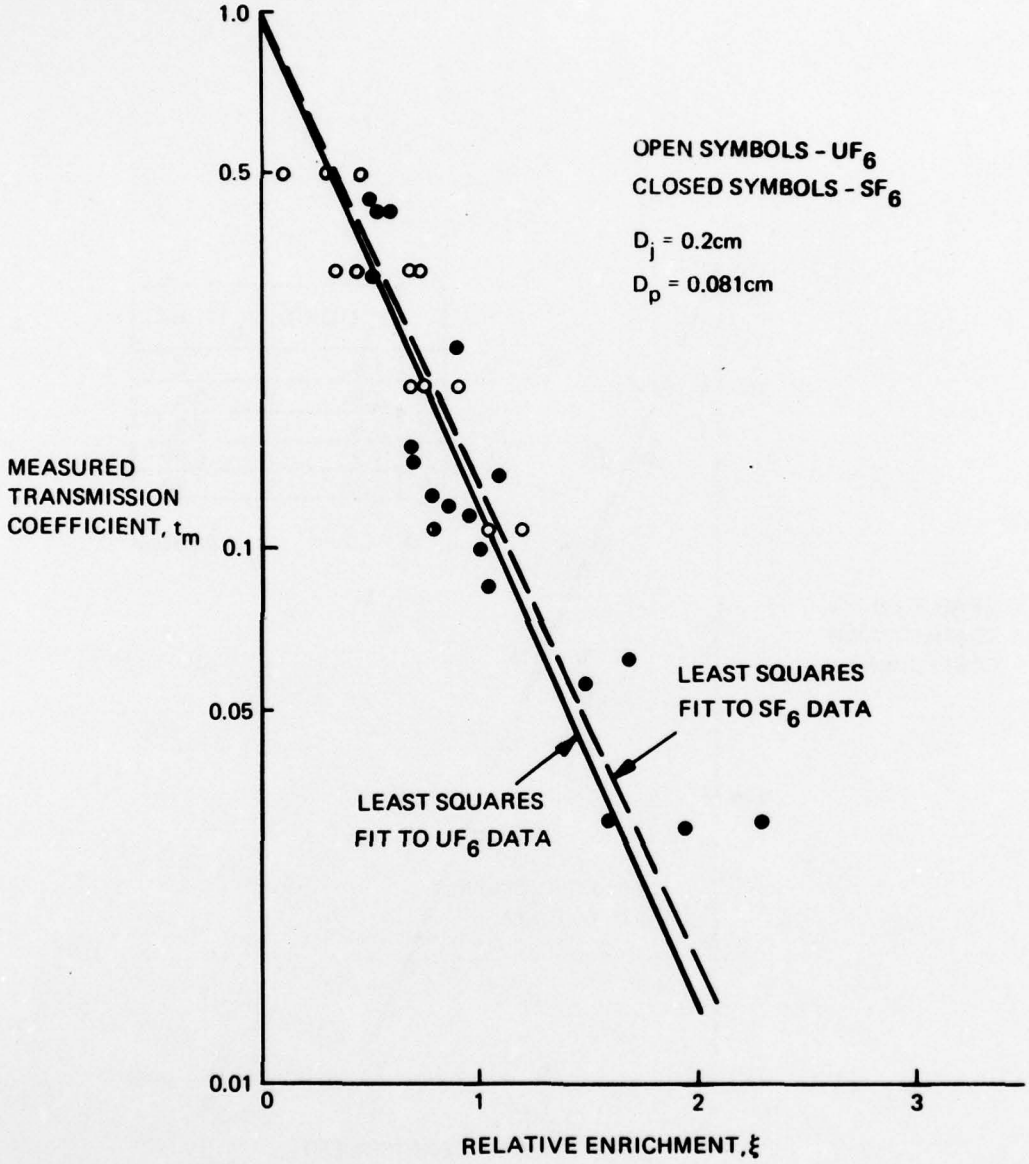

Figure 3-6. Comparison of UF_6 and SF_6 Performance: FC-43 Jet: Small Cylindrical Collector Probe

- The measured data for both cases are in excellent agreement; least squares curve fits to both sets of data are virtually identical
- The observed agreement between SF_6 and UF_6 results is consistent with model predictions (see Section 5)
- SF_6 performance results should be transferable to UF_6.

3.2 CONCLUSIONS

In this section we have presented experimental results that demonstrate isotopic enrichment, by means of the jet membrane process, of the light isotope in Ne, SF_6, and UF_6 gases. These data were obtained in a jet membrane unit process apparatus which was operated in the near continuum flow regime using a heavy molecule (FC-43) condensible jet gas. In addition, for neon separation, data obtained in a different apparatus that employed a Nitrogen jet gas were presented. In this case a performance envelope was shown for process conditions (pressure and scale) that covered the range from rarefied to the continuum flow regimes.

Based on the experimental results it is concluded that

- The light isotope of uranium can be enriched by the jet membrane process
- The UF_6 results are virtually identical to those obtained in SF_6, therefore the SF_6 results are transferable to UF_6
- Transmission decreases exponentially with increasing enrichment
- A heavy condensible jet can be used to separate isotopes
- The same separation performance can be obtained over a broad range of nozzle pressure ratios; a pressure ratio as low as 1.5 was employed in the FC-43/Ne tests.

SECTION 4

PROGRAM SUPPORTING EXPERIMENTS

Within the limitations of our scale-up economic model, we have been able to identify certain key technical issues that are the primary capital and energy cost drivers of the jet membrane process. In this section, we present the results of experiments performed to investigate these issues. In general, two specific questions have been addressed: 1) what are the limitations on process parameters, particularly as they affect unit process performance? and 2) how do we scale these parameters to a full-scale UF_6 enrichment plant? The experiments were carried out in parallel with the UF_6 experiments (reported in Section 3) using apparatus 1 and 2. The process gases employed were SF_6 and He/Ar mixtures. Based on these experiments and the UF_6 results a rational basis for extrapolating the UF_6 data base to full scale process conditions has been established.

The technical issues which have been studied, the jet membrane feature they relate to, and the area of primary economic impact are summarized below:

- Probe/orifice area ratio-Jet mass flow - Energy
- Pressure ratio p_s/p_b-Jet mass flow/Scaling-Energy/Capital
- Probe/orifice configuration-Jet mass flow/Suction pressure-Energy/Capital
- Backflow into collector probe-Jet mass flow/Suction pressure-Energy/Capital
- Pressure limits/Scaling-Suction pressure/Size-Capital
- Suction pressure - Capital

As can be seen, the primary thrust of these experiments has been to try to optimize the geometry of the unit process probe/orifice configuration in order to reduce the required jet mass flow without sacrificing performance; and to attempt to raise the overall system operating pressure. The former is to reduce the thermal energy required and the latter to reduce the capital costs, particularly of mechanical pumping. Other factors, which relate to system or engineering issues, such as the effect of multiple probes, stage design, and

interstage connections, have not been addressed here. Descriptions of the apparatus in which the experiments were performed are contained in Section 6. The experimental procedure is discussed in Section 7.

4.1 EFFECT OF PROBE TO ORIFICE AREA RATIO

These experiments were conducted in apparatus no. 1 with the collector probe dimensions fixed (D_p and D_c) and the probe to orifice area ratio was increased by making D_j smaller. Thus, for fixed source conditions increased area ratio results in actual reduction of jet mass flow. The effect of probe to orifice area ratio on the performance of a N_2/He-A system is shown in Figures 4-1a, 4-1b, and 4-1c where three sets of data are shown corresponding to A_p/A_j = 0.09, 0.32, and 0.62, respectively. From these data we see

- Jet membrane performance for mixtures is not significantly changed as relative probe area is increased. Apparent improvement in performance as D_p/D_j is increased, is probably within the scatter in the data
- Performance remains algebraic ($t \sim \alpha^{-s}$/see Section 5.1) as D_p/D_j increases
- Although not apparent from the figures, as the area ratio increases, at the same level of transmission, separation occurs closer to the orifice plate or even inside the source chamber.

It should also be noted from Fig. 4-1a that the background mixture ratio does not effect performance.

Subsequent to the above experiments, similar experiments were carried out using FC-43/SF_6. The transmission in these data was measured on-line in apparatus no. 2 using the small magnetic mass spectrometer, and the enrichment was measured by collecting samples and analyzing them on the Nuclide 12-CG-90 mass spectrometer. The results are shown in Fig. 4-2 for p_s = 2 and 7 torr and a pressure ratio p_s/p_b = 2. From this figure we see

- Performance is exponential, as for the small probe
- Performance is not noticeably affected by pressure level.

Again, significant enrichment was observed near the orifice plate or within the source chamber.

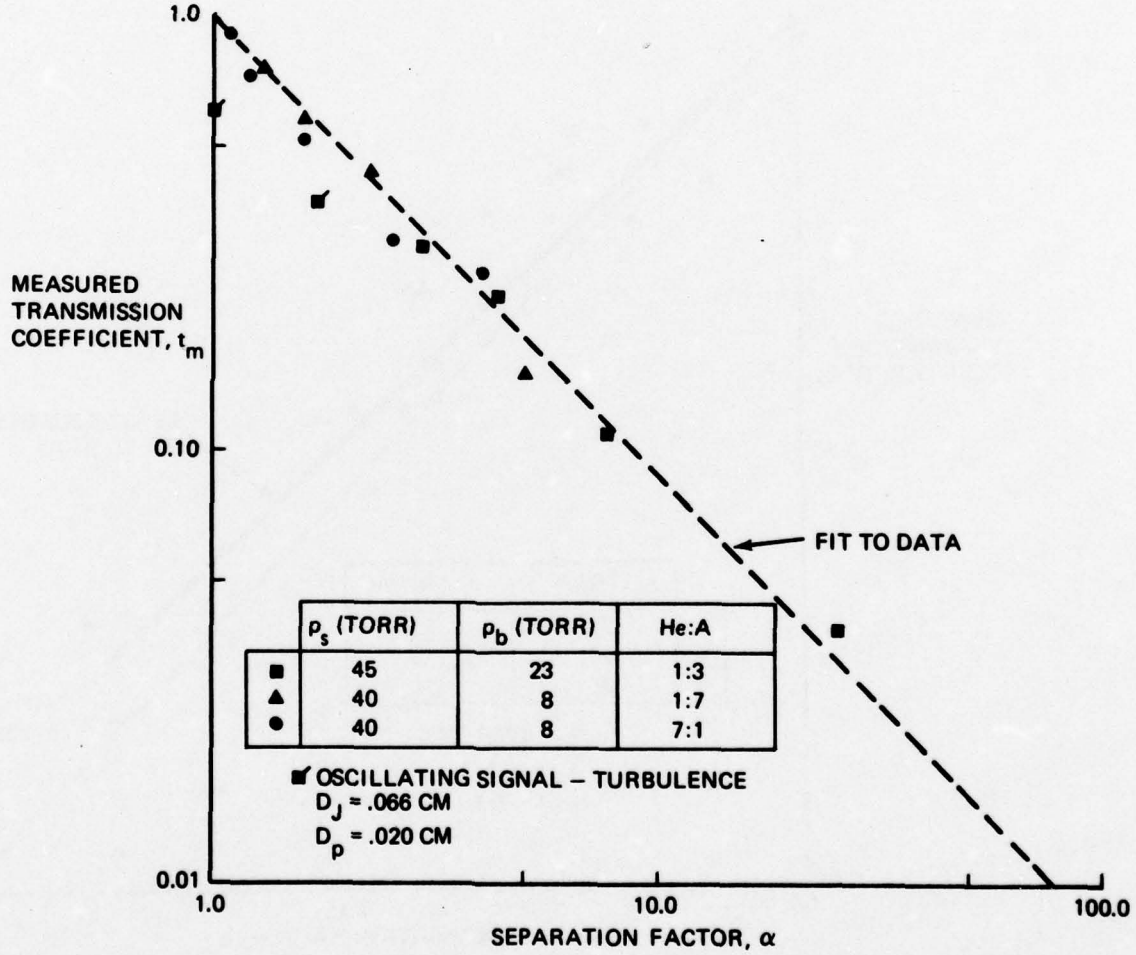

Figure 4-1a. He/A Separation: N_2 Jet: Small Cylindrical Collector Probe

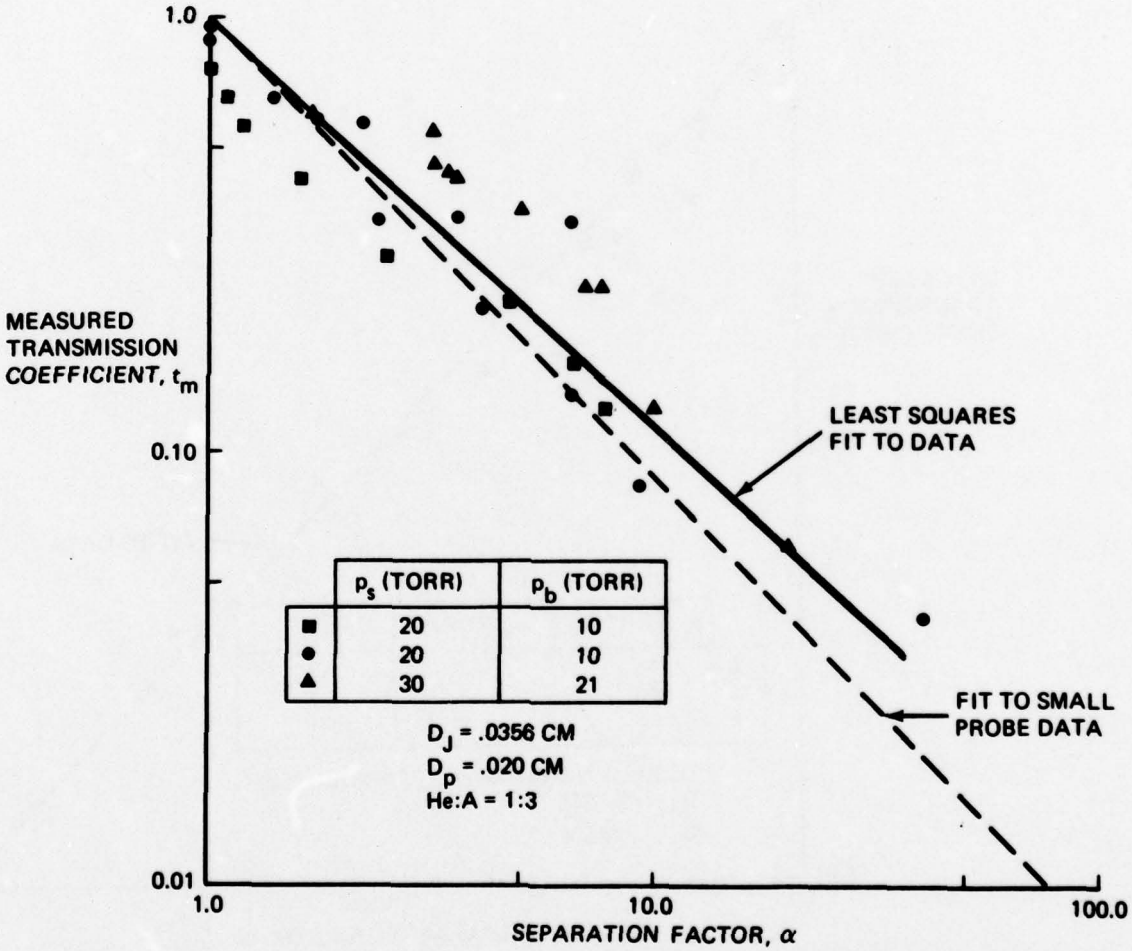

Figure 4-1b. He/A Separation: N_2 Jet: Intermediate Cylindrical Collector Probe

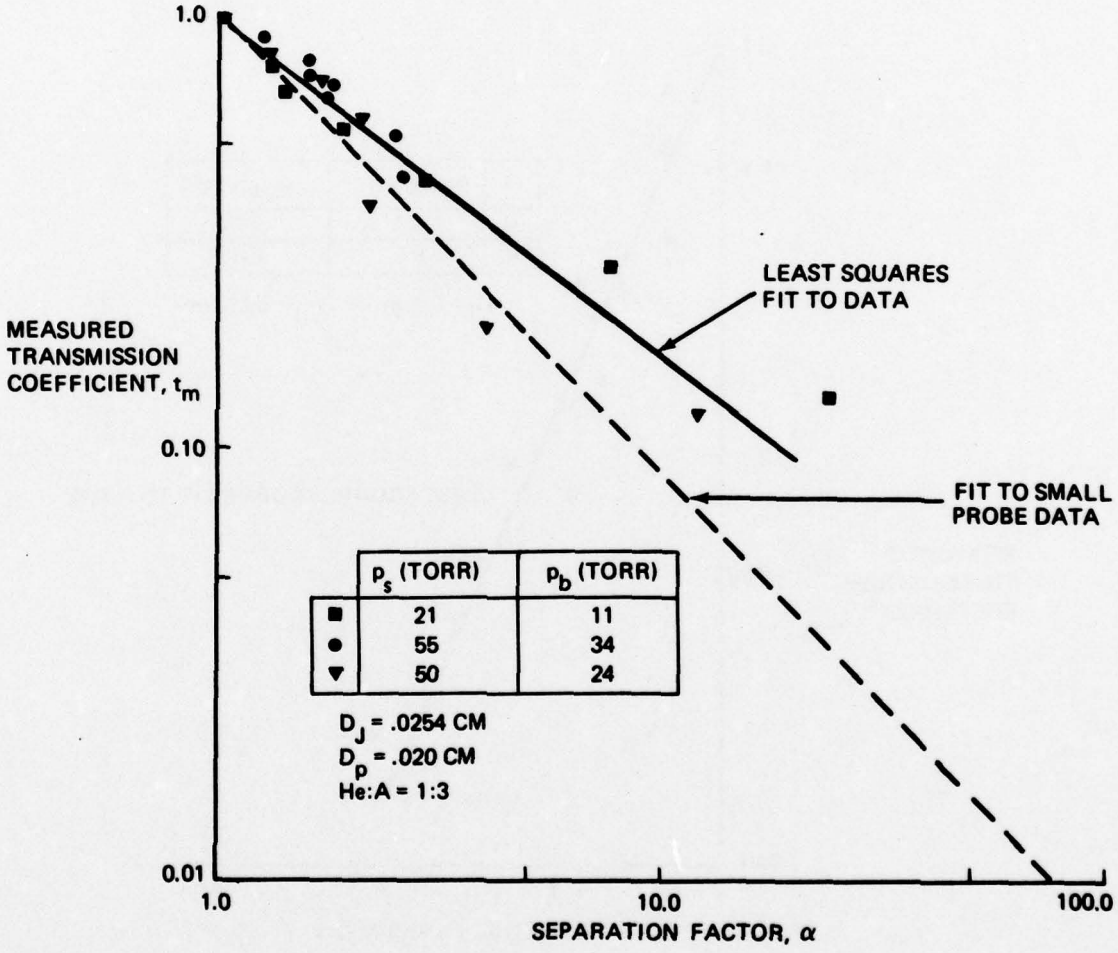

Figure 4-1c. He/A Separation: N_2 Jet: Large Cylindrical Collector Probe

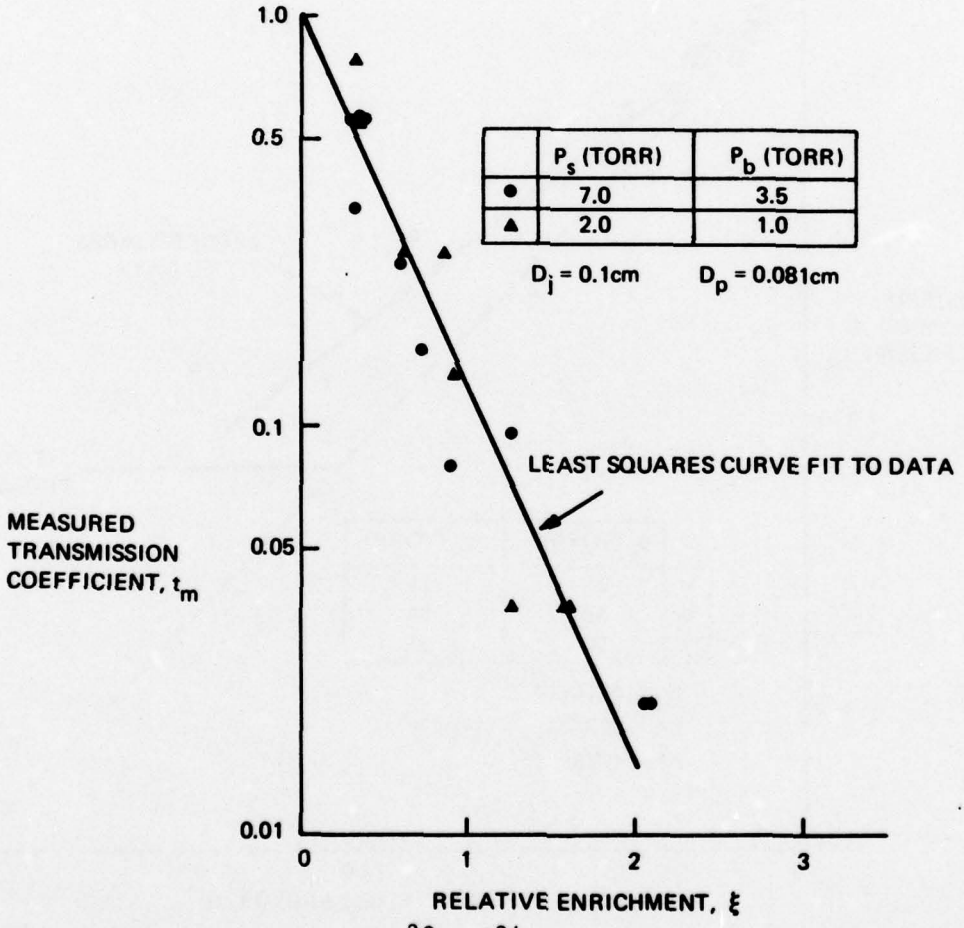

Figure 4-2. Separation of $^{32}SF_6/^{34}SF_6$: FC-43 Jet: Large Cylindrical Collector Probe

In Fig. 4-3, a comparison of all FC-43/SF_6 data (for which enrichment was analyzed on the Nuclide 12-CG-90 mass spectrometer) is presented. Also shown are the exponetial curve fits to each set of data. Based on these data, and the data in Fig. 4-1, we conclude:

- Jet membrane performance is not affected significantly by probe/orifice area ratio
- Based on the agreement between FC-43/SF_6 and FC-43/UF_6 small probe performance, we draw the same conclusion for FC-43/UF_6 large probe performance, i.e., SF_6 data are transferable to UF_6.

The latter comment is, of course, the basis for including all of the data shown in Fig. 2-2 in the economic analysis.

Since it has been observed that significant enrichment can occur near the orifice plate or inside the source chamber, the question arises as to whether this enrichment has indeed occurred at a reduced jet mass flow, or whether the increase in geometric area between the collector probe and the orifice plate, as the probe is withdrawn into the source chamber, has led to an increase in jet mass flow. The results of an experiment to investigate this aspect of large probe performance are shown in Fig. 4-4. In this figure the solid curve represents the ideal jet mass flow relative to the maximum ideal mass flow as a function of collector probe position, x_p. In both cases the ideal mass flow is calculated on the basis of the minimum geometric area and a discharge coefficient of 1.0. The maximum ideal mass flow is, of course, based on the orifice diameter D_j alone. The plus symbols represent mass flow measured by collecting the fluid leaving the condenser in a tube and measuring the change in height of the fluid. The solid squares and circles are the enrichment data shown earlier. From Fig. 4-4, the main point is

- Unchanged jet membrane performance as the probe area increases is obtained with a reduction of jet mass flow.

This figure also demonstrates explicitly that significant enrichment and changes in enrichment, can occur within the thickness of the orifice plate, w.

4.2 EFFECT OF ORIFICE PRESSURE RATIO P_s/P_b

All of the small and large probe data were analyzed to see if any systematic effect of pressure ratio could be ascertained. Due to the limited data base, scatter in the data, and the fact that the experiments were not specifically designed to investigate this effect, we conclude that

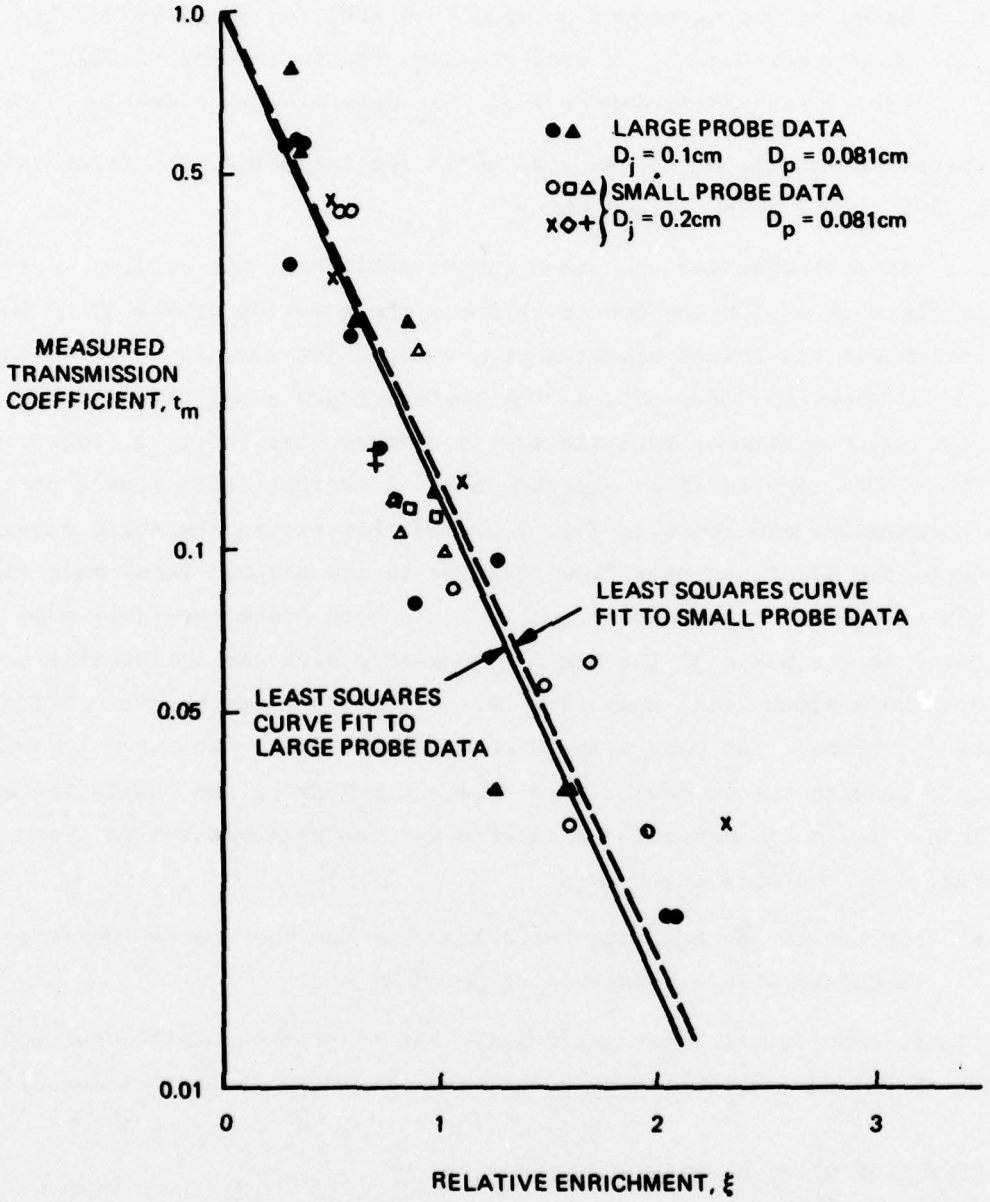

Figure 4-3. Comparison of Large and Small Cylindrical Probe Performance: SF_6 Isotopes: FC-43 Jet

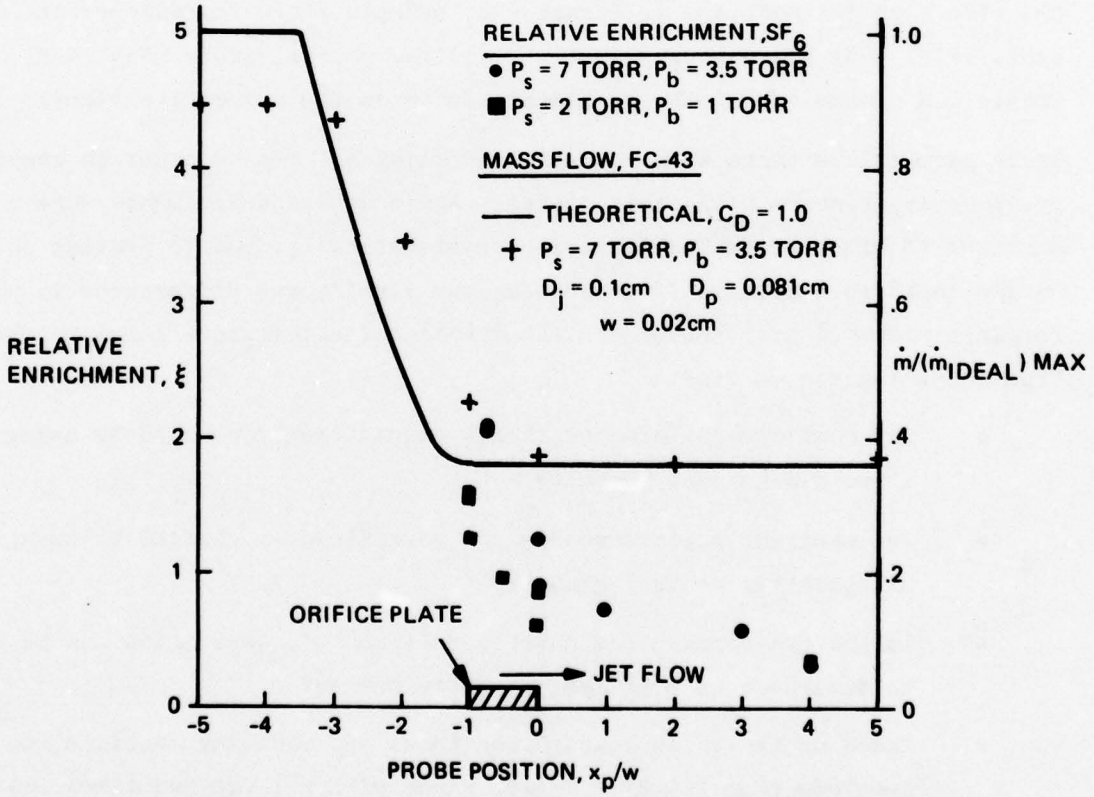

Figure 4-4. Relative Enrichment and Jet Mass Flow: SF_6 Isotopes: FC-43 Jet Large Cylindrical Collector Probe

- Within the available data, there does not appear to be any systematic effect of the pressure ratio p_s/p_b on jet membrane performance
- Performance for mixtures remains unchanged for p_s/p_b as low as 1.5.

4.3 PROBE/ORIFICE GEOMETRY

It is clear that a cylindrical collector probe is not satisfactory for an enrichment plant. First of all, for the same dimensions, a two-dimensional collector probe has a larger collector area relative to the orifice open area than does an axisymmetric collector probe In addition, it may prove easier to manufacture a two-dimensional geometry. Secondly, a cylindrical collector probe will have large internal losses. In order to reduce these losses it is necessary to open the interior of the probe to some kind of conical shape. Therefore, experiments were conducted in apparatus no. 1 in order to investigate the effect on jet membrane performance of using a large two-dimensional collector probe (Fig. 4-5) and a large axially symmetric conical probe (Fig. 4-6). The shapes and dimensions of the probes are shown on the respective figures.

These geometric effects were investigated using N_2/He-A in order to compare with previous experiments using this system. Again, these experiments were not designed to study these configurations systematically, but to provide only a "quick look" to ascertain if there were any significant differences in performance compared with the small cylindrical collector probe baseline data. From these figures we find

- Jet membrane performance is not significantly changed by using a two-dimensional geometry
- Jet membrane performance is not significantly changed by using axisymmetric conical geometry
- In the two-dimensional case (open symbols), separation can be made to disappear at high enough source pressures
- Based on the above results and those of preceding sections, we conclude that FC-43/UF_6 performance with a large two-dimensional or conical probe will not differ greatly from the measured small probe performance.

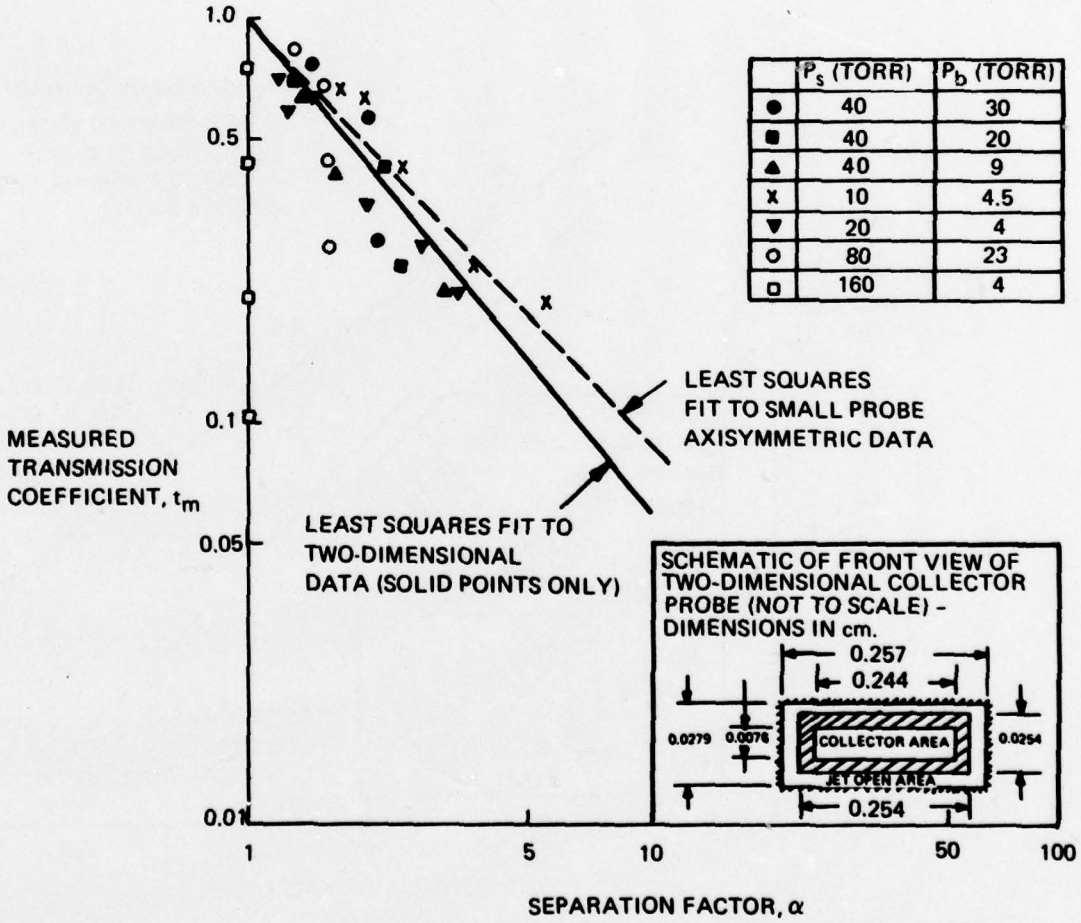

Figure 4-5. Separation of He/A: N_2 Jet: Two-Dimensional Collector Probe

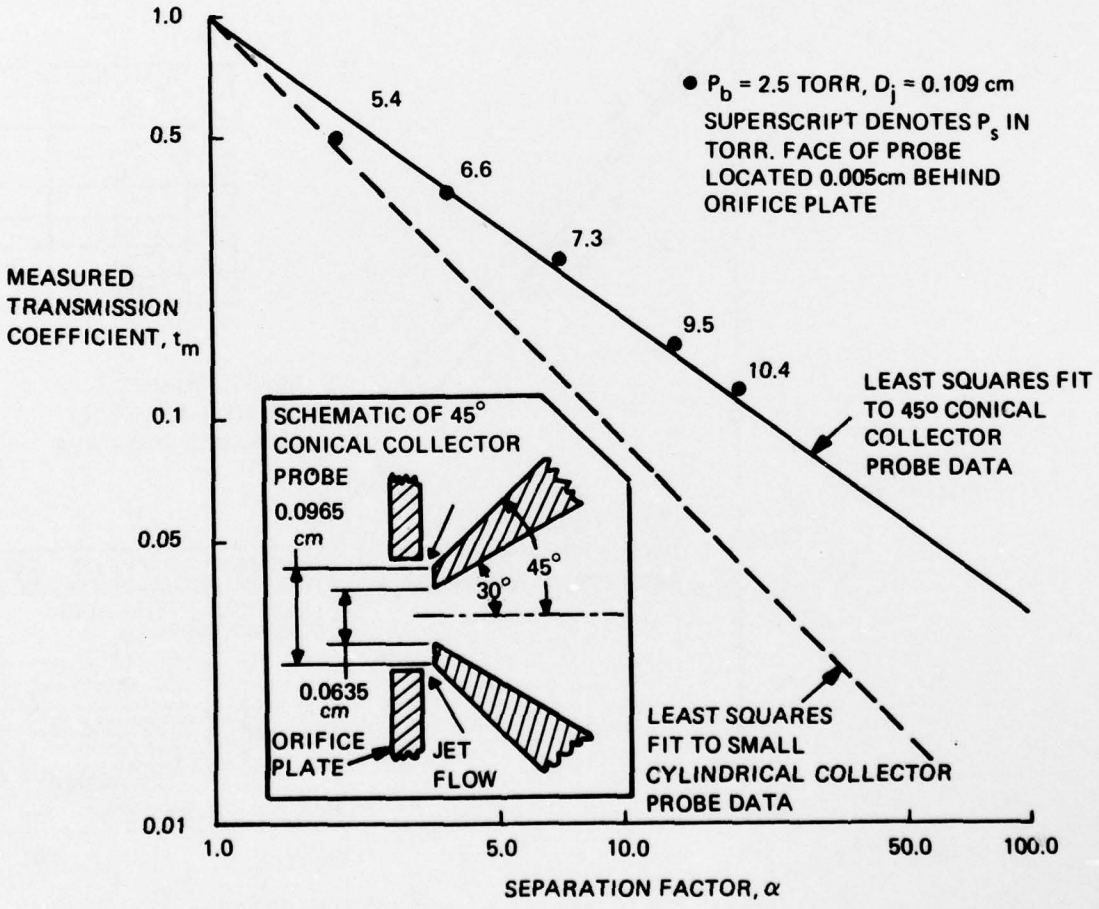

Figure 4-6. Separation of He/A: N_2 Jet: 45° Conical Collector Probe

Note that the conical probe data have been obtained at fixed probe position and background pressure by varying the source pressure. Past experience (Ref. 14) indicates that performance obtained in this manner will be identical to that obtained by fixing the pressures and moving the collector probe. Due to the limited data base, it is not clear at present whether the improved performance shown in Fig. 4-6 can always be achieved.

4.4 BACKFLOW INTO COLLECTOR PROBE

Backflow is the jet fluid which passes into the collector probe along with the process gas. Backflow can arise from jet fluid which turns the corner at the face of the collector probe or from the penetration of jet gas in the test chamber through the jet by the jet membrane penetration phenomena itself. Interest in backflow stems from two concerns: 1) the problem of handling jet fluid in the heads stream along with the process gas; and 2) the possibility of feed process gas dissolving in the jet fluid at the condenser, issuing from the orifice along with the jet, and passing into the collector probe by backflow, thus decreasing the separation of the background species.

A qualitative assessement of the amount of jet backflow has been made using FC-43/SF_6 and a large cylindrical collector probe. The results of this experiment are shown in Figs. 4-7 and 4-8. In Fig. 4-7, the ordinate represents the relative ion current in the mass spectrometer of both $^{32}SF_6$ and FC-43 in the upflow. For SF_6, the ion current is normalized by the jet off signal so that the SF_6 data are simply the measured transmission. For FC-43 the ion current has been normalized by the signal at $x_p/w = -18$, i.e., for the collector probe withdrawn well into the stagnation chamber. These data are then equivalent to the backflow flux relative to the flux through the collector probe from a static FC-43 supply at stagnation pressure. Figure 4-7 shows that the backflow increases as the transmission decreases.

In Fig. 4-8 measurements of the initial rate of rise of pressure, P_c, in the collector chamber, normalized to the same quantity with the jet-off, are shown as a function of the collector probe position. The measurements were obtained, with a barotron manometer, by closing the isolation valve that is located between the collector chamber and the mass spectrometer (see Fig. 6-4). Since the rate of rise of pressure is proportional to the flux into the collector chamber, the near constancy of this quantity with probe position indicates that the total flux (FC-43 + SF_6) into the collector probe is nearly constant. Therefore, from Figs. 4-7 and 4-8 we conclude:

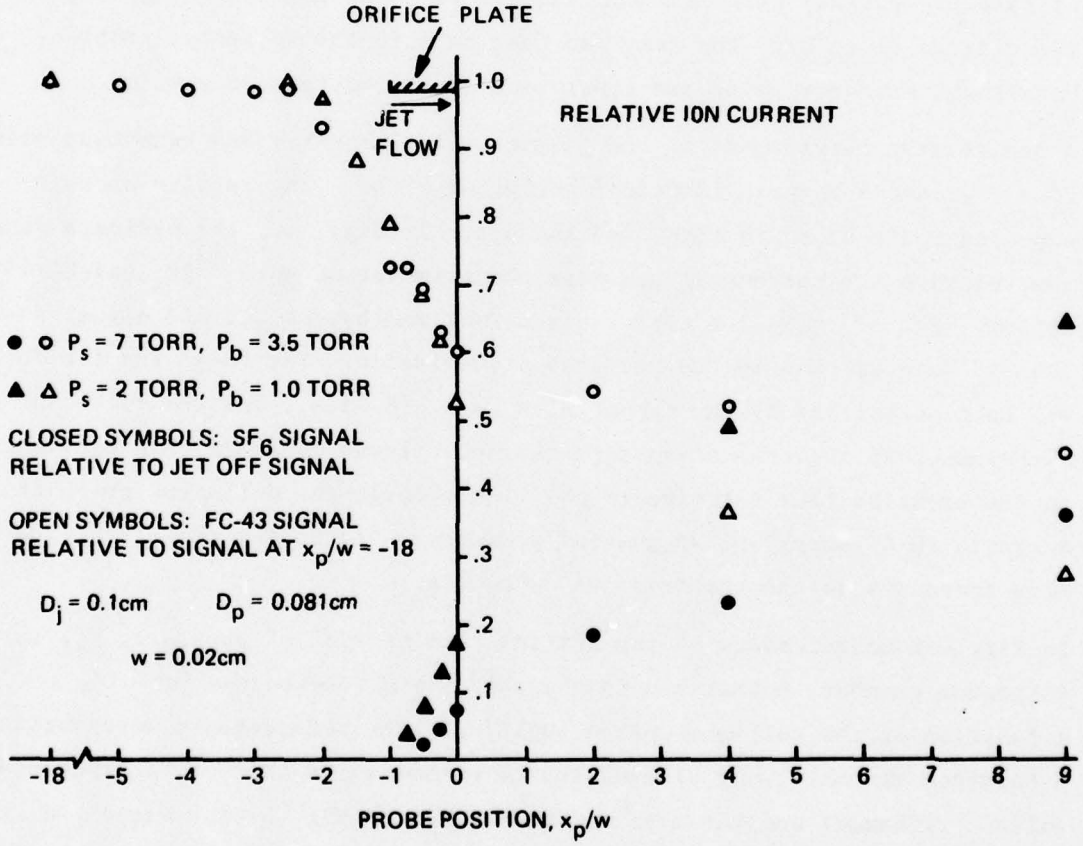

Figure 4-7. Variation of Jet Backflow and Process Gas Upflow with Probe Position: SF_6/FC-43: Large Cylindrical Collector Probe

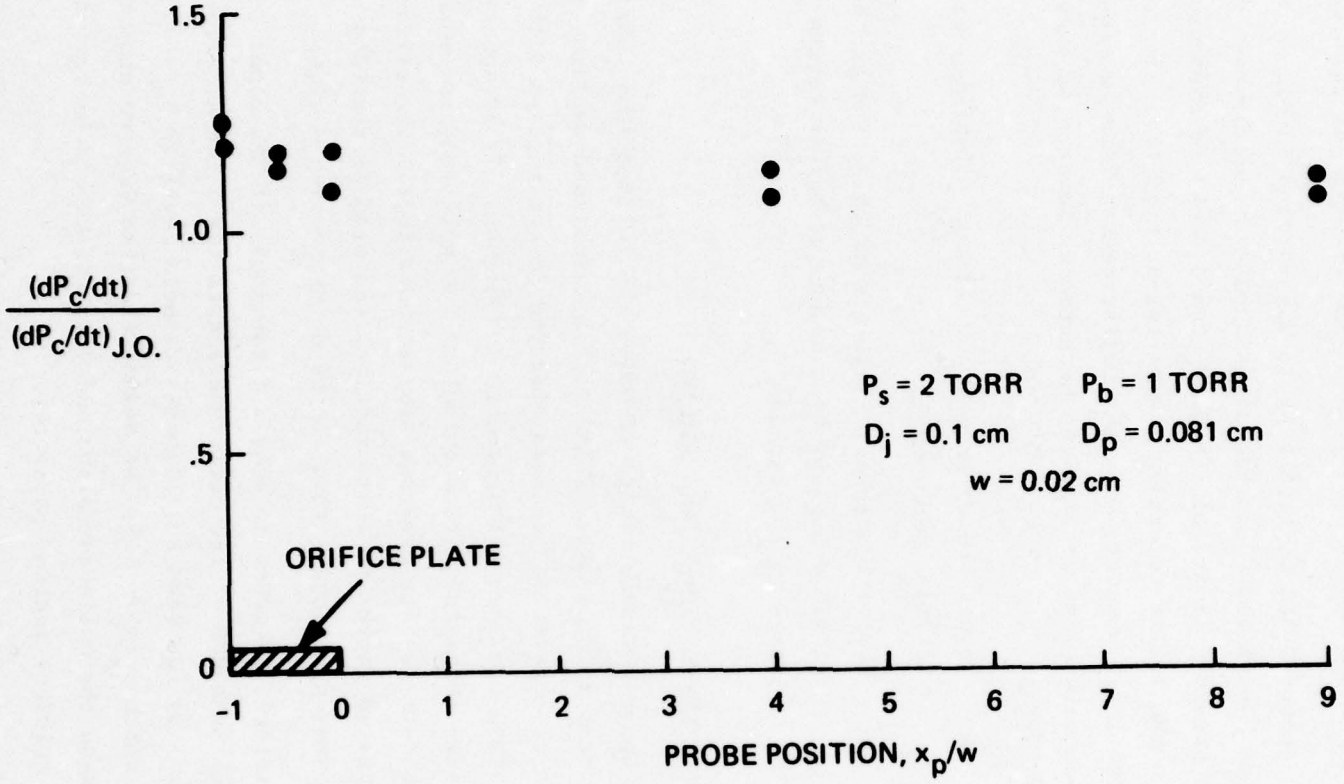

Figure 4-8. Rate of Rise of Collector Chamber Pressure vs Probe Position: SF_6: FC-43 Jet: Large Cylindrical Collector Probe

- The backflow of jet fluid into the collector probe increases as the transmission of process gas decreases in such a way as to keep the total collected flux nearly constant.

We shall see in Section 4.6 that this increase in backflow can be used to increase the suction pressure of the process gas upflow.

The second point (solubility) is illustrated in Fig. 4-9. This was a single point "quick look" experiment in apparatus no. 3 whose purpose was to investigate the pressure limits of FC-43/SF_6 small probe performance. As can be seen, with the boiler return on the performance is severely reduced due to solubility; however, when the boiler return line is closed, the performance becomes very close to what was measured at lower pressures. This leads to the conclusion

- As the pressure level is raised, solubility can become a factor in limiting performance
- However, sclubility effects of this kind can be eliminated in an enrichment plant by routing the boiler return line to a different stage in the cascade.

4.5 PRESSURE LIMITS AND SCALING

The upper pressure limits at which the jet membrane continues to perform have not been studied systematically. As mentioned earlier, in some configurations loss of separation has been observed in conjunction with oscillating signals and this has been attributed to turbulence. It is apparent that the increased mixing associated with a turbulent jet will tend to reduce or completely eliminate the jet membrane separation effect. The effect of solubility, as discussed in the previous section, can also be regarded as a pressure-limiting phenomenon; however, this can be eliminated by design.

Therefore, in order to make a first guess at the upper limit on pressure we shall make use of the performance data for N_2/He-A. From Fig. 4-1 (largest probe) we see that the highest pressure level is p_s = 55 torr, p_b = 34 torr, for which $p_s/p_b \sim 1.5$. We assume that the Knudsen number, based on gap width between the collector probe and jet orifice and background-jet collisions, is the relevant scaling parameter.

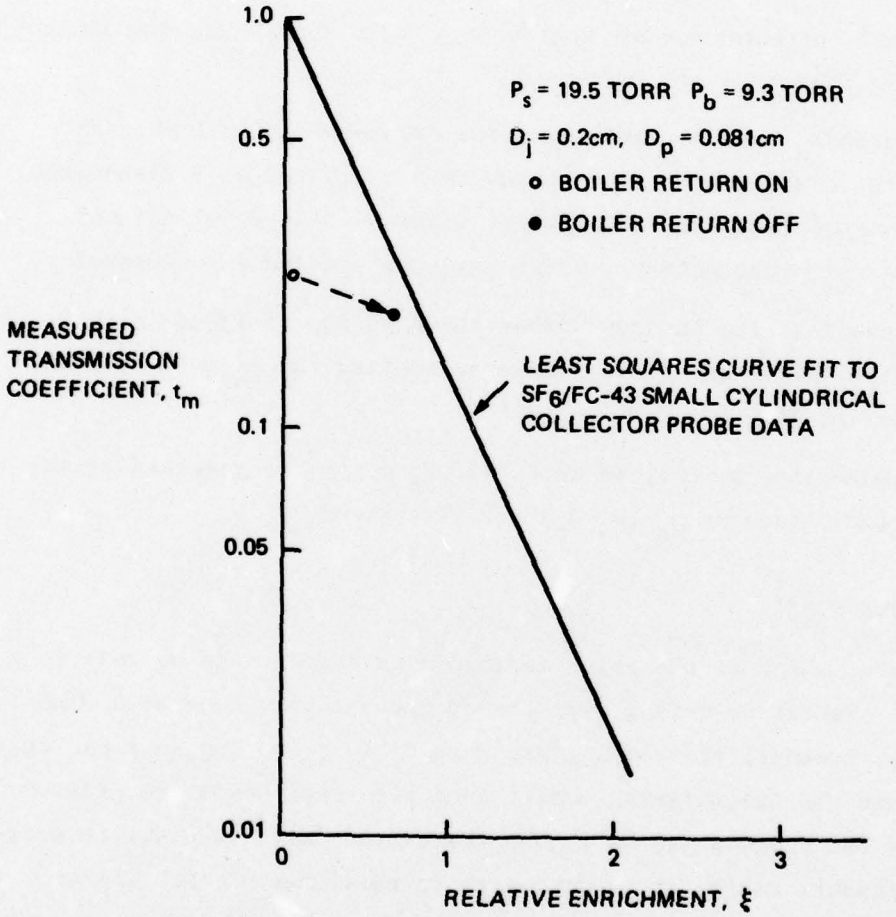

Figure 4-9. Effect of Solubility on Separation of SF_6 Isotopes: FC-43 Jet: Small Cylindrical Collector Probe

$$K_{n_{bj}} = \frac{\lambda_{bj}}{D_j - D_p} \sim \frac{1}{P_s \Omega_{bj} (D_j - D_p)} \qquad (4\text{-}1)$$

where λ_{bj} is the mean free path of background-jet collisions and Ω_{bj} is the appropriate cross-section. Using the applicable dimensions shown in Fig. 4-1 and viscosity cross-sections for UF_6, FC-43, N_2, He and A, we can use Eq. (4-1) to estimate the corresponding source pressure for FC-43/UF_6 for the similar large cylindrical collector probe geometry shown in Fig. 4-4. This pressure is approximately p_s = 21 torr, which is close to the value shown in Fig. 4-9 for FC-43/SF_6. Therefore, as far as limitations on the pressure levels are concerned

- A systematic study of the upper limits of pressure for which reasonable jet membrane performance is obtained has not been made; however, performance has been observed to degrade in some cases as the pressures are increased.
- Based on N_2/He-A performance and a cross-collisional Knudsen number, a value p_s = 21 torr has been estimated as a reasonable stagnation pressure for FC-43/UF_6, using a large cylindrical collector probe geometry which has been studied experimentally.

Now, if we assume that the Knudesn number shown in Eq. (4-1) can also be used to relate physical size and source pressure, we find for p_s = 21 torr and the dimensions shown in Fig. 4-4.

- Pressure-size scaling in an FC-43/UF_6 system is governed by the scaling parameter $p_s (D_j - D_p)$ = 0.42 torr-cm.

4.6 SUCTION PRESSURE

Suction pressure, which is the major capital cost driver, can be raised by increasing the overall operating pressure of the sytems. Even at a higher pressure level, however, the pumping pressure ratio p_h/p_ℓ ($\sim p_b/p_\ell$) can still be large because the transmission coefficient also represents the pressure drop experienced by the process gas as it penetrates the jet. In order to decrease the pumping pressure ratio, it is necessary to raise the partial pressure of the process gas between the entrance to the collector probe and the mechanical pump to the next stage. A concept to achieve this, called partial pressure condensation pumping*, has been proposed and preliminary experiments to test this concept have been performed.

---

*Patent applied for.

Briefly, the idea behind the partial pressure condensation pump (PPCP) is the following. As can be seen from Fig. 4-8 the total flux (process gas plus jet gas) into the collector probe is not sensitive to probe position. The inference from this is that the effective total pressure (process gas plus jet gas) at the face of the collector probe is nearly constant. Therefore, as the transmission of the process gas decreases, its partial pressure decreases relative to the partial pressure of the jet fluid collected due to backflow (Fig. 4-7). Then, if the jet fluid is condensed downstream of the collector probe, and the partial pressure of the process gas is allowed to rise by throttling the outlet from the collector probe to match the mass flow of the process gas into the probe, it should be possible to recover a significant fraction of the total pressure that exists at the probe face. The resulting pressure is now produced almost entirely by process gas and is the suction pressure that would exist at the inlet to the pump to the next stage.

In order to verify this phenomenon, experiments have been performend using CO_2 as a jet gas to separate a He-A mixture. These experiments were carried out in a modified version of apparatus no. 1. A schematic of the experimental setup is shown in Fig. 4-10. In this apparatus, the upflow (CO_2/He-A mixture) was passed to the PPCP, which utilized LN_2 to condense the CO_2. The pressure of the collected He-A mixture was regulated by the throttle valve downstream of the PPCP. Separation factors and the low pressure in the system, p_ℓ, were measured by the mass spectrometer and pressure gauge located downstream of the PPCP. Results of the experiment are shown in Fig. 4-11.

The ordinate in Fig. 4-11 is the ratio of the measured separation factor α divided by the separation factor $\alpha(0)$ taken with the suction (low) pressure $p_\ell \sim 0$, i.e., the normal experimental conditions. The abscissa is the ratio of p_ℓ to the background pressure p_b. From an inspection of Fig. 4-11, we conclude

- The partial pressure condensation pumping concept works
- Suction pressures on the order of 20% of background pressure have been demonstrated without a loss in separation as compared with the normal experimental results ($p_\ell \sim 0$).

There was an estimated 20-30% pressure drop between the collector chamber and the gauge that was used to measure p_ℓ. Most of this can be eliminated in a properly designed system so that a value $p_\ell/p_b \sim 0.25$, i.e., an interstage compression ratio of 4 can probably be achieved without difficulty. The latter number has been used as input to the economic model.

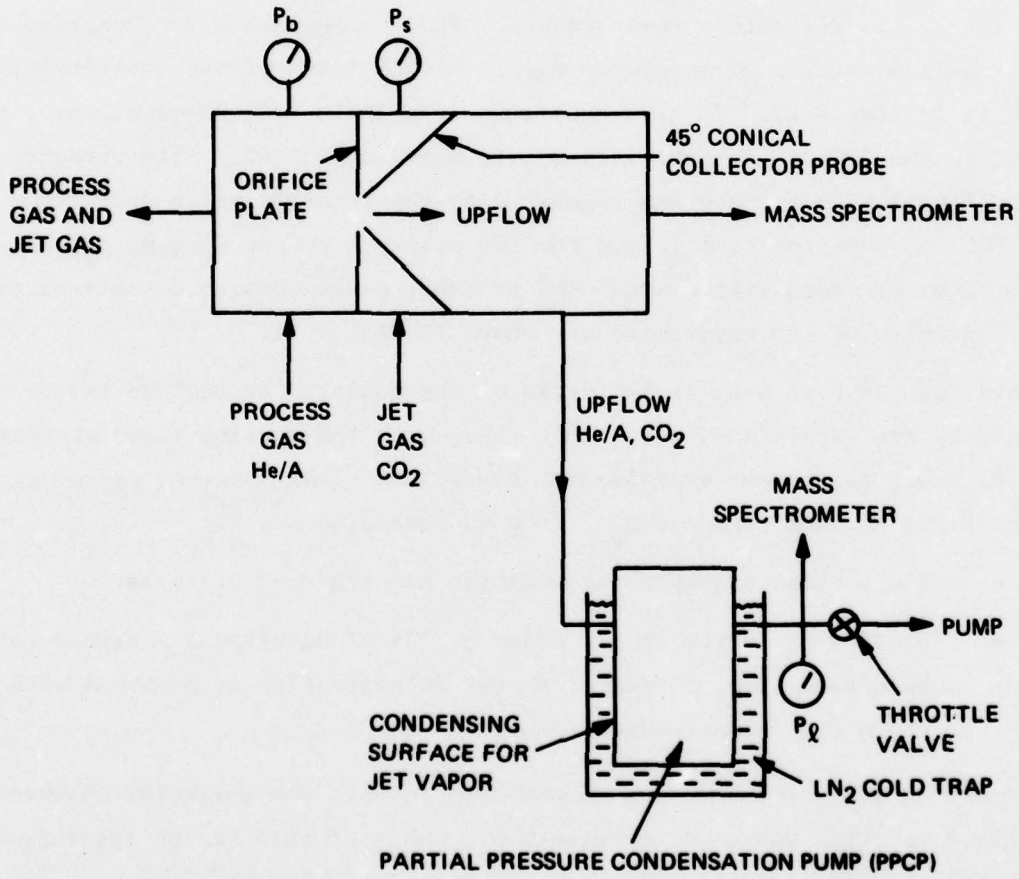

Figure 4-10. Partial Pressure Condensation Pumping Experiment: Schematic

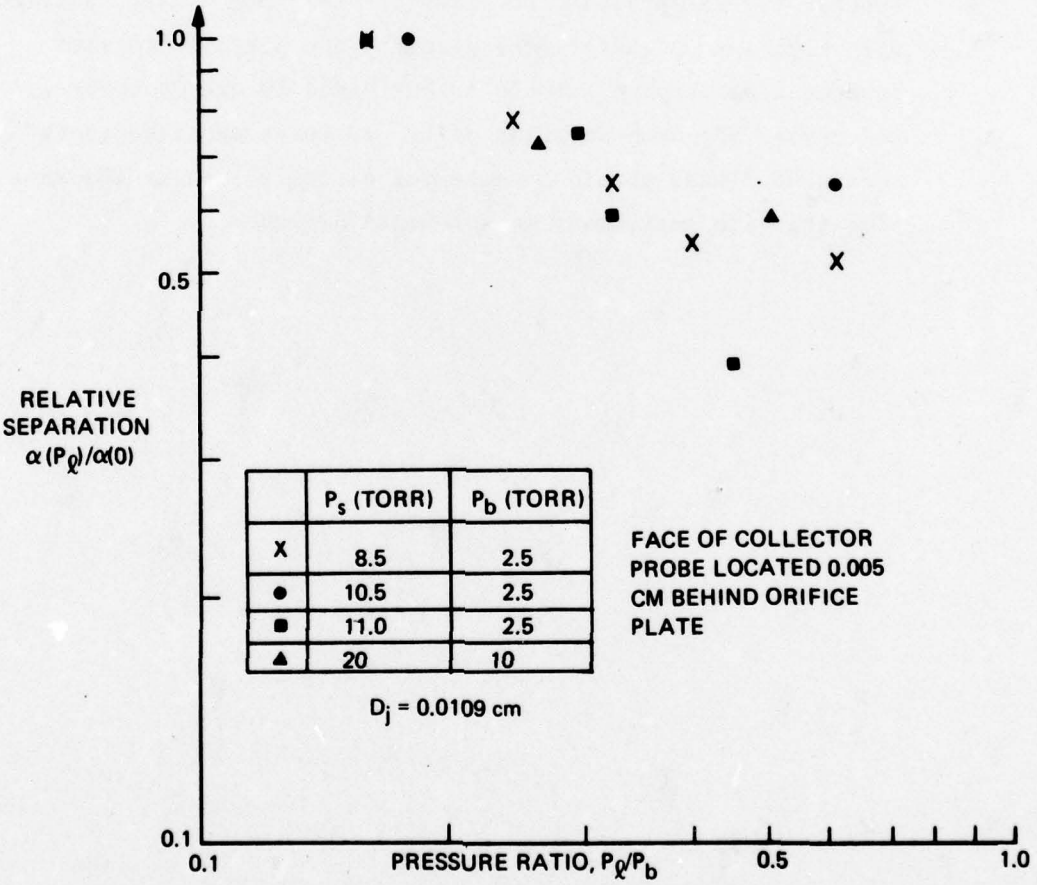

Figure 4-11. Effect of Suction Pressure on He/A Separation: CO_2 Jet: 45° Conical Collector Probe: Partial Pressure Condensation Pumping

4.7 CONCLUSIONS

The results of this section are the primary source of process parameter input to the economics model. As has been shown, in some sense each of the values used in Section 2 have been demonstrated experimentally (with the exception of dependence on actual physical size). However, many of these numbers have been generated by inference and transferability to UF_6 remains to be demonstrated unambiguously. Therefore, we may conclude from the results of this section

- Each of the numerical values of process parameters used as input to the economics code (except actual size) have been demonstrated experimentally
- Some of the data were generated in nonisotopic systems and transferability to UF_6 is by inference
- Further experiments with at least an FC-43/SF_6 system, particularly with regard to probe/orifice geometry and partial pressure condensation pumping, should be performed before proceeding to a multistage UF_6 demonstration unit. In these experiments the pertinent fluxes should be measured directly, and at the same time that the enrichment measurements are made.

SECTION 5
THEORETICAL CONSIDERATIONS

In this section we shall briefly outline the theoretical modeling of the jet membrane that has been done to date and indicate the degree of agreement between the models and experiment. In the previous sections we have been concerned primarily with experimentally determined jet membrane performance, i.e. transmission vs enrichment. In this section we shall also address the details of the process, and the variation of transmission and enrichment with collector probe position. The primary considerations of this section will be threefold: 1) are theory and experiment in agreement, at least qualitatively? 2) do we have some understanding of any quantititive differences? and 3) is the available information useful for extrapolating to a full scale UF_6 system? It should be kept in mind, however, that the experiments were not designed to test a particular theory, but were performed for the purpose of process development. Therefore, the information available is not as complete as would be if the former were the purpose.

This section is divided into two topics: small cylindrical collector probe and large cylindrical collector probe (see Section 6.1.1 for a discussion of probe geometry). The small collector probe results refer to configurations where the probe is primarily a diagnostic tool and does not occupy a significant fraction of the orifice area. The large collector probe results refer to configurations where the collector probe occupies a significant fraction of the orifice area. Therefore, in the latter case, the probe is not only representative of a possible economically attractive configuration, but also creates a large disturbance to the jet flow.

Most of the small collector probe theoretical results have been presented in some detail in Ref. 1. Only that which is required for the discussion herein will be repeated in the following discussion. Similarly, although the large collector probe modeling is new, only a skeleton outline is presented.

The basic conclusions we draw from this section are

- Regardless of the particular probe/orifice geometry we have studied theoretically or experimentally, jet membrane performance for isotopes appears to be exponential, i.e., the transmission is an exponentially decreasing function of the level of enrichment
- We have a reasonable understanding of the physics underlying the jet membrane process although we are unable at present to predict the fine structure. This is because our models are too simplistic and also because the experiments performed were not designed to test theory systematically. Qualitatively, however, the models and experiments are in agreement.
- Theoretically, there are not large differences in performance between FC-43/UF_6 and FC-43/SF_6 systems. This provides further justification for transferring FC-43/SF_6 data to a full scale configuration
- Large collector probe attenuation data for FC-43/SF_6 taken at a pressure ratio $p_s/p_b = 1.5$ are qualitatively similar to data taken at $p_s/p_b = 2.0$. From this we conclude that it is reasonable to expect the same performance at a pressure ratio of 1.5 as was obtained at a pressure ratio of 2.

5.1 SMALL COLLECTOR PROBE CONFIGURATION

5.1.1 Gas Dynamics Regimes

The idea for using the jet membrane for separating isotopes originated with a rarefied jet-background interaction model developed by Muntz, Hamel and Maguire (MHM) (Ref. 15). The original jet membrane economic predictions were based upon this model. It rapidly became apparent, however, that the economics of the jet membrane process for enriching uranium required higher pressure levels and lower jet/background pressure ratios when applied under rarefied conditions. Experiments were then performed which showed that the basic separation effect persisted to higher pressures. A continuum (diffusion) model was also developed which showed that, on theoretical ground, the separation effect should persist at higher pressures and lower pressure ratios. Based on a rarefaction parameter developed in Ref. 16, we depict in Fig. 5-1 the regimes in which these solutions apply. Again, further details may be found in Ref. 1.

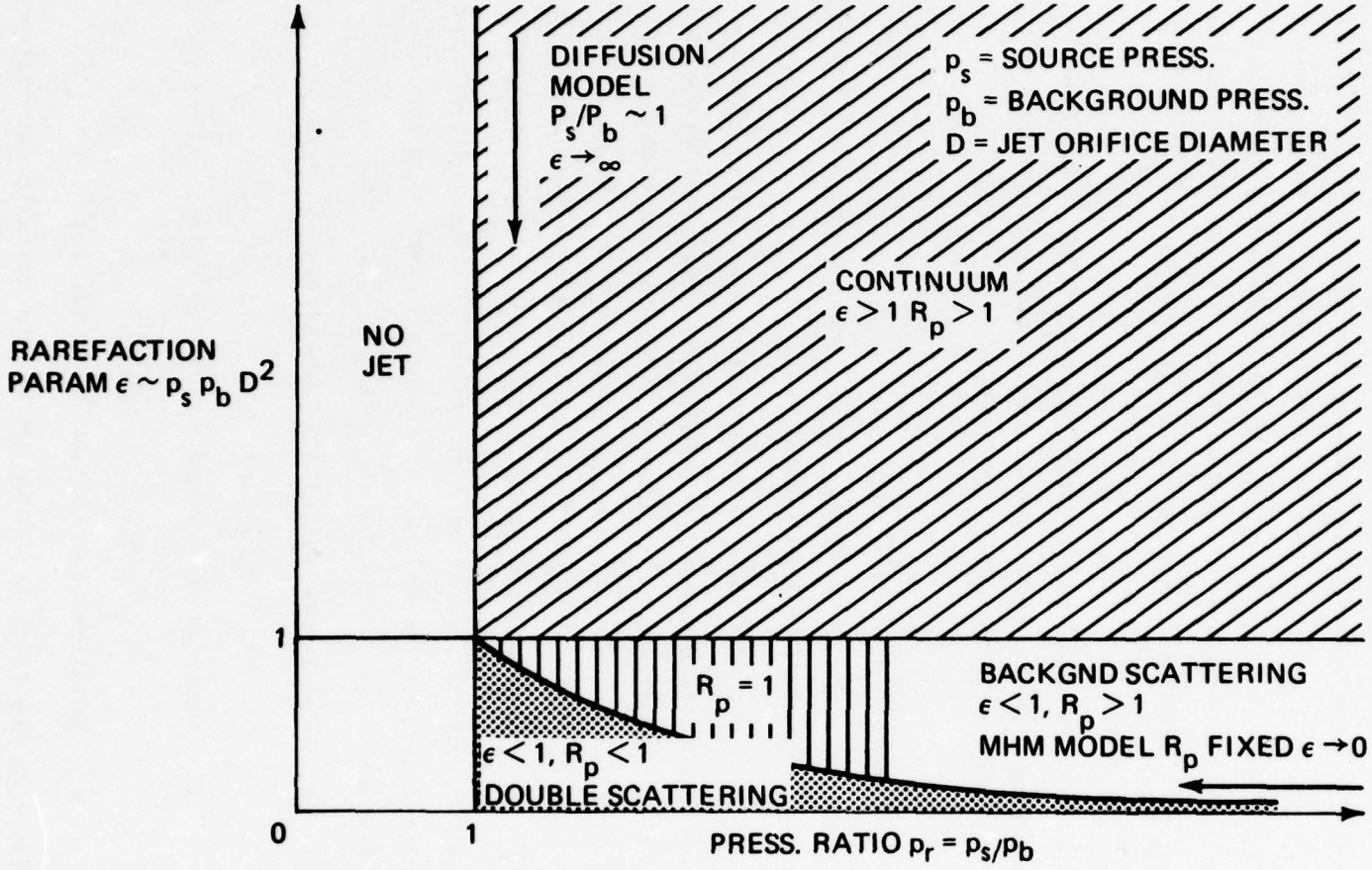

Figure 5-1. Jet Membrane Gas Dynamics Regimes

The ordinate in Fig. 5-1 is the rarefaction parameter ϵ which is proportional to $p_s p_b D_j^2$; the abcissa is the pressure ratio p_s/p_b. As indicated earlier, the rarefied model (background scattering; MHM) occupies the lower right corner of this figure; $\epsilon < 1$ roughly indicates a rarefied interaction. The diffusion model, on the other hand, occupies the upper left hand corner of the figure; in particular, it applies for a fixed pressure ratio close to one (taken here as identically one). In both of these areas separation has been demonstrated both experimentally and theoretically. Furthermore, for large ϵ and large p_s/p_b, a combination of contiuum (diffusion) and rarefied separation effects should apply.

From this we conclude, by extrapolation, that separation should be expected everywhere in parameter space except, perhaps, in the limit $\epsilon \to p_s/p_b$ fixed ~1. This limit will be commented on later.

5.1.2 Rarefied (MHM) Model

A schematic of the rarefied, or MHM, separation model is depicted in Fig. 5-2. The main features of this model are:

- The jet plume is represented as a source flow
- Collisions are treated on an individual basis (scattering)
- Boltzmann type kinetic equations are used
- Jet velocity = V_{max} = maximum adiabatic velocity
- Background particle velocity = $\bar{c}_b$ = mean thermal speed
- Separation of species is calculated by superposition

The solution of the kinetic equations is presented approximately in Ref. 1 and more rigorously in Ref. 17. The major features of the rarefied model are as follows:

- Two length scales are identified

$$R_p \sim p_s D_j^2 \quad , \quad R_\infty \sim 1/p_b$$

- Rarefaction parameter ϵ is the ratio of these scales

$$\epsilon = R_p/R_\infty \sim p_s p_b D_j^2$$

- Solution is valid for R_p fixed, $\epsilon \to 0$.

Based on the limit indicated above, the approximate solution has the following properties

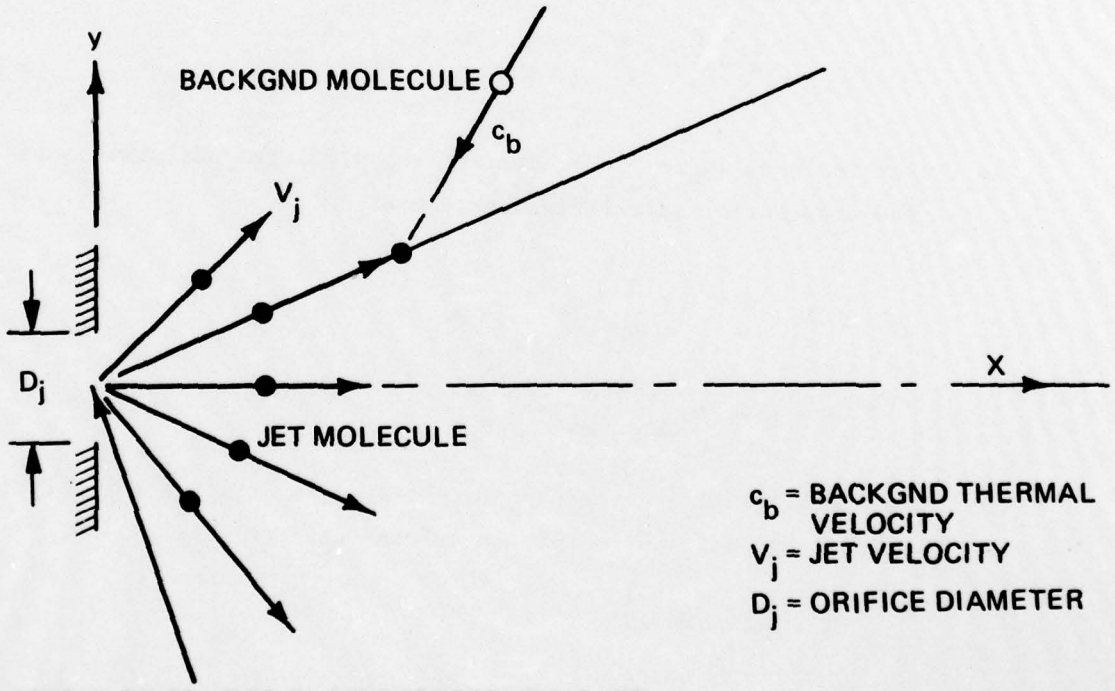

Figure 5-2. Rarefied (MHM) Model

- The distribution of background species number density on the centerline of the jet is exponential in inverse probe position, x_p

$$n/n_b = \exp\ (-R_p/x_p) \tag{5-1}$$

The value of n/n_b for the light species (L) is defined as the transmission coefficient t_{JM}

$$t_{JM} = (n/n_b)_L \tag{5-2}$$

- By superposition, large separations of light (L) and heavy (H) species are possible ($R_{pH} > R_{pL}$, in general)

$$\alpha = (n/n_b)_L/(n/n_b)_H = \exp\left(\frac{R_{pH}-R_{pL}}{x_p}\right) \tag{5-3}$$

where α is the separation factor.

- Jet membrane performance (transmission vs separation) in general is algebraic

$$t_{JM} = \alpha^{\left(\frac{R_{pH}}{R_{pL}} - 1\right)} \tag{5-4}$$

- For isotopes ($m_H/m_L \sim 1$) however, the predicted performance is now exponential in relative enrichment

$$t_{JM} = \exp\left(-\frac{\xi}{\bar{s}}\right)$$

$$\xi = (\alpha-1)/e_{GD}\ ;\ e_{GD} = \sqrt{\frac{m_H}{m_L}} - 1 \tag{5-5}$$

- The coefficient $\bar{s}$ depends primarily on m_j/m_H through the relative velocity of jet and background collisions (see Ref. 1)

$$\bar{s} = \frac{(R_{pH}/R_{pL})-1}{e_{GD}} \tag{5-6}$$

- For isotopes, relative enrichment is proportional to inverse probe position

$$\xi = \bar{s}\ \frac{R_{pL}}{x_p} \tag{5-7}$$

- The model addresses jet effects only - the actual collection process and collector probe effects are not accounted for. All particles which reach the axis are assumed to be collected.

5.1.3 Continuum (Diffusion) Model

The features of the diffusion separation model are depicted in Fig. 5-3. The major features of this model are

- Jet is a cylinder of fluid with a constant velocity equal to sonic velocity (mixing ignored)
- Background species penetrate jet by transverse diffusion (heat conduction equation)
- Separation of background species is calculated by superposition
- Assumption of diffusion is equivalent in some sense to Chapman - Enskog solution of Boltzmann equation (in our notation p_s/p_b fixed ~ 1, $\varepsilon \to \infty$).

The major features of the solution are (details may be found in Ref. 1):

- Species distribution on the centerline for small values of the probe position, x_p, is exponential in inverse probe position

$$n/n_b \cong \exp\left(-\frac{D_j^2 V_j}{16 \mathcal{D}_{bj} x_p}\right) \tag{5-8}$$

V_j = jet velocity; $\mathcal{D}_{bj}$ = diffusion coefficient of each species into jet.

- From elementary kinetic theory this result is remarkably similar to rarefied result

$$\frac{\mathcal{D}_{bj}}{D_j^2 V_j} \sim \frac{1}{R_p} \sim \frac{1}{p_s D_j^2} \tag{5-9}$$

Therefore

$$n/n_b \sim \exp\left(-R_p/x_p\right)$$

- Performance and enrichment results will also be identical in form to rarefied result

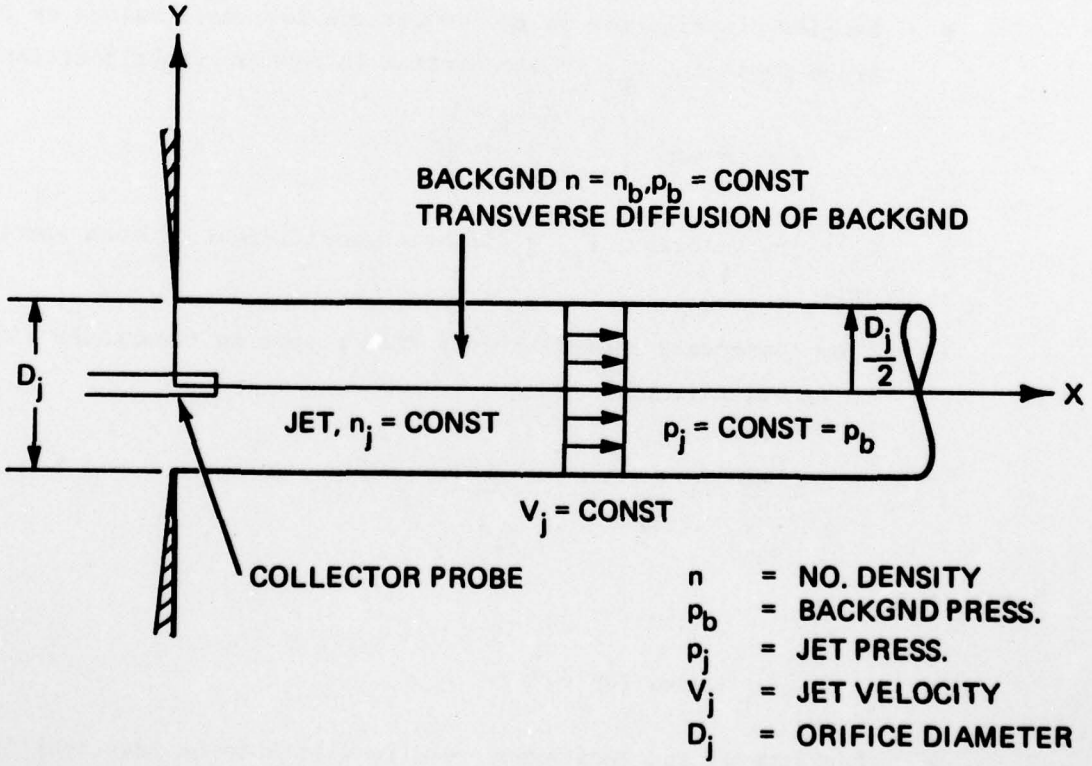

Figure 5-3. Continuum Diffusion Model

$$t_{JM} \sim \exp\ (-\xi/\bar{s}) \quad ; \quad \xi \sim 1/x_p \tag{5-10}$$

- Separation is also predicted to occur in the two-dimensional case (Ref. 1) where jet is represented as a slab (solution cannot be represented analytically as in Eq. (5-8). Two-dimensional rarefied solution has not been worked out
- Again, the model addresses jet effects only; the actual collection process is not addressed.

5.1.4 Analysis of Performance Data

A comparison of calculated performance for both rarefied and continuum solutions are presented in Fig. 5-4 for both FC-43/SF_6 and FC-43/UF_6. In this figure the full diffusion solution has been employed. From Fig. 5-4 we draw the following conclusions concerning performance:

- Predicted continuum and rarefied performance is quantitatively similar for both gas pairs
- FC-43/SF_6 and FC-43/UF_6 performance is quantitatively similar and SF_6 performance results should be transferable to UF_6 for the small probe configuration.

As was shown earlier in Section 3, the performance data for SF_6 and UF_6 can be represented quite reasonably by exponential curve fits. Comparison between these curve fits and a simplified version of the MHM model is shown in Fig. 5-5. The simplified MHM model is used here because analytical results can be obtained. The simplification comes from expressing the relative velocity of jet background collisions, $\bar{V}_{bj}$, as

$$\bar{V}_{bj} = V_j + \bar{c}_b \tag{5-11}$$

Using Eq. (5-11), and neglecting isotopic cross section differences, the parameter $\bar{s}$ can be expressed

$$\bar{s} = \frac{V_j/\bar{c}_L}{1+V_j/\bar{c}_L} \tag{5-12}$$

In the original MHM formulation (Ref. 15) V_j was taken as the maximum adiabatic velocity V_{max}

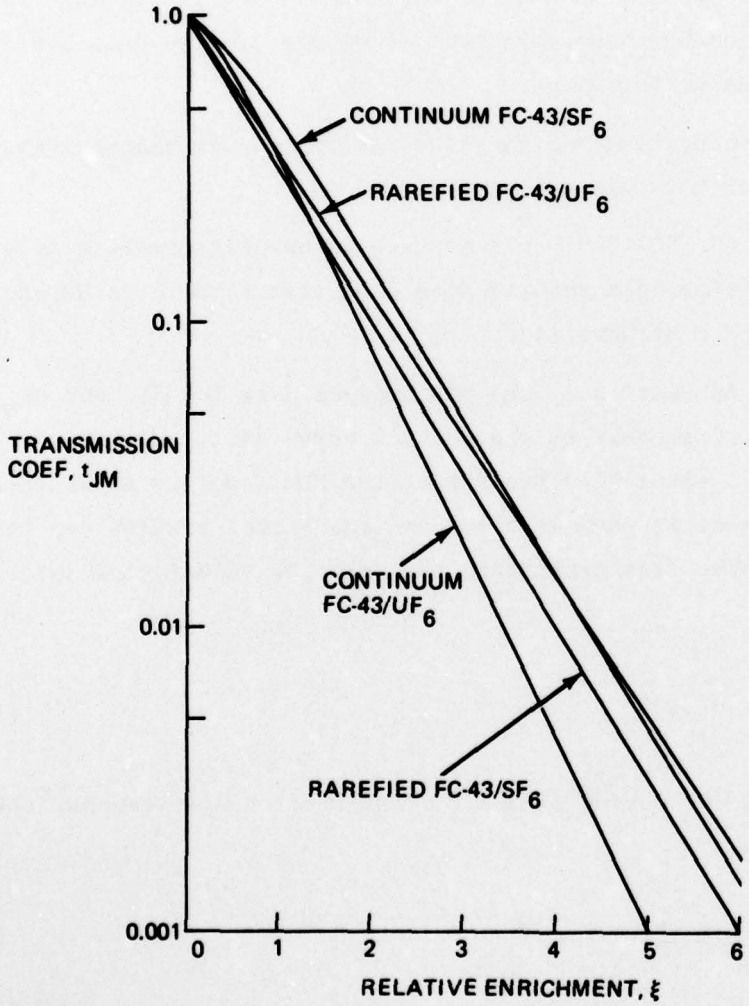

Figure 5-4. Predicted Rarefied and Continuum Performance

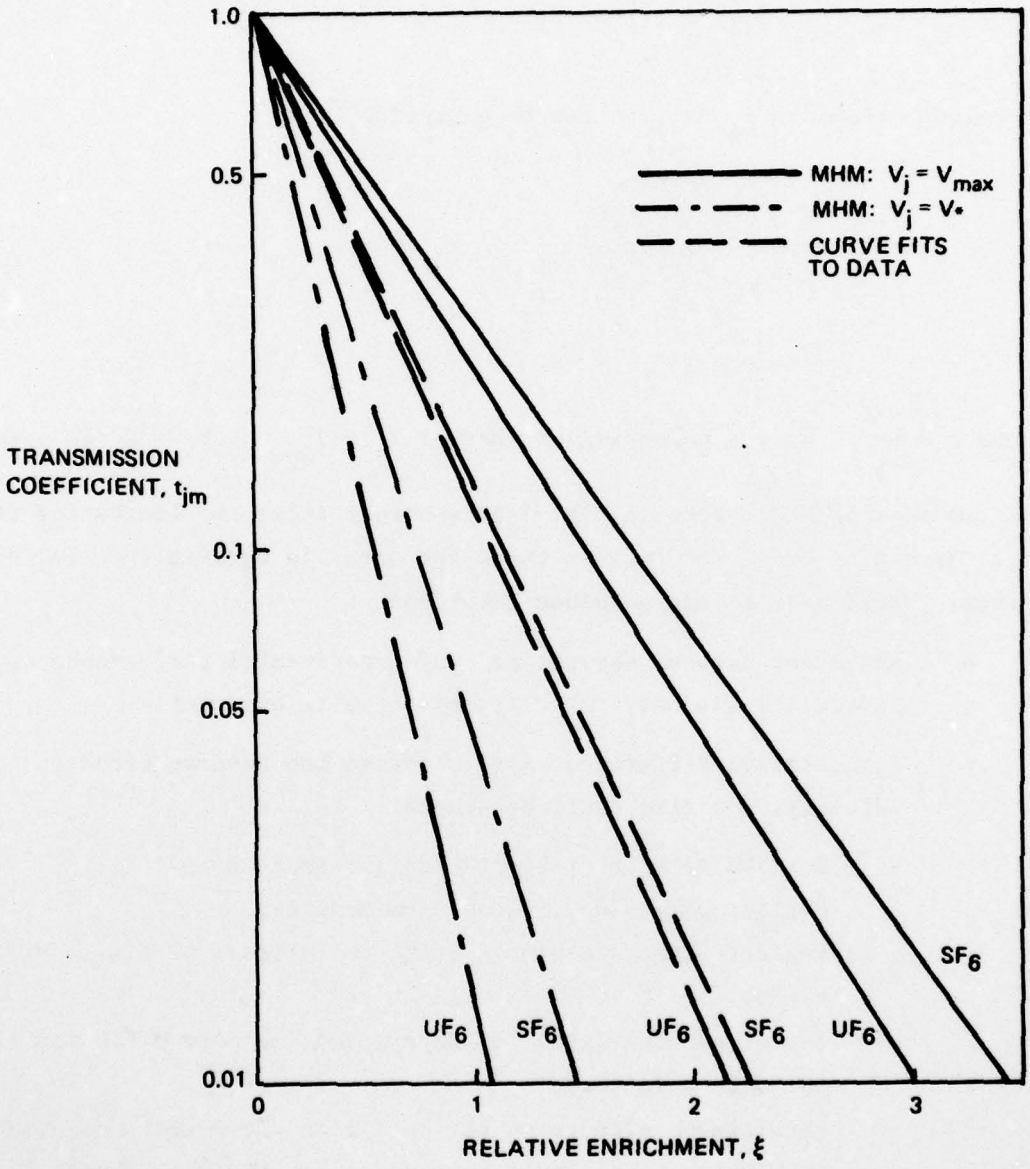

Figure 5-5. Comparison of Predicted and Experimental Performance: SF_6 and UF_6 Isotopes: FC-43 Jet: Small Cylindrical Collector Probe

$$V_{max} = \sqrt{\frac{2\gamma_j}{\gamma_j - 1} \frac{kT_s}{m_j}} \qquad (5\text{-}13)$$

However, at the lower pressure ratios at which the experiments were performed, the jet will not expand to V_{max}. A lower bound to the jet velocity is sonic velocity, V_*,

$$V_* = \sqrt{\gamma_j \frac{kT_s}{m_j}} \qquad (5\text{-}14)$$

Therefore, assuming $T_s = T_b$, $\bar{s}$ can be expressed

$$\bar{s} = \frac{\sqrt{\frac{\pi c}{8} \frac{M_L}{M_j}}}{1 + \sqrt{\frac{\pi c}{8} \frac{M_L}{M_j}}} \qquad (5\text{-}15)$$

where $c = \frac{2\gamma_j}{\gamma_j - 1}$ or γ_j, depending on whether $V_j = V_{max}$ or $V_j = V_*$ is assumed.

The two sets of MHM curves in Fig. 5-5 represent these two limits for SF_6 and UF_6. As can be seen, the curve fits to the data lie between the theoretical curves. Therefore, we can conclude only that

- Agreement between theoretical and experimental performance curves is qualitative only; both are essentially exponential
- Quantitative differences may be due to the unknown effective jet velocity, but also could be due to:
  - Unknown details of the collection process
  - Neglect of mixing in continuum modeling
  - Neglect of actual plume structure (effects of finite pressure ratio)
  - Use of superposition for separation (ternary diffusion effects could be a factor)
  - Persistence effects on the collision cross-sections associated with the complicated structure of the FC-43 molecule.

5.1.5 Analysis of Transmission and Enrichment Data

As described above, in both the rarefied and continuum models, the transmission is exponential in inverse probe position. In Figs. 5-5 and 5-6 we have plotted the measured transmission (t_m) coefficient vs D_j/x_p for both the FC-43/SF_6 and FC-43/UF_6 systems. In spite of the relatively small data base, we can conclude the following from these figures

- Both FC-43/UF_6 and FC-43/SF_6 transmission is exponential in D_j/x_p
- UF_6 dissolving in FC-43 at the condenser and returning to the collector probe by means of backflow from the jet effects the slope of the transmission data. As with the SF_6 data shown in Fig. 4-9, this effect was eliminated by shutting off the boiler return line.

The solid and dashed lines in Figs. 5-6 and 5-7 are least squares fits to the transmission data of the form

$$t_m = A \exp\ (-R_p'/X_p) \quad ; \quad X_p = x_p/D_j \tag{5-16}$$

In Fig. 5-8, the values of R_p' are plotted as a function of p_s (the value of R_p' at $p_s \sim 4.7$ torr for FC-43/SF_6 came from a single data point not shown in Fig. 5-6). From this figure we see

- In both systems, in the absence of the effects of solubility, R_p' is a linear function of p_s
- The lines of R_p' vs p_s do not pass through the origin as predicted (Eq. 5-8).

It is not clear why the lines of R_p' vs p_s do not pass through the origin. It should be noted, however, that this extrapolation is equivalent to the limit $\epsilon \to o$, p_s/p_b fixed, alluded to earlier, which has not yet been modeled. Hence, it is possible that R_p' remains finite as $p_s \to o$ in this limit.

In Figs. 5-9 and 5-10, relative enrichment ξ is plotted vs D_j/x_p for FC-43/SF_6 and FC-43/UF_6. The solid and dashed lines are curve fits to the data. From these curves

- For both FC-43/SF_6 and FC-43/UF_6 relative enrichment is reasonably linear in D_j/x_p, as predicted.

As stated in Section 3, the effect of solubility on UF_6 enrichment was not investigated because it was not possible to operate with the boiler return off for the long periods of time necessary to collect adequate samples.

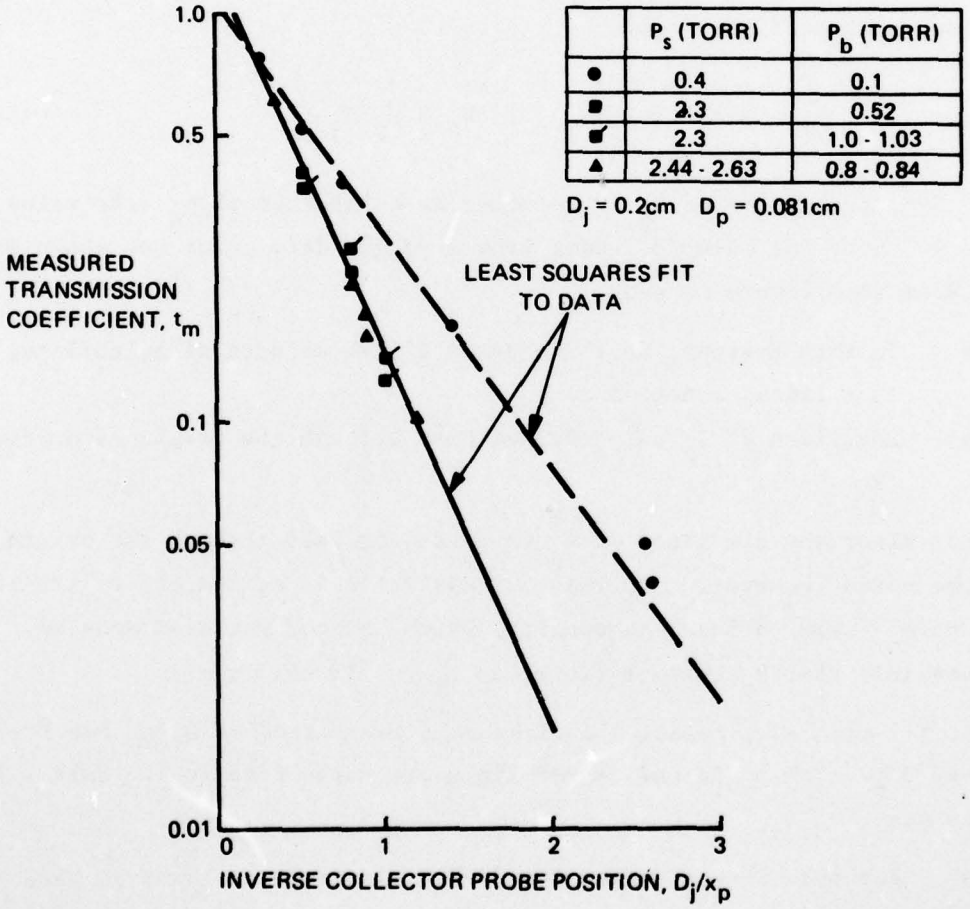

Figure 5-6. Attenuation of $^{32}SF_6$: FC-43 Jet: Small Cylindrical Collector Probe

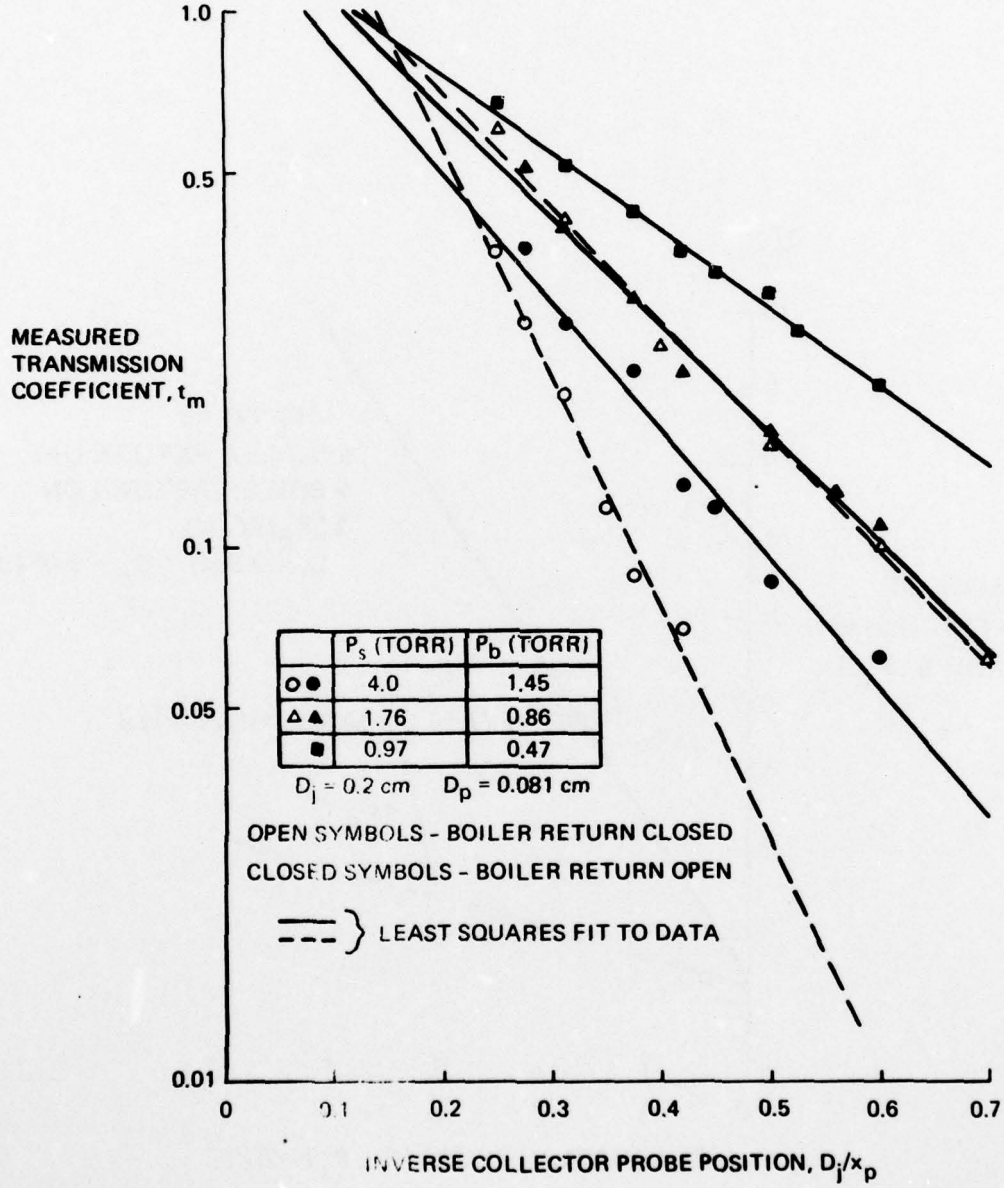

Figure 5-7. Attenuation of $^{238}UF_6$: FC-43 Jet: Small Cylindrical Collector Probe

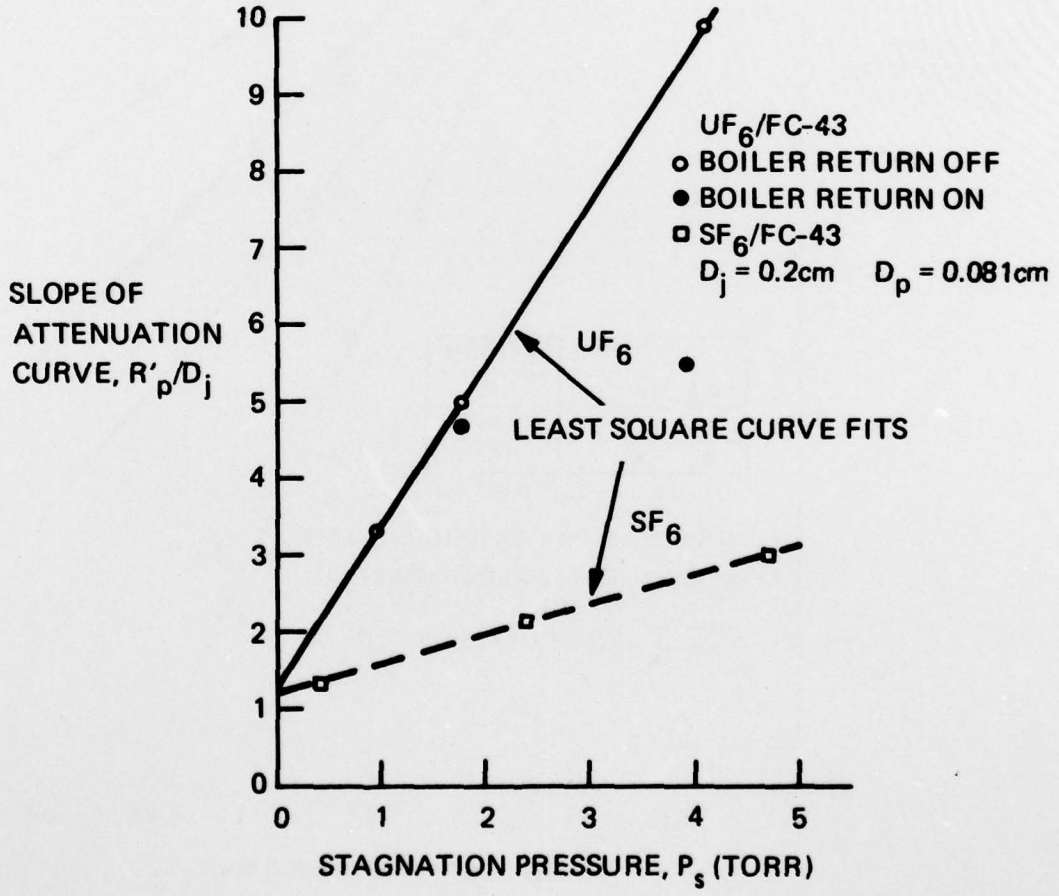

Figure 5-8. Variation of R'_p with Stagnation Pressure: UF_6, SF_6: FC-43 Jet: Small Cylindrical Collector Probe

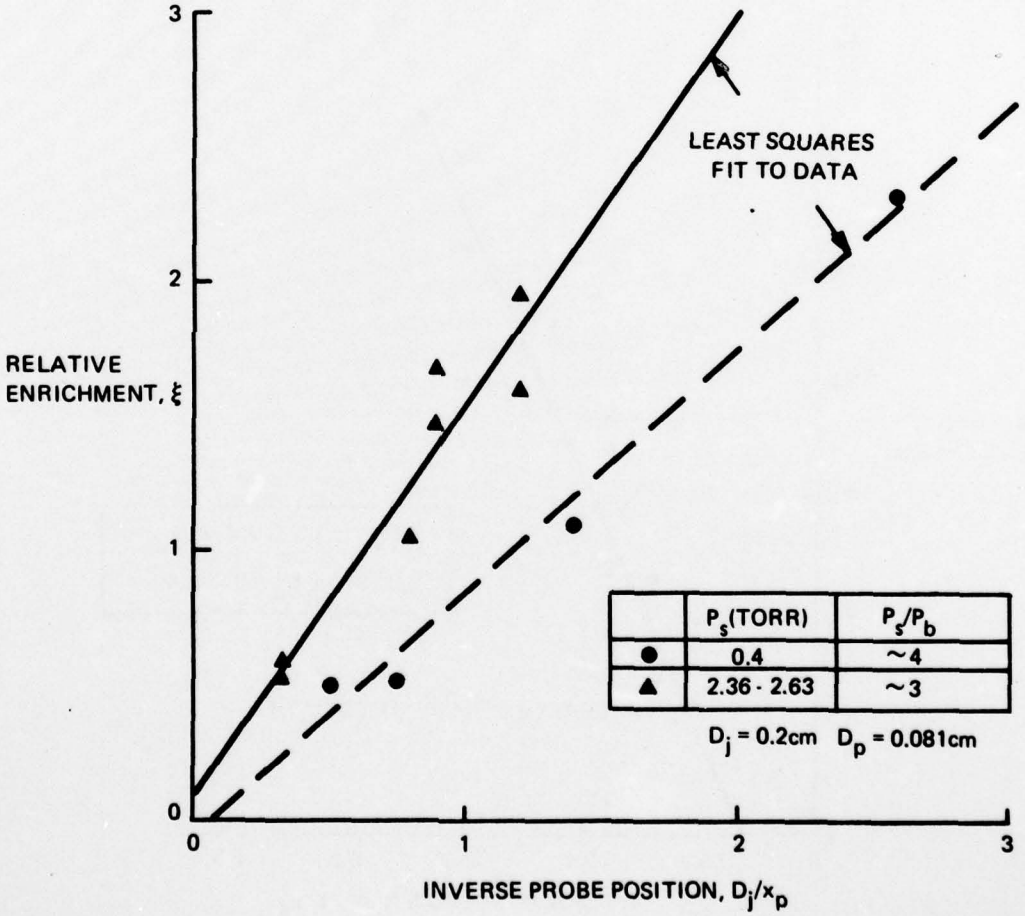

Figure 5-9. Variation of Enrichment Factor with Probe Postiion: SF_6 Isotopes: FC-43 Jet: Small Cylindrical Collector Probe

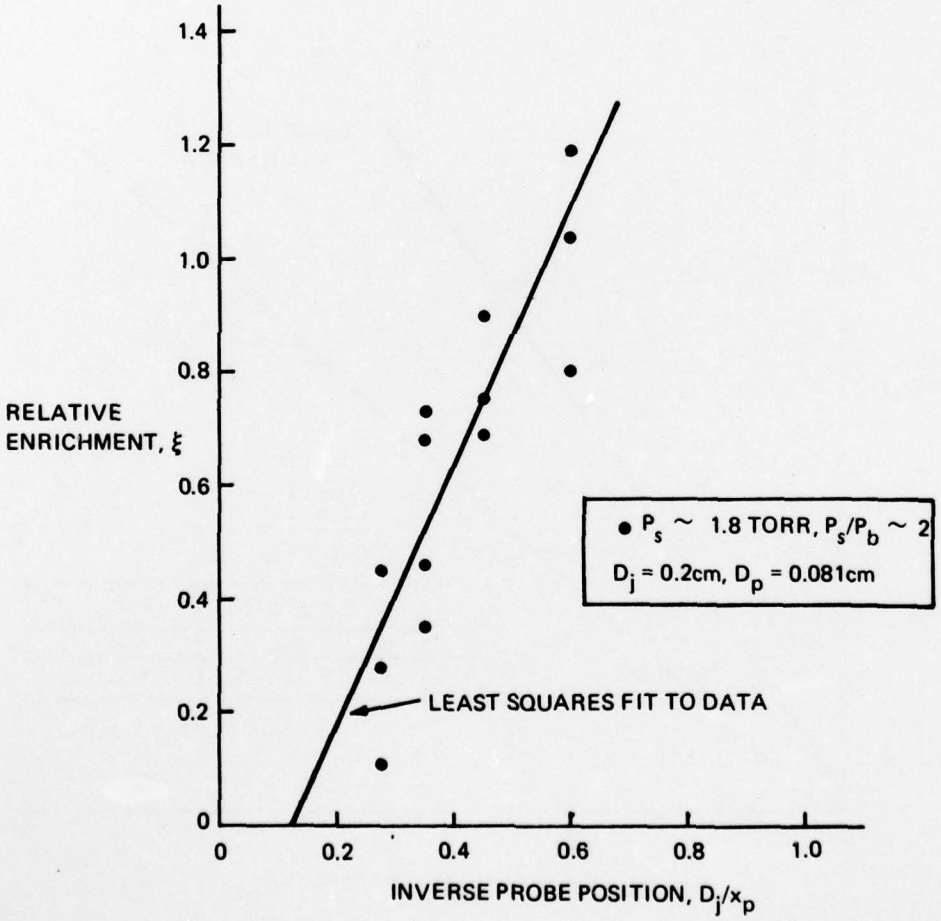

Figure 5-10. Variation of Enrichment Factor with Probe Position: UF_6 Isotopes: FC-43 Jet: Small Cylindrical Collector Probe

AD-A076 907 GRUMMAN AEROSPACE CORP BETHPAGE N Y RESEARCH DEPT F/G 18/2
THE JET MEMBRANE PROCESS FOR URANIUM SEPARATION AND ENRICHMENT.(U)
SEP 79 J W BROOK , V CALIA
UNCLASSIFIED RE-586 NL

2 OF 2
AD
A076907

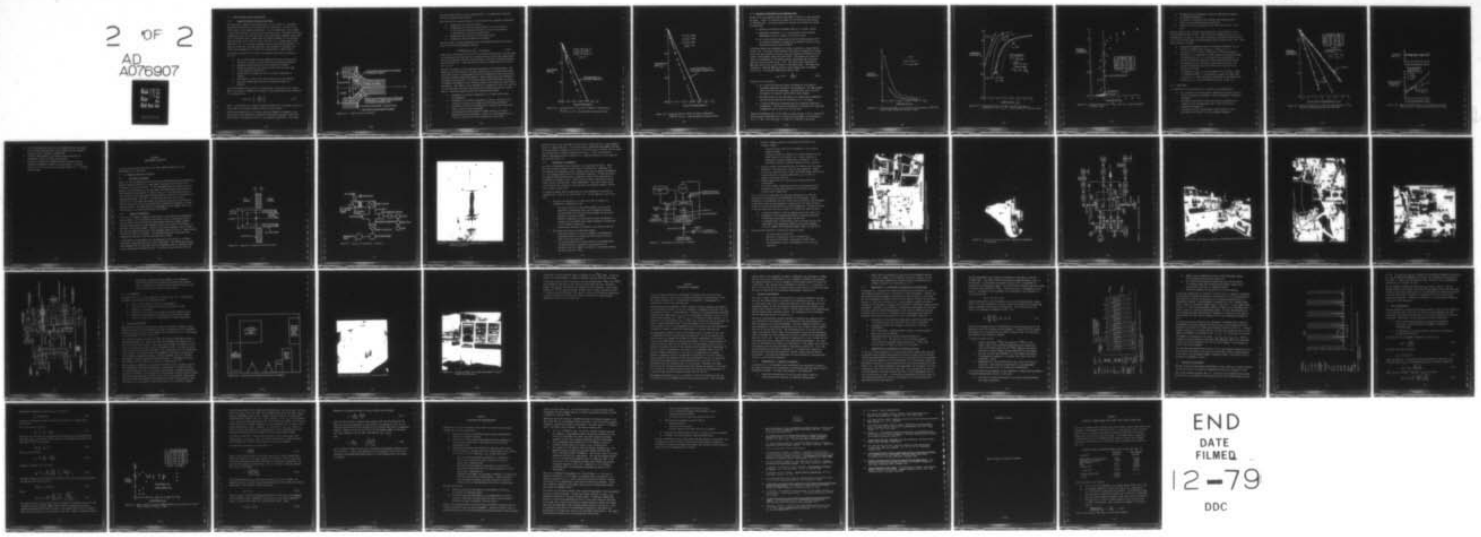

END
DATE
FILMED
12-79
DDC

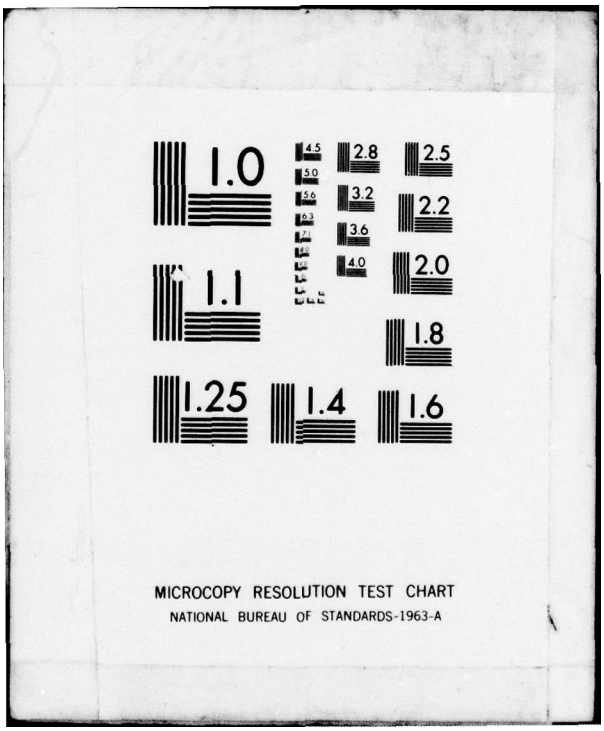
1.0
1.1
1.25
1.4
1.6
1.8
2.0
2.2
2.5
2.8
3.2
3.6
4.0
4.5
5.0
5.6
6.3
MICROCOPY RESOLUTION TEST CHART
NATIONAL BUREAU OF STANDARDS-1963-A

5.2 LARGE COLLECTOR PROBE CONFIGURATION

5.2.1 Large Cylindrical Collector Probe Model

The model that is briefly described below is a first attempt to investigate analytically the effects of increased collector probe area, relative to jet orifice area, on jet membrane performance. It also represents a first attempt to deal with the physics of the actual collection process. Experiments with this configuration gave the surprising result that significant enrichment takes place near or inside the source chamber when the external diameter of the collector probe D_p becomes of the order of $1/2\ D_j$ (see Fig. 4-7). Another aim of this model was to see if the latter phenomenon could be predicted analytically. It should be noted that, although this model was developed to investigate the large probe configuration, it should also be applicable to small probes.

The essential features of the model are summarized below and by reference to Fig. 5-11

- The jet fluid forms a conical lamina which meets at the axis and then forms a single jet (sonic velocity) which moves downstream
- Background species penetrate the jet lamina by diffusion
- Particles stream into the collector probe from the inside edge of the lamina free molecularly
- Superposition is assumed in order to calculate separation of species
- Thicknesses of orifice plate and collector probe are neglected
- Angle that lamina makes with axis is determined solely by geometry.

To further simplify the solution, the distribution of particles on the inside edge of the lamina is assumed to be similar to the distribution of the centerline of a cylindrical jet

$$n/n_b \sim \exp\left(-\frac{a^2 V_j}{4D_{bj}\, s}\right) \qquad (5\text{-}17)$$

Here a is the width of the lamina, assumed constant, and s is distance along the inside edge of the lamina, measured from the collector probe.

Particles streaming into the collector probe are assumed to originate at the inside edge of the lamina with a Maxwellian distribution function, having zero mass velocity and temperature equal to the background temperature. Once these

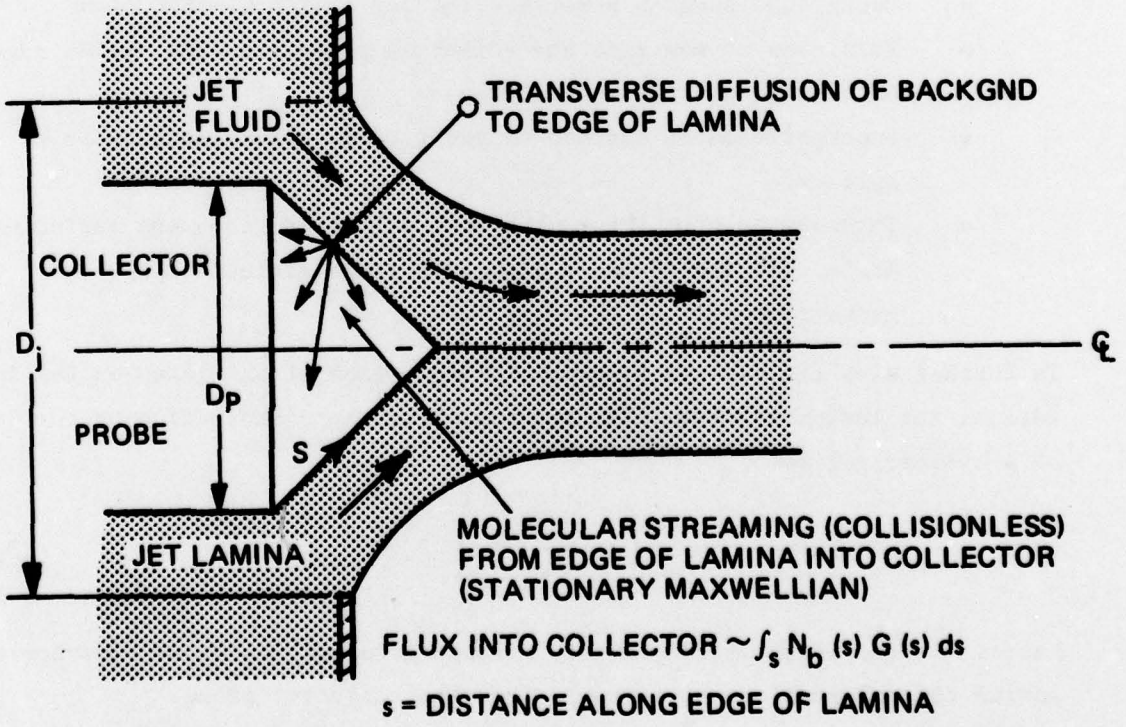

Figure 5-11. Large Collector Probe Model

particles reach the face of the collector probe it is assumed that they pass through it without backscattering.

The flux into the collector probe is then calculated by a quadruple integration:

- Integration over particle velocity
- Integration over the solid angle formed by a point on the face of the collector probe and an element of area on the lamina at a fixed distance s from the collector face
- Integration over the area of the collector probe
- Integration along the length of the lamina.

The first three of these quadratures can be performed analytically; the final result is (for either background species)

$$t = \text{FLUX}/(n_b \bar{c}_b A_c/4) \int_o^L (n/n_b) G(s)\, ds \qquad (5\text{-}18)$$

where (n/n_b) is given by Eq. (5-17), G is an analytic function of s and the angle the lamina makes with the axis (G is obtained from the first three quadratures), and L is the distance from the collector probe to the point at which the lamina reaches the axis ($L \to \infty$ when the collector probe is outside the orifice plate, i.e., $x_p \geq 0$).

Based on this model, we have performed calculations for an N_2/Ne system. This system was selected because of the early availability of data and also because calculation (as well as experimental) errors are magnified as the relative mass difference between isotopes gets smaller. These calculations were performed to investigate two questions: 1) how does relative collector/orifice area affect jet membrane performance; and 2) how does pressure level (mean free path) affect performance. The results of the calculation are presented in Figs. 5-12 and 5-13 (A_o here represents the open area between the collector probe and the orifice plate). From these figures we make the following observations:

- Performance is basically exponential, as in small probe theory and experiment
- Performance is relatively insensitive to area of collector probe relative to orifice, as in N_2/He-A and FC-43/SF_6 experiments
- Performance is relatively insensitive to pressure level (mean free path), as seen in most experiments
- Calculations with large open area (small probe) do not agree quantitatively with experiment. This is not surprising since the actual jet structure for this configuration is not known.

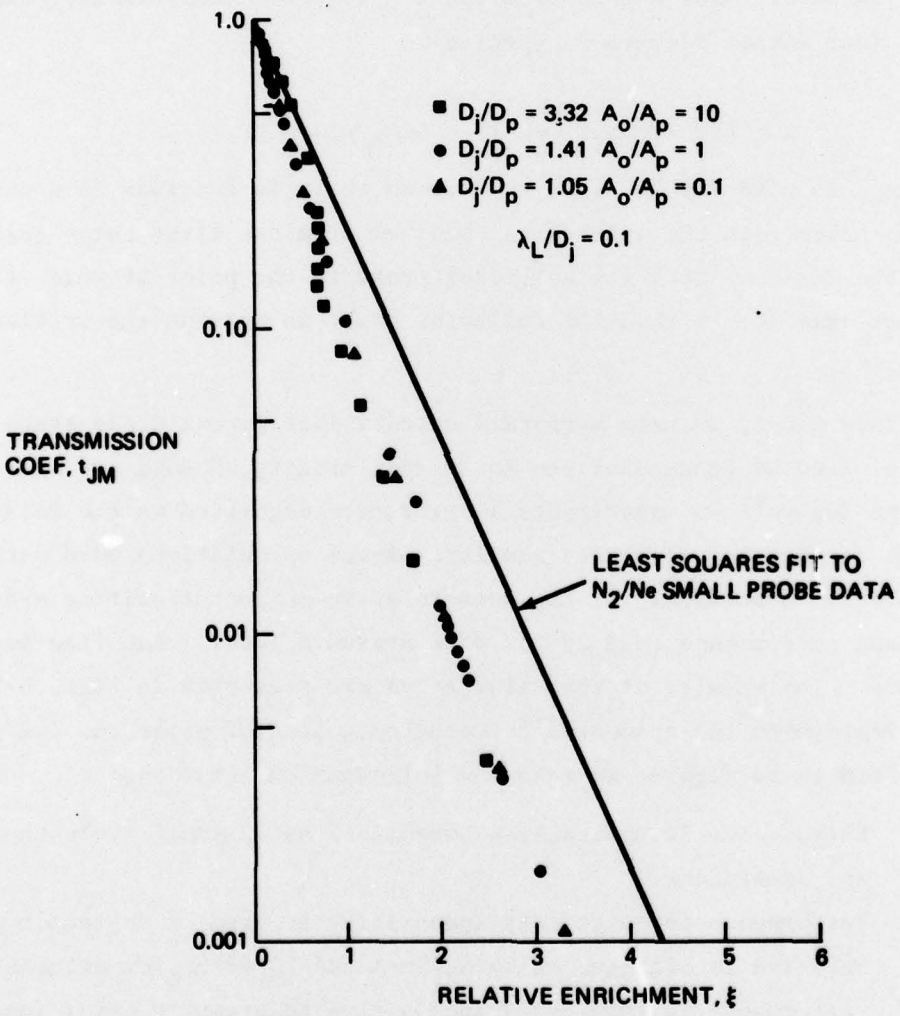

Figure 5-12. Predicted Effect of Collector Diameter on Separation of $^{20}Ne/^{22}Ne$: N_2 Jet: Large Cylindrical Collector Probe

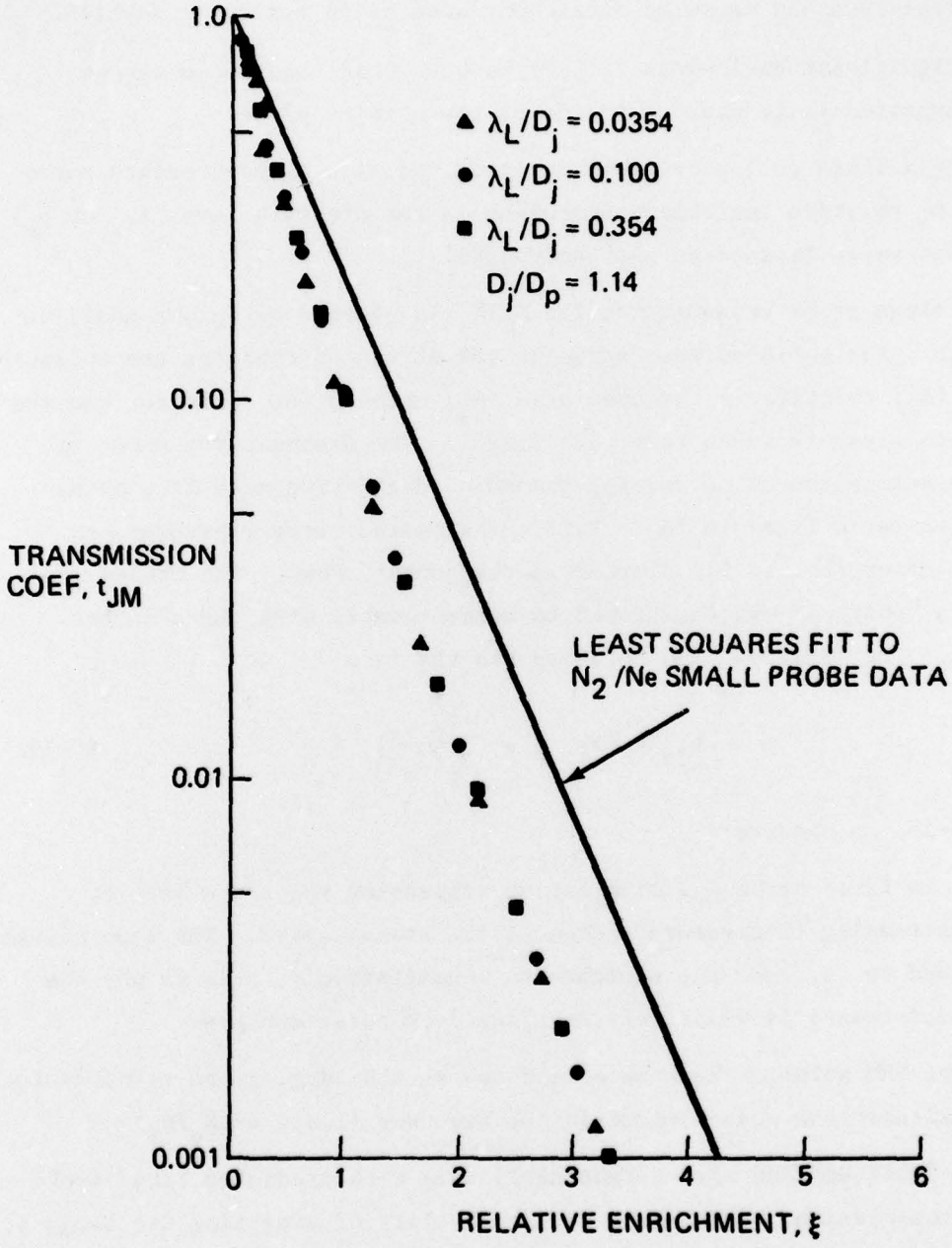

Figure 5-13. Predicted Effect of Mean Free Path on Separation $^{20}Ne/^{22}Ne$: N_2 Jet: Large Cylindrical Collector Probe

5.2.2. Analysis of Enrichment and Transmission Data

In Fig. 5-14, the predicted relative enrichment is plotted vs probe position for N_2/N_e. In Fig. 4-7 measured enrichment for FC-43/SF_6 has been plotted vs probe position. From these figures we conclude (even though the systems are different):

- Predicted and measured enrichment behaves in a similar fashion
- Significant enrichment ($\xi \gtrsim 1$) is both predicted and observed experimentally near or inside of the orifice plate.
- At a fixed collector probe position and with fixed pressure ratio the relative enrichment increases as the pressure level (p_s or p_b) increases (mean free path decreases).

Calculated large probe transmission for N_2/N_e is plotted vs. probe position in Fig. 5-15. The solid curves represent the effect of changing the collector probe area (A_p) relative to the open area (A_o) between the collector and the orifice, with pressure (mean free path fixed). The dashed curve shows the effect on transmission of increasing pressure (decreasing mean free path) with the area ratio fixed ($A_o/A_p = 1.0$). The dotted curve represents an MHM type solution (Eq. (5-1)) plotted in the manner shown. The broken line represents a "shifted" MHM positioned to agree roughly with the adjacent solid curve. The "shifted" MHM solution has the form

$$t_{JM} = \exp\left(-\frac{R_p'}{X_p/X_o}\right) \qquad (5\text{-}19)$$

From Fig. 5-15, we observe

- At a fixed probe position either increasing the probe area or decreasing thepressure increases the transmission. The same changes tend to decrease the enrichment. Qualitatively, this is why the performance is relatively unaffected by these changes.
- The MHM solution has the same shape as the large probe transmission calculations when plotted in the same way (i.e., vs X_p/D_j)
- A "shifted" MHM agrees reasonably well with predicted large probe transmission. This opens the possibility of analyzing the large probe transmission data by curve fits of this type.

Measured transmission data for FC-43/SF_6 are shown in Fig. 5-16 as a function of probe position (normalized here by orifice plate thickness, for convenience) for P_s = 2 and 7 torr and P_s/P_b = 1.5 and 2.0. From Fig. 5-16 we see:

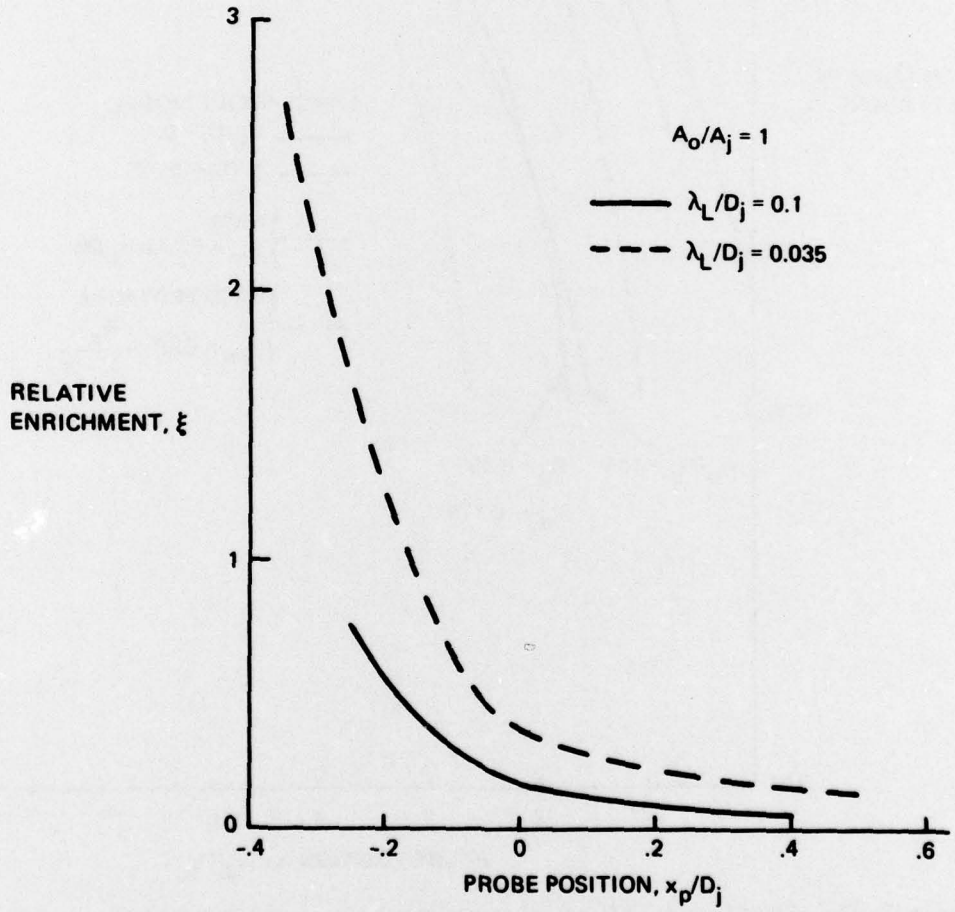

Figure 5-14. Predicted Enrichment as a Function of Probe Postiion: $^{20}Ne/^{22}Ne$: N_2 Jet: Large Cylindrical Collector Probe

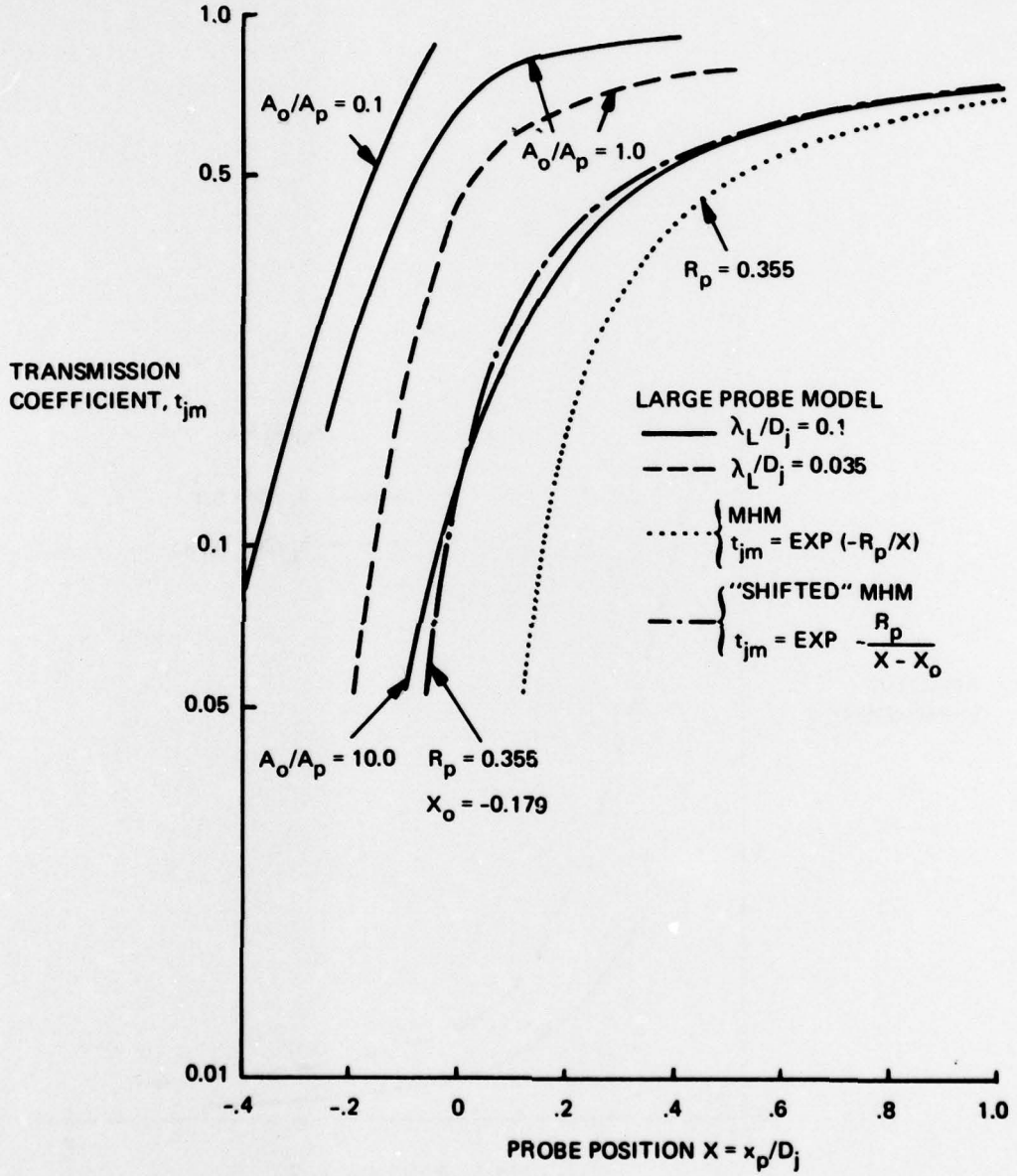

Figure 5-15. Predicted Effect of Area Ratio and Mean Free Path on Attenuation of ^{20}Ne: N_2 Jet: Large Cylindrical Collector Probe

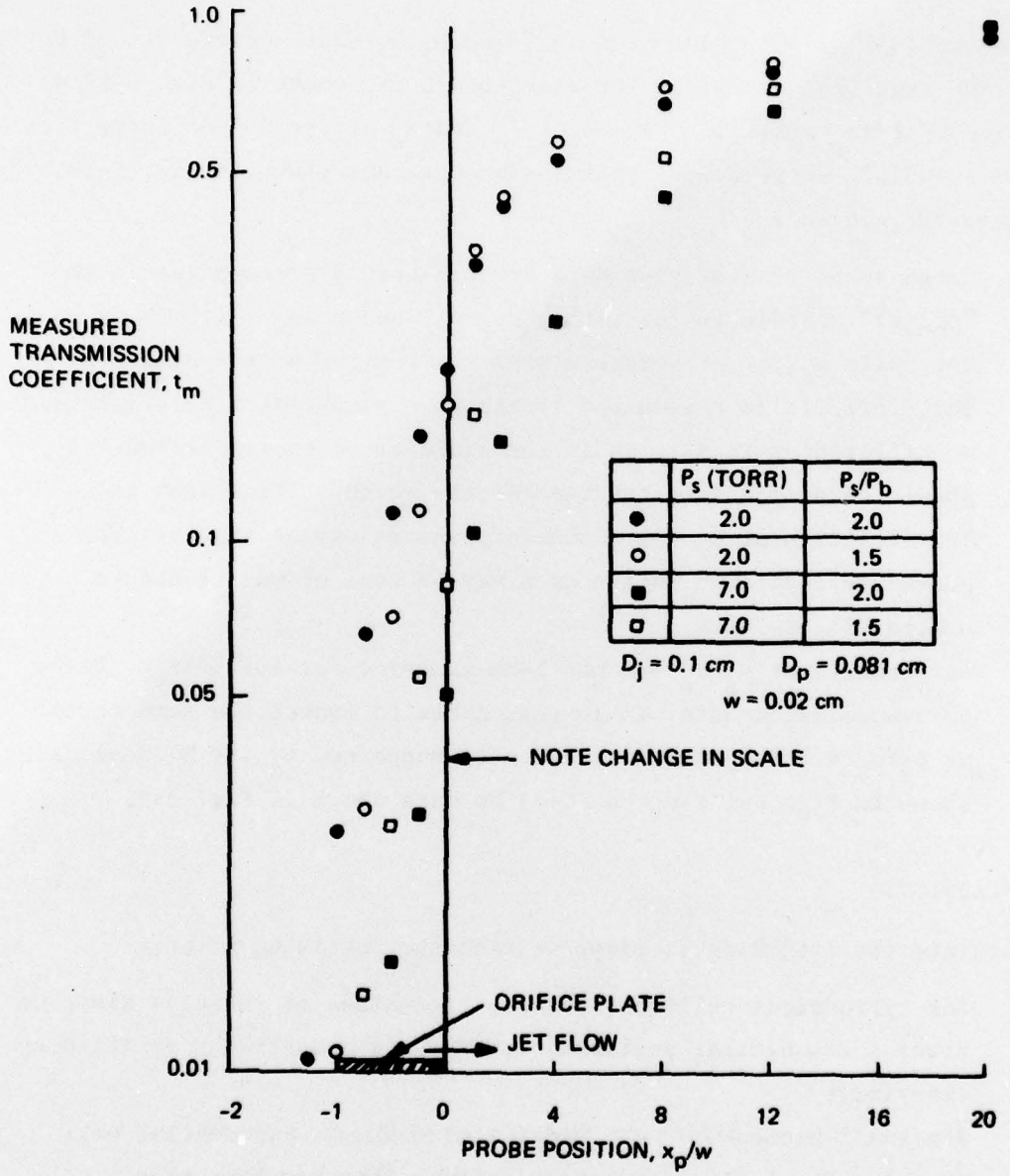

Figure 5-16. Measured Attenuation: $^{32}SF_6$: FC-43 Jet: Large Cylindrical Collector Probe

- The shape of the transmission curves are qualitatively similar to the model prediction
- The effect of increased source pressure (decreased mean free path) is in the same direction as predicted
- Pressure ratio p_s/p_b appears to have only a small effect on the data.

The data shown in Fig. 5-16 have been analyzed by a least squares fit of a "shifted" MHM type (Eq. (5-19)). The results are presented in Fig. 5-17 as transmission vs $1/(x_p-x_o)$. The values of R_p' and x_o obtained from curve fits of all of the FC-43/SF_6 large probe transmission data are shown in Fig. 5-18. From these figures we conclude

- Large probe transmission data are reasonably exponential in the "proper" coordinate for both $p_s/p_b \approx 2$ and $p_s/p_b = 1.5$
- The shift x_o is, at worst, a weak function of source pressure. Therefore, it is reasonable to expect exponential separation based on differences in R_p', as in the small probe configuration. x_o should be primarily a function of the probe/orifice area ratio
- The variation of R_p' with source pressure may be linear. The curvature indicated in the data may be real or may be due to scatter in the data.
- Performance at $p_s/p_b = 2$ has been measured for FC-43/SF_6. Based on transmission data, it is reasonable to expect the same result at $p_s/p_b = 1.5$. This conclusion is supported by the N_2/He-A data shown in Fig. 4-1 and the FC-43/Ne data shown in Fig. 3-2.

5.3 CONCLUSIONS

To recapitulate the preceding section, we make the following points:

- For cylindrical collector probes, regardless of relative size, we predict exponential performance. This is essentially verified by experiment
- The small probe diffusion model also predicts exponential performance in the two-dimensional case. This has been also observed experimentally.
- The models provide a qualitatively correct picture of both performance and details of the jet membrane phenomena

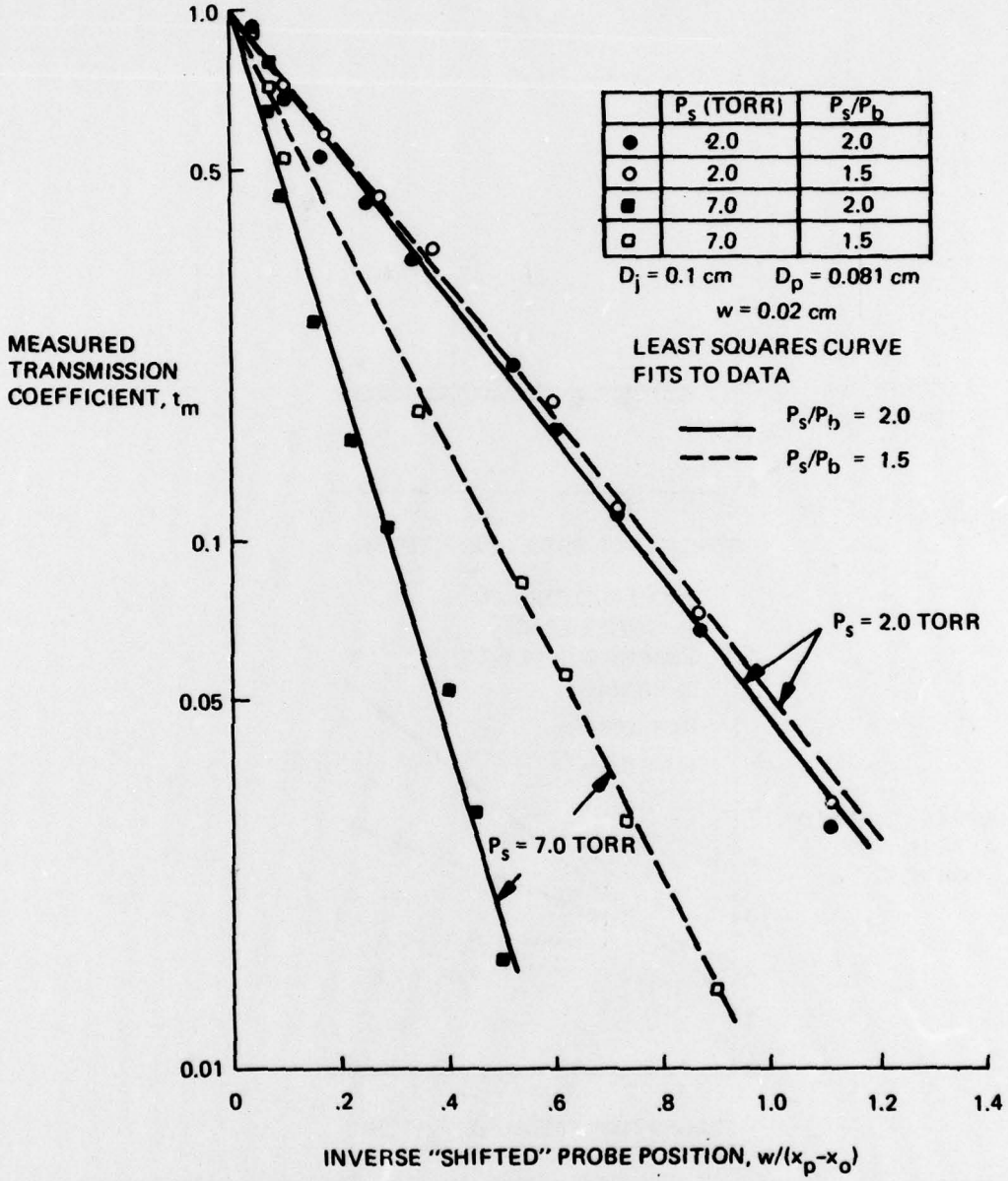

Figure 5-17. Measured Attenuation vs "Shifted" Probe Position: $^{32}SF_6$: FC-43 Jet: Large Cylindrical Collector Probe

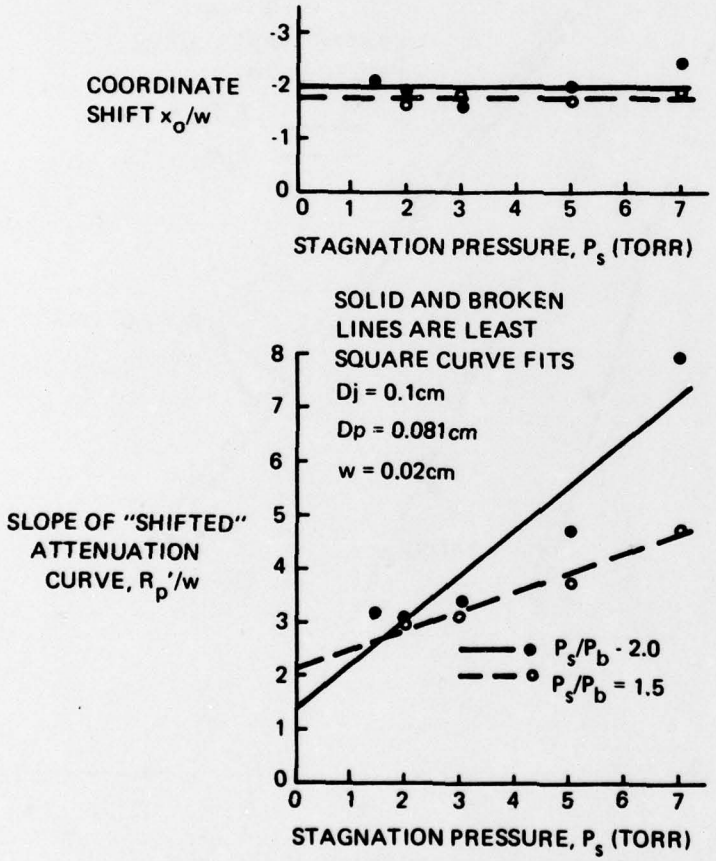

Figure 5-18. "Shifted" MHM Parameters vs Jet Stagnation Pressure: $^{32}SF_6$: FC-43 Jet: Large Cylindrical Collector Probe

- Due to the simplified nature of the assumptions made, the models do not provide quantitatively correct predictions and therefore cannot be used to optimize configurations
- The small probe models do not predict large differences in performance between FC-43/SF_6 and FC-43/UF_6
- Analysis of large probe transmission data indicates that the unchanged performance observed in mixtures down to a pressure ratio of 1.5 will also be true for heavy isotopes (i.e., FC-43/SF_6 and FC-43/UF_6).

SECTION 6
EXPERIMENTAL FACILITIES

In this section the main features of the three apparatus employed in the experiments will be described.

6.1 JET MEMBRANE SEPARATION APPARATUS

6.1.1 Probe/Orifice Geometry

Except for the two-dimensional and conical probe configurations, the probe/orifice geometry employed consists of a long slender cylindrical tube located on the centerline of a circular orifice. In the two-dimensional and conical cases, the geometry has been depicted in the data plots. The nomenclature associated with the cylindrical probe geometry is shown in Fig. 6-1. The distinction between a large collector probe and a small collector probe is related to the difference in the area ratio $A_p/A_j = D_p^2/D_j^2$, or the effective open area ratio $A_o/A_j = (D_j^2-D_p^2)/D_j^2$. For those cases where the collector probe area is less than one tenth of the orifice area we have arbitrarily classified the geometry as "small collector probe". The probe position is measured from test chamber side of the orifice plate, and is positive into the test chamber.

6.1.2 Gaseous Jet Apparatus

In Fig. 6-2 a schematic diagram of apparatus no.1, the gaseous jet experimental setup is shown. In this apparatus the collector probe is positioned relative to the orifice plate by moving the plenum (source) and test chamber assembly. The test chamber portion of the apparatus, which is not shown in the figure, is attached to the plenum chamber. Details of the drive mechanism, source chamber, and collector probe may be seen in the photograph shown in Fig. 6-3. Repositioning accuracy of 0.002 cm is possible. The sampling probes were constructed from commercially available, thin wall stainless steel tubing.

In the gaseous jet experiments the concentration of the species in the heads stream was continuously monitored with an ULTEC QUAD. 150 residual gas analyzer. The instrument has a conventional electron bombardment ionizer, quadrupole mass filter, and electron multiplier output. The current output from the electron

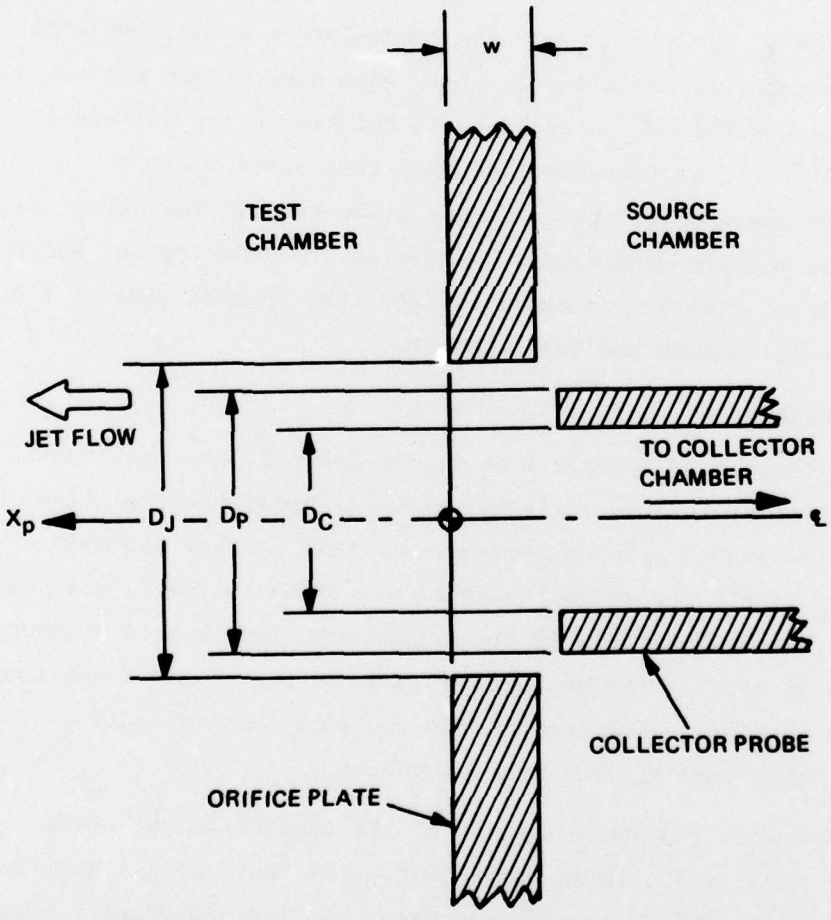

Figure 6-1. Geometry of Cylindrical Collector Probe

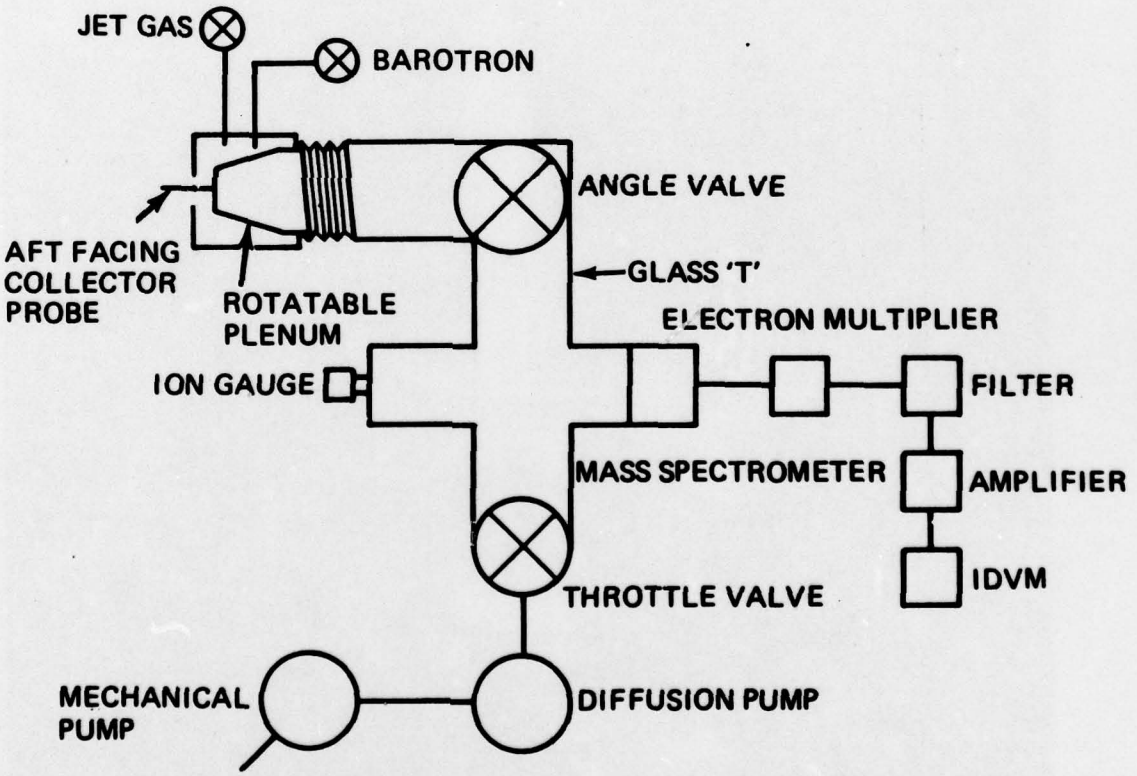

Figure 6-2. Gaseous Jet Experiment: Schematic

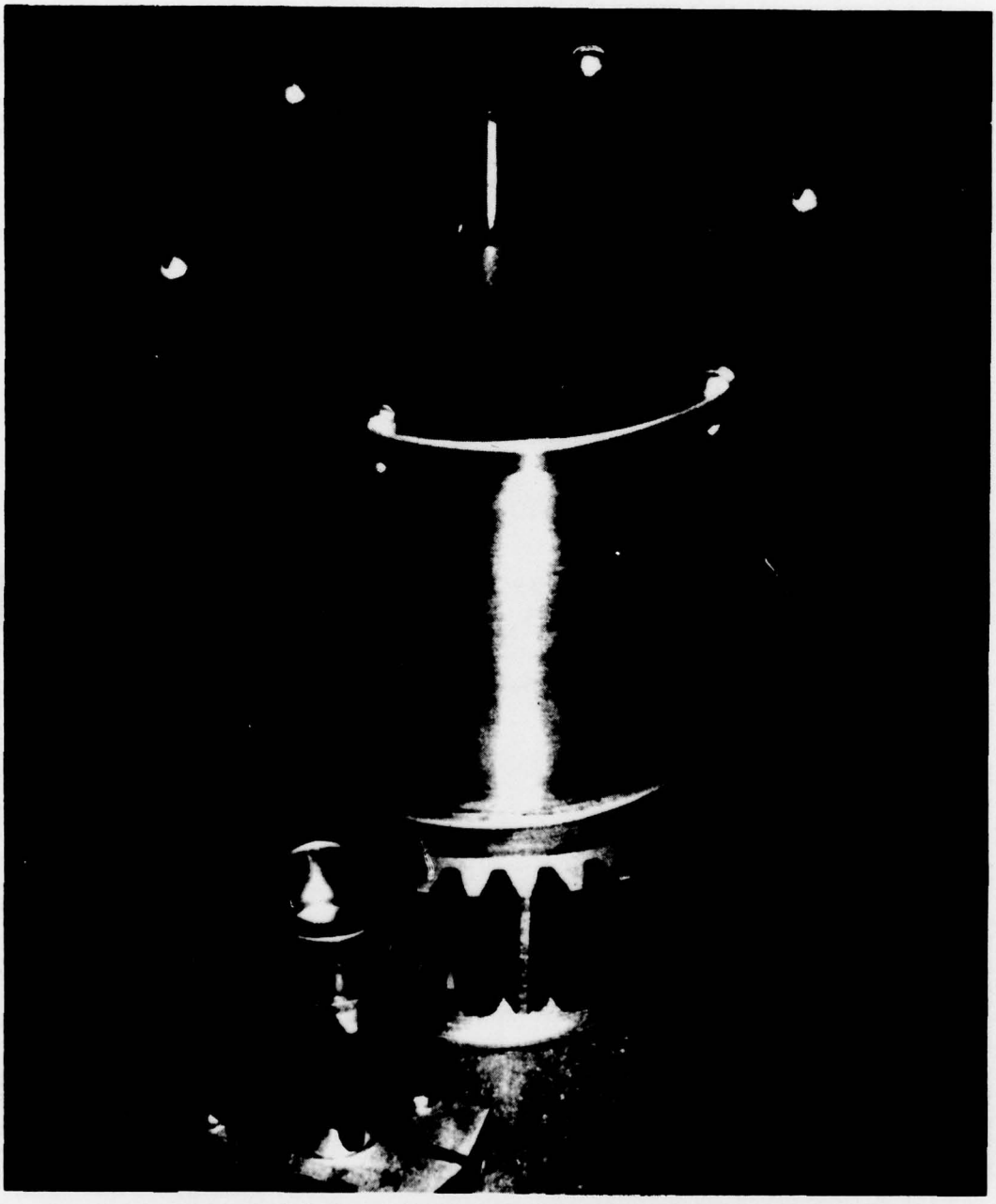

Figure 6-3. Orifice and Collector Probe: Gaseous Jet Separation Apparatus

multiplier was fed via a shielded low capacitance coaxial cable to a high impedance device for signal detection. In the Neon isotopic separation measurements the mass filter was manually adjusted to the center of the mass peak of interest and the signal was processed with a digital integrating voltmeter. It was not possible to observe simultaneously mass 20 and mass 22. Additional details of this apparatus may be found in Ref. 18.

6.1.3 Condensible Jet Apparatus

The vapor jet experiments were performed in two separate facilities. These facilities differed primarily in materials of construction. Apparatus no 2 was designed for experiments using a benign process gas (or gases) and apparatus no. 3 was designed specifically for experiments using UF_6. In both facilities the sampling probe (stainless steel tubing) was located on the centerline of an axisymmetric convergent nozzle. Probe position could be controlled to within 0.0025 cm with a Varian linear vacuum feedthrough. The scale of these bench type facilities was selected so that additional nozzle/probe elements could be easily added in future work.

A schematic diagram, which is applicable to both condensible jet facilities (apparatus nos. 2 and 3), is shown in Fig. 6-4. In this sketch it can be seen that

- The vapor jet operates in a closed cycle that is similar to a conventional refrigeration cycle.
  - Jet source pressure is controlled primarily by the boiler temperature; superheated vapor can be obtained by heating the line between the boiler and source chamber and by direct heating of the source chamber.
  - Condenser temperature is controlled by direct refrigeration cooling; the fluorocarbon test chamber pressure is established by the condenser temperature.
  - Fluorocarbon condensate is returned to the boiler by gravity.
- The process gas upflow is mechanically pumped
  - Process gas pressure in the test chamber is established by adjusting either/or a variable leak valve and the throttle valve in the tails gas line
  - In the UF_6 apparatus, the system leak rate was insignificant and hence mechanical pumping on the apparatus was not necessary; the test chamber was loaded to the desired pressure and then sealed by a valve.

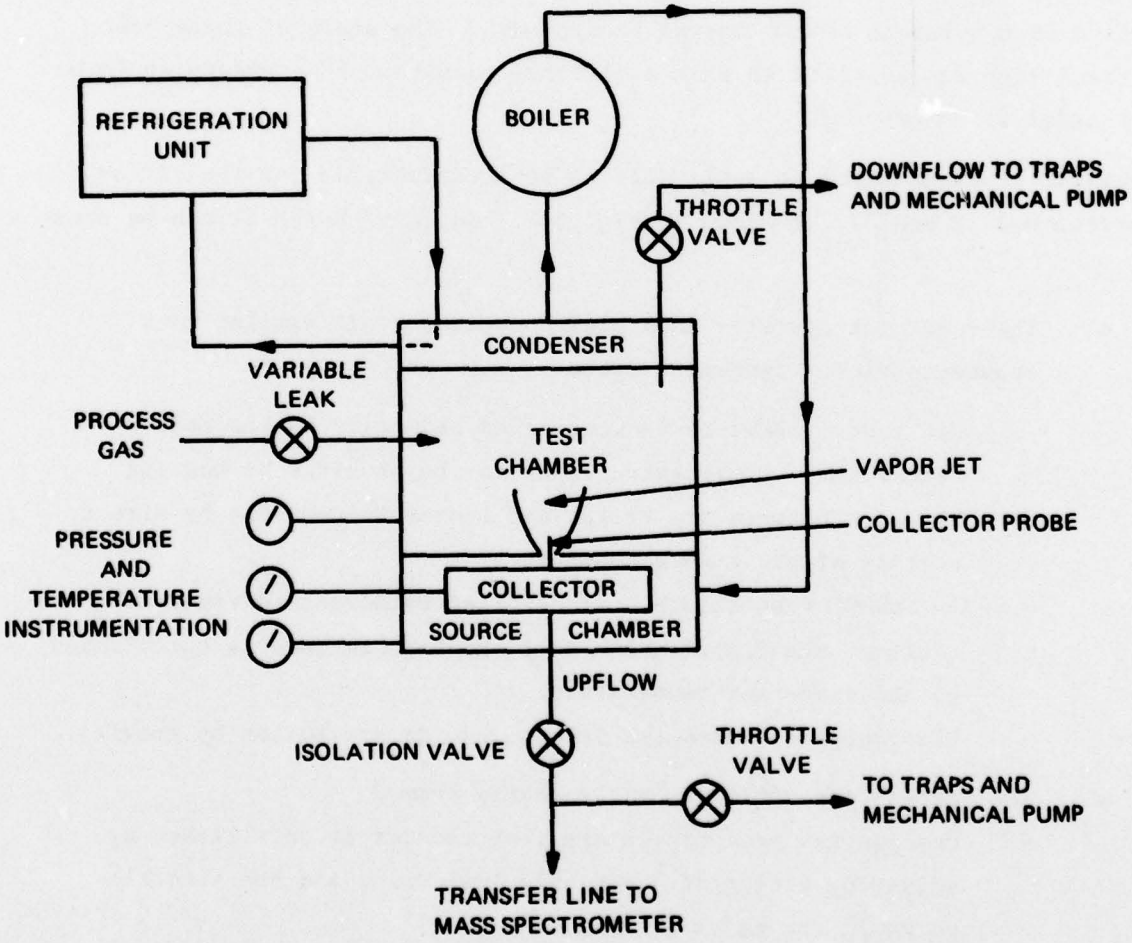

Figure 6-4. Condensible Jet Apparatus: Schematic

- Collector chamber pressure is established by mechanical and cryogenic pumping
  - A throttle valve permits fine adjustment of the collector chamber pressure
  - Provision is made for removal of jet vapor backflow from the heads stream in the transfer line. Simple cryotraps at appropriate operating temperatures are employed. In the FC-43/UF_6 experiments complete separation was not possible.
- Process pressures were measured with three MKS barotron electronic manometers. The manometers, which are UF_6 compatible, covered the pressure range from 0-10, 0-100, and 0-1000 mm Hg, respectively, Linear operation at elevated temepratures, up to 150°C, is possible with these detectors.
- Process temperatures were monitored with Copper-Constantan thermocouples
- The source chamber thermocouple was used in conjunction with a Thermoelectric model 300 proportional controller to maintain constant source temperature.

Fig. 6-5 shows the condensible jet apparatus (apparatus no.2) that was constructed for purposes of testing separation in benign gases. Major components of the apparatus that can be seen here are labeled in the photograph. An additional photo of this apparatus is shown in Fig. 6-6 where we show a closeup of the orifice plate/collector probe configuration. The major features of the UF_6 apparatus can be seen in Figs. 6-7 through 6-11 where we show:

- A detailed schematic of the UF_6 apparatus flow chart (Fig. 6-7)
- Photographs of the assembled apparatus, including the Nuclide 12-90-CG mass spectrometer (Figs. 6-8 and 6-9)
- A photograph and a cross-sectional view of the test section that shows some of the engineering details of the source chamber, collector chamber, and background chamber (Figs. 6-10 and 6-11).

Several special features of construction should be noted:

- All fusion weld construction
- Material of construction is 304 stainless steel
- All access joints employ copper metal-to-metal seals
- All accessories (valves, instrumentation, etc.) are UF_6 compatible

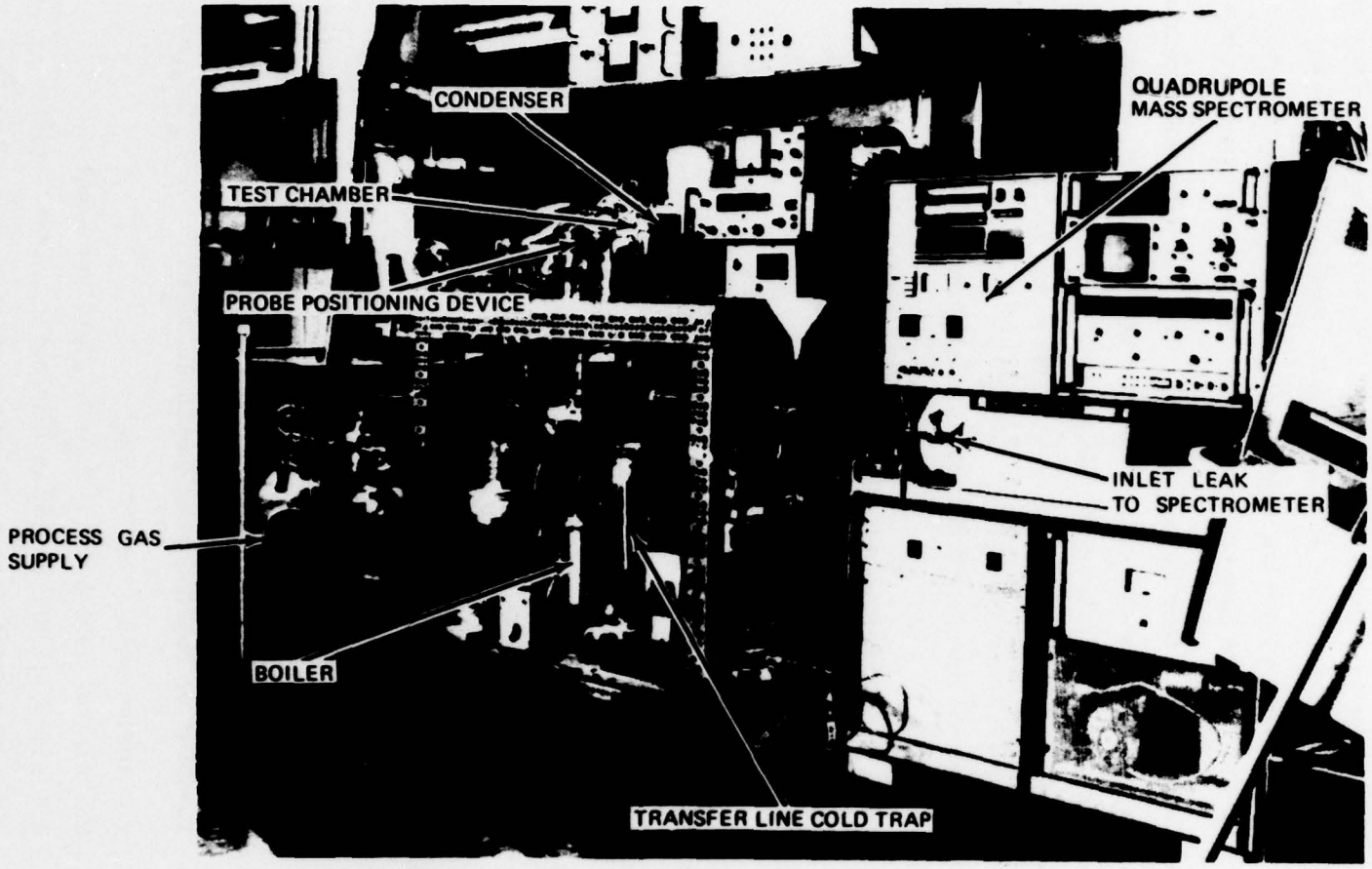

Figure 6-5. Condensible Jet Separation Apparatus with Quadrupole Mass Spectrometer

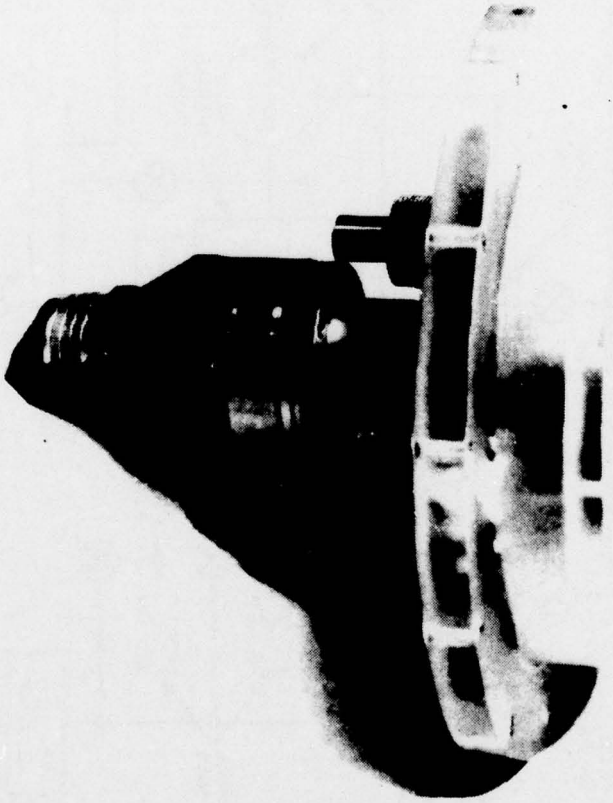

Figure 6-6. Orifice and Collector Probe: Benign Gas Condensible Jet Apparatus

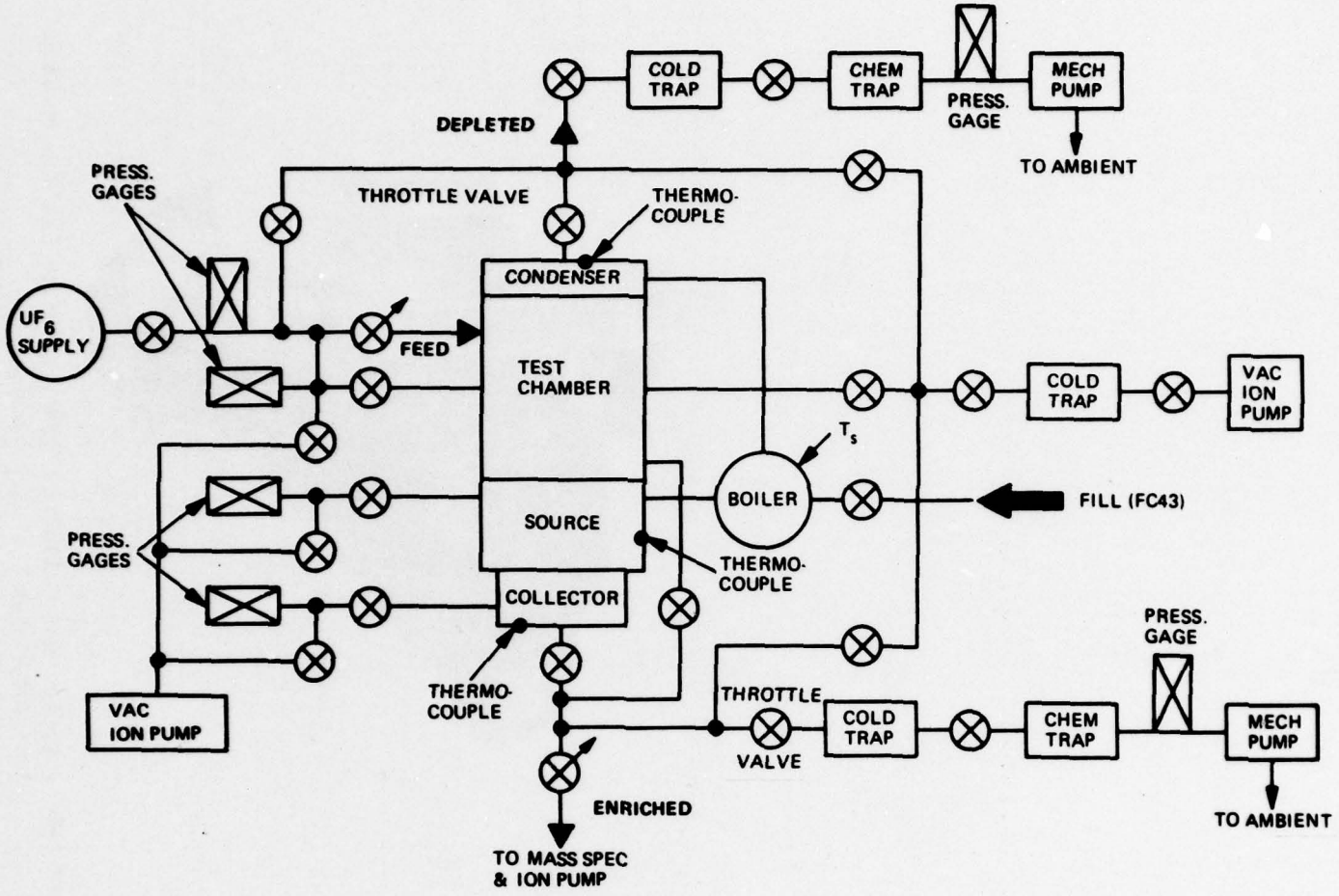

Figure 6-7. UF_6 Separation Apparatus: Schematic

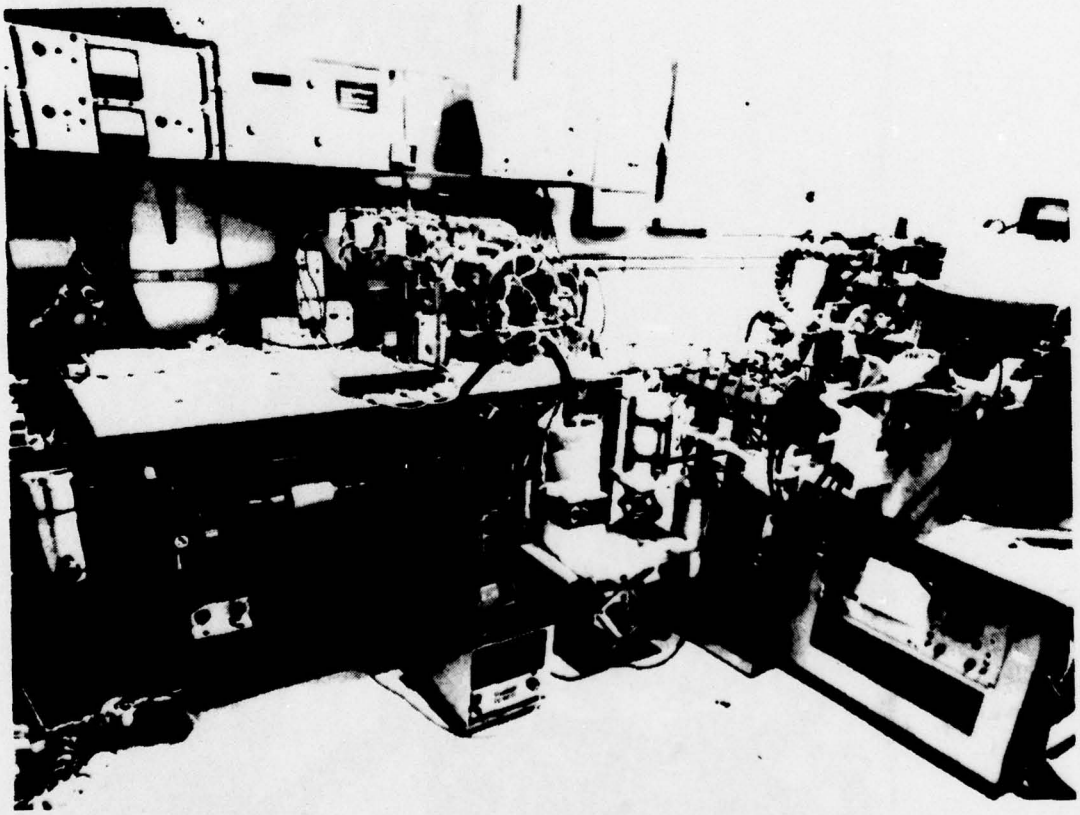

Figure 6-8. UF_6 Separation Apparatus, Instrumentation and Mass Spectrometer

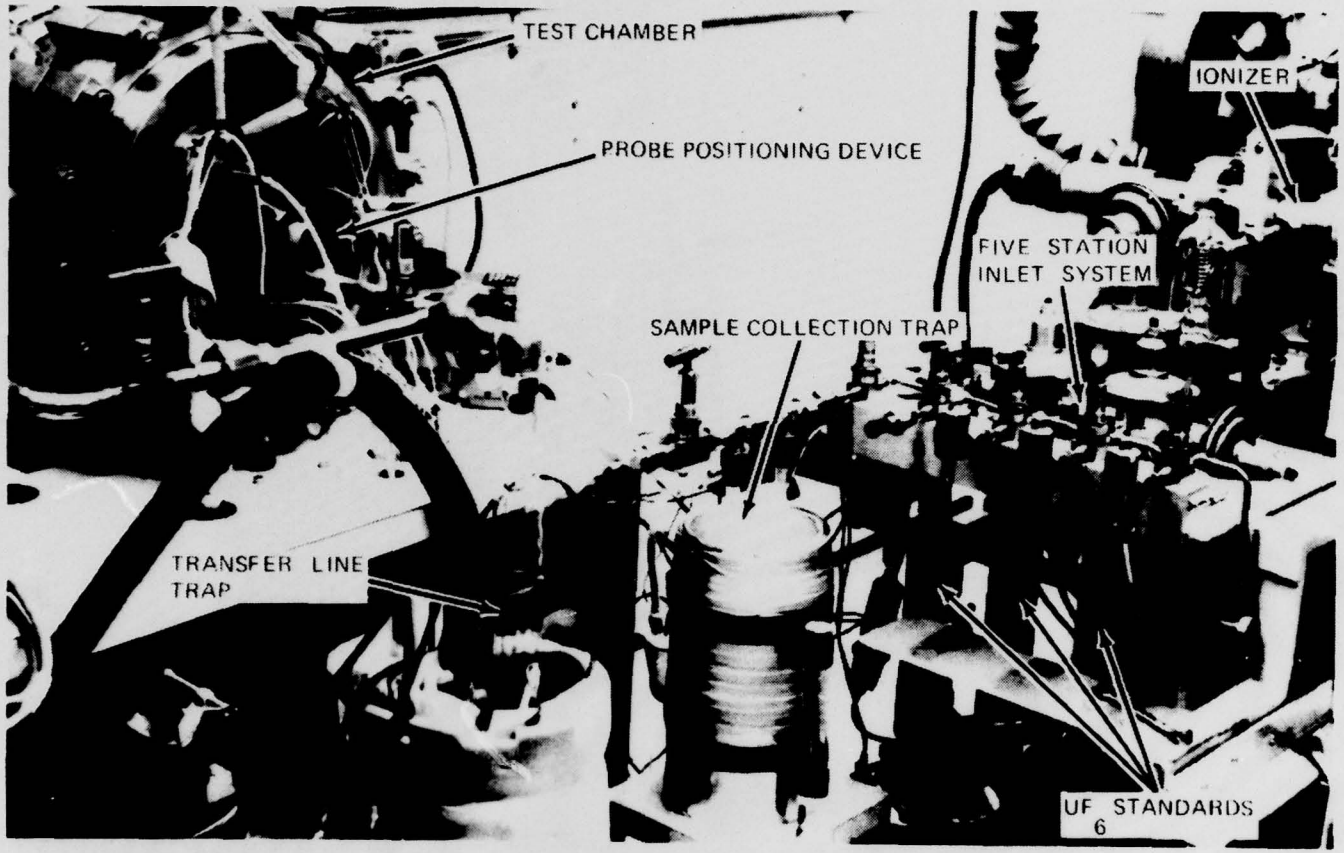

Figure 6-9. UF_6 Separation Apparatus, Transfer Line, and Mass Spectrometer Inlet System

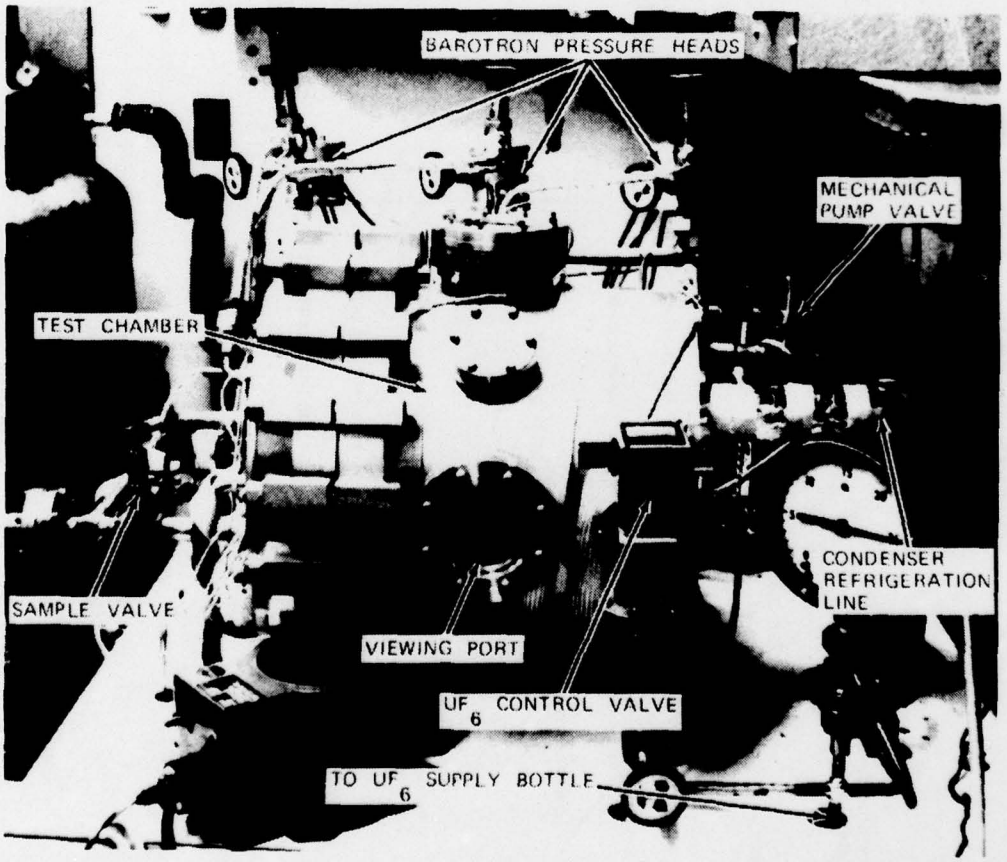

Figure 6-10. Side View of UF_6 Separation Apparatus

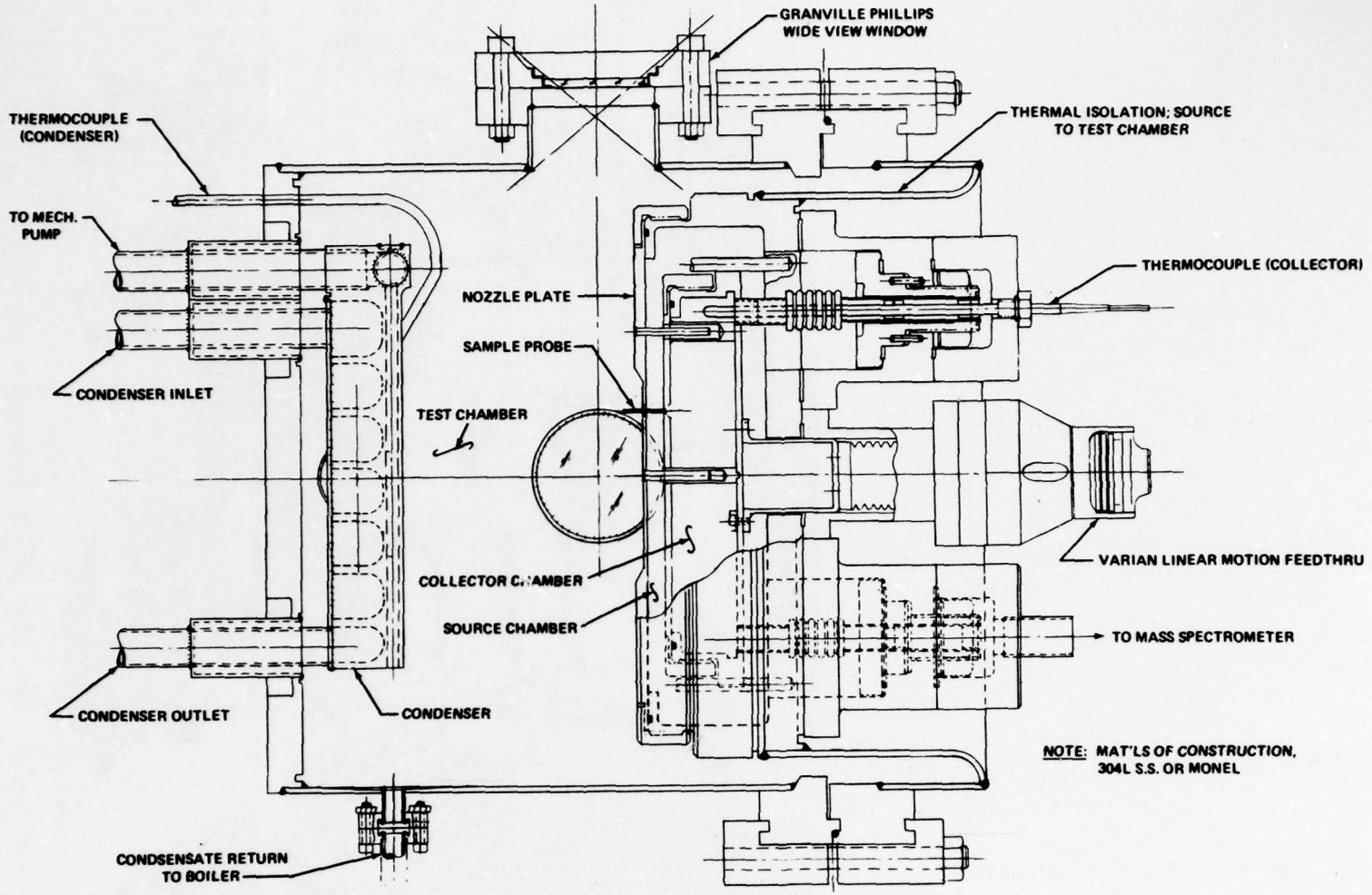

Figure 6-11. Cross Sectional View of UF_6 Separation Apparatus

- UF_6 release, through flow paths leading to the atmosphere is prevented with liquid nitrogen and aluminum oxide chemical traps. Automatically controlled valves physically seal off the the flow paths in the event of a trap failure.

6.2 UF_6 LABORATORY

A schematic layout of the UF_6 laboratory is shown in Fig. 6-12. The essential features of the laboratory are summarized below.

- Direct hood and exhaust system to the atmosphere
- Floors and walls are smooth and specially treated for easy removal of contaminants
- Laboratory air is continuously sampled for Alpha radiation level
- Laboratory is maintained at negative pressure relative to atmosphere to prevent outlfow of contaminants to nearby laboratories.

6.3 UF_6 MASS SPECTROMETER

The Nuclide 12-90-CG mass spectrometer, which is specifically designed to make precision isotopic ratio determinations in UF_6, was selected for our experiments. Detailed specifications for this instrument can be found in Ref. 19. A photograph of the instrument is shown in Fig. 6-13.

The standard instrument consists of a Nier type electron bombardment ionizer, a direction focusing 12 in. radius, 90° sector electromagnet ion analyzer, and a dual ion beam collector system. Three high speed ion pumps are employed to pump on the ion source and on both ends of the analyzer section. Test gas is introduced to the ionizer through an automatic inlet system which has five independent inlet stations. A Tektronix Model 31 programmable caclulator, in conjunction with a digital integrating ratiometer, permits automatic control of the mass spectrometer for data acquisition and data analysis. A photograph of the mass spectrometer control console and calculator is shown in Fig. 6-14.

Mass analyzed ion beams may be collected simultaneously with the dual collector for instantaneous isotopic determinations. Alternatively, a single collector can be used with the analyzer in the peak stepping mode, to measure successively the peaks of interest. In our version of the instrument the dual collector system has been slightly modified (a double slit is used at the collector plate rather than the conventional single slit arrangement)to provide for UF_6 isotopic ratio measurements in the presence of fluorocarbon peaks; e.g., the FC-43 cracking

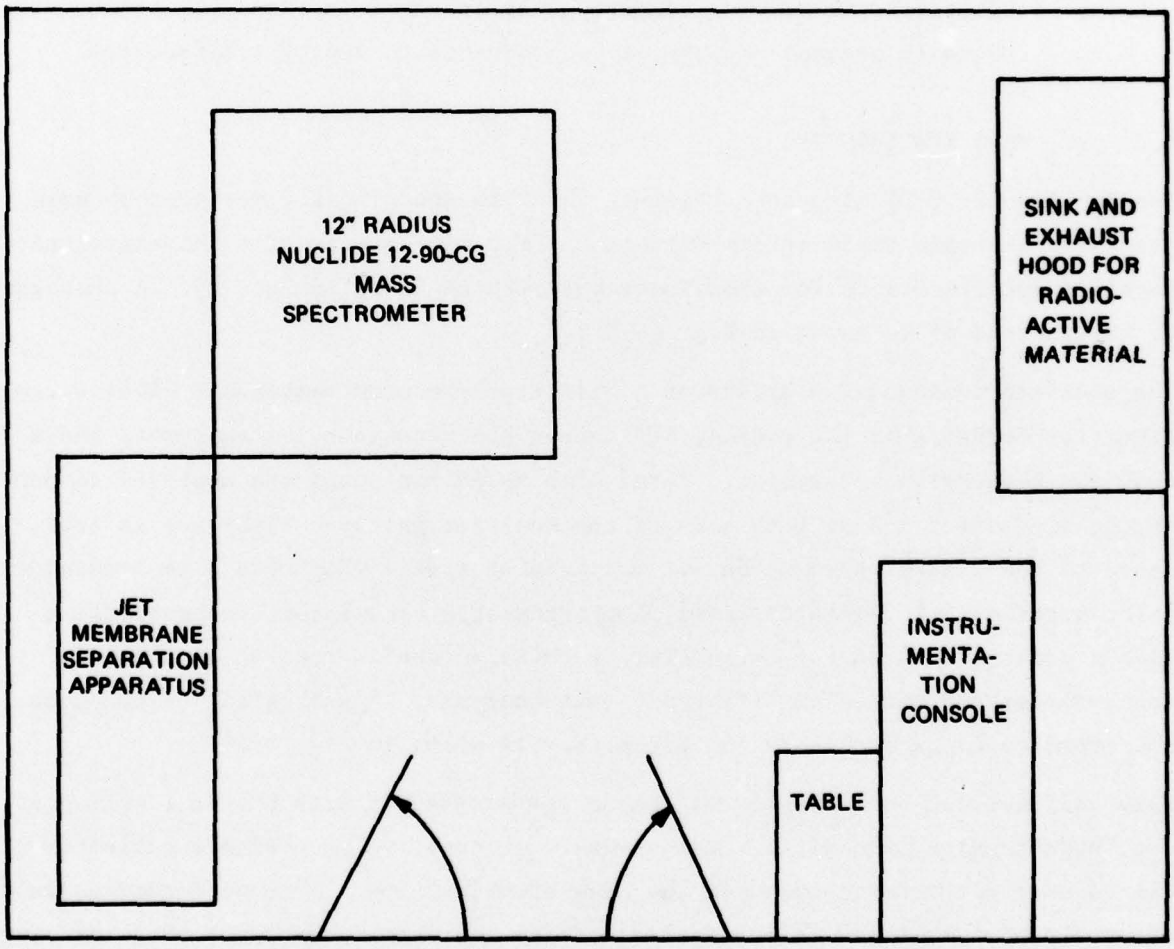

Figure 6-12. Uranium Isotope Separation Laboratory: Schematic

Figure 6-13. Nuclide 12-90-CG 12 in. Mass Spectrometer

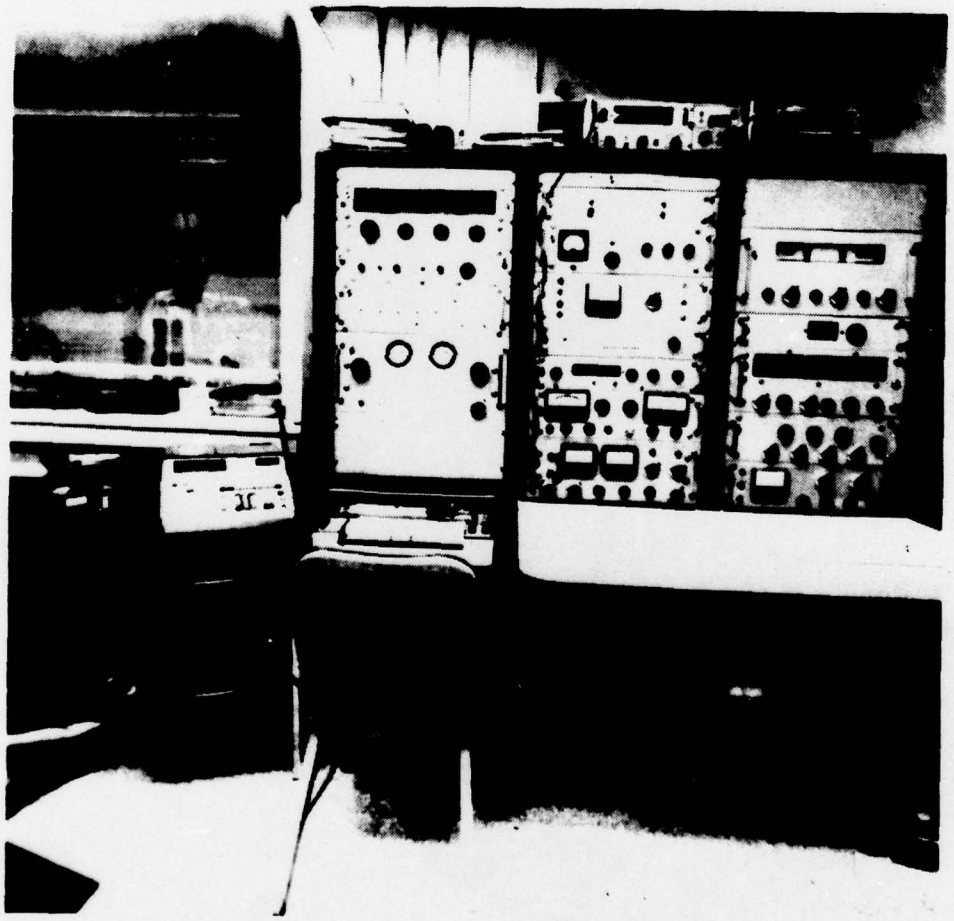

Figure 6-14. Nuclide 12-90-CG 12 in. Mass Spectrometer: Control Console and Calculator

pattern has a peak at mass 331 which is adjacent to the $^{235}UF_5^+$ peak. It was not possible in the experiments to separate completely UF_6 and FC-43 in the upflow.

In the dual collector mode of operation the mass analyzed beams $^{235}UF_5^+$ and $^{238}UF_5^+$ pass through the two slits in the collector plate where they are collected on Faraday cups and the ion currents are measured with electrometers. The low mass Faraday cup ($^{235}UF_5^+$) may be removed, without loss of vacuum, and replaced with a 14 stage electron multiplier. This special feature is particularly advantageous in those cases where an insufficient sample is available to obtain adequate signal/noise ratio in the low mass cup.

SECTION 7

EXPERIMENTAL PROCEDURES

In this section we discuss the experimental procedures used in each of three experiment setups to obtain the jet membrane performance curves previously shown. The topics discussed are: 1) measurement of separation; 2) measurement of transmission, and 3) data interpretation.

Because precision measurements of small changes in relative abundance (enrichment) are very difficult to make, it was not convenient to determine the upflow flux, L_{PG}, and separation factor, α, simultaneously. Therefore, for fixed operating conditions (pressures and temperatures), L_{PG} and α were determined separately, each as a function of probe position, x_p. The flux, L_{PG}, as a function of probe position, x_p, is referred to as an attenuation curve. Cross plots of these two sets of data were then used to obtain performance data. Since some degree of error is introduced by this procedure, one of our recommendations for future work is that the experimental technique be revised to enable both measurements to be made simultaneously.

The measurements, material upflow and enrichment factor, are made for each type of experiment with one of several mass spectrometers. In the spectrometer ionization source ion signals are produced (by electron bombardment) in proportion to the local number density of each species present. The local species density is related to the flow rate of that species into the spectrometer source so that a measure of material flow rate of any species can be obtained from a measurement of the ion current corresponding to that species. The abundance ratio of any two species is simply proportional to the ratio of the appropriate ion signals. Therefore, separation factor is determined by measuring the ion ratio (light to heavy species) in gas samples that have been processed by the jet (at some probe position and dividing by the ion ratio measured with the jet off; a jet off measurement gives the abundance ratio of the feed gas. Similarily the transmission data are obtained by measuring the light species ion signal($\propto$ to the flux) as a function of the sampling probe position and normalizing each measurement to a measured light species ion signal obtained with the jet off.

The measured performance, t_m vs ξ, in general, reflects the separation that can be acnieved in the jet membrane/collector probe system studied. Since the probe

used in many of the experiments is simply a diagnostic tool (necessary to sample the jet), and is not representative of an acceptable enrichment plant geometry, the question arises as to how the diagnostic probe results relate to results for a real plant. This question will be addressed in Section 7.3. In Sections 7.1 and 7.2 we describe the basic procedure used in each apparatus to obtain and reduce the data for separation and transmission measurements, respectively.

7.1 SEPARATION MEASUREMENTS

The ratio of light to heavy species density in the upflow divided by the same ratio in the background gas is a measure of the separation factor α. In all of our experiments there was no significant depletion of the light species in the background chamber so that the separation factors measured are related to the heads-to-feed separation factor β (Refs. 7 and 8) rather than to the conventionally defined heads-to-tails separation factor. The consequence of this difference has been discussed earlier in Section 2.3.1.

Details of the measurement approach employed to determine the separation factor $\alpha(x_p)$ differed in each apparatus, as was indicated in the data presentation. With the exception of the UF_6 measurements, the point separation factors, $\alpha(x_p)$, were determined by successively measuring the ion ratio (light to heavy species) with the jet-on and jet-off (JO). The alternating cycle, jet-on and jet-off sample, was repeated several times and the separation factor was then determined from the averaged ion ratio measured with the jet on divided by the same measurement with the jet off. Tests conducted in apparatus nos. 1 and 2, except for the large probe SF_6 results, employed on-line spectrometer measurements. The large probe SF_6 experiments were conducted in apparatus no. 2 but samples were collected and analyzed in the Nuclide spectrometer, described in Section 6.3. In the SF_6 and UF_6 experiments performed in apparatus no. 3, samples were collected at selected probe positions and analyzed for isotopic content with the Nuclide spectrometer. The separation measurement for each apparatus are discussed individually in the following paragraphs.

7.1.1 Apparatus No. 1 - Gaseous Jet Apparatus

In apparatus no. 1 the quadrupole mass spectrometer was successively focused on each peak of interest and the amplitude of the resolved peaks was measured with an integrating voltmeter. The major shortcomings of this method are:

- Fluctuation instabilities in the ion source tend to bias the results because the peaks are not measured simultaneously

- Signal level is determined by the process gas background pressure in the test chamber, the attenuation in the jet, $L_{PG}(x_p)$, and the sampling probe conductance; therefore signal-to-noise ratio was a problem, especially for cases where $t_m \leq 0.1$.

7.1.2 Apparatus No. 2 - Condensible Jet Apparatus for Benign Gases

In apparatus no. 2 provision for manually adjusting the spectrometer ion focus (with adequate stability) was not available for either instrument. Instead, both spectrometers employed (magnetic and quadrupole) were operated in a scan mode. The ion focusing was repeatedly scanned over the peaks of interest and the output spectra, for each scan, were sent to an on-line computer system for analysis. Co-addition and averaging of numerous scans resulted in significant signal-to-noise improvement. However, the precision of a single point measurement (at one probe position), based on repeated measurements of that point on different days was no better than ±1.0% at the 1σ confidence level. Measurement error resulted primarily from the following limitations of the spectrometers employed:

- Nonlinearity in the scanning voltage which caused very small shifts in the peak position and, therefore, bias in the co-additions
- Instrument resolution was marginal, particularly in the SF_6 measurements
- Flat topped peaks, a highly desirable feature in isotope measurements, could not be obtained
- Averaging methods that utilize spectrum scanning are inefficient, i.e., the majority of the time spent is wasted in the valleys or on peaks of no interest (e.g., $^{33}SF_6^+$, when only the ratio of $^{32}SF_5^+$ to $^{34}SF_5^+$ is of interest).

7.1.3 Apparatus No. 3 - Condensible Jet Apparatus for UF_6

In the UF_6 facility (apparatus no. 3) process gas upflow samples were collected at selected probe positions and analyzed for isotopic content with the Nuclide 12-90-CG mass spectrometer (see Section 6.3 for a description of this instrument). It was especially important in these measurements to collect samples having the same amount of material to ensure identical inlet leak source pressures for each sample; e.g., the relative abundance ratio measurement can be biased if the flow conductance of the inlet leak varies (Ref. 20). By operating with all of the collected samples at the same pressure the ratio of ratio measurements will be free of this source of error. To establish the appropriate collection time for each sample the attenuation results corresponding to the particular process operating conditions were employed.

The UF_6 measurements were obtained by operating the instrument in the dual collector mode. The double standard interpolative method described in Ref. 21 was employed. In this method the unknown isotopic ratio is determined by comparison with measurements taken in two UF_6 reference standards which have lower and higher concentrations of $^{235}UF_6$. A six entry cycle is recommended for best results. The sample (X) and standards (S) are admitted to the instrument in the following order

$$(S_L, X, S_H, S_H, X, S_L)$$

where the subscripts L and H correspond to the low and high standards, respectively. For each introduction ion signal ratios are recorded on an integrating digital ratiometer and stored in the calculator. From these data the mole ratio in the unknown is determined from Eq. (7-1)

$$H_x = \left(\frac{\bar{R}_x - \bar{R}_L}{\bar{R}_H - \bar{R}_L} \right) (H_H - H_L) + H_L \qquad (7\text{-}1)$$

where $\bar{R}_i$ are averaged values of the measured ion ratios and H_H and H_L are the known mole ratios for the high and low standards. A typical two cycle measurement sequence of a collected jet off sample is shown in Fig. 7-1 along with a reproduction of the calculator printout.

It should be noted that the

- Relative amplitudes ($^{235}UF_5^+$ as compared to $^{238}UF_5^+$) of the signals shown in the recording have no particular significance since the multiplier gain for the $^{235}UF_5^+$ signal is arbitrarily selected to provide roughly the same amplitude for both signals
- UF_6 flow rate into the instrument, for each sample introduction, is automatically adjusted to a constant level before the ratio measurement is made
- Repeatability of the calculated mole ratio in the two cycles is quite good. This result is representative of the measurement quality obtained in all of the UF_6 ratio measurements.

In the SF_6 separation measurements it was convenient to operate the spectrometer in the peak stepping mode, because, in this case

- The sources of error noted above for the earlier SF_6 measurements are largely eliminated

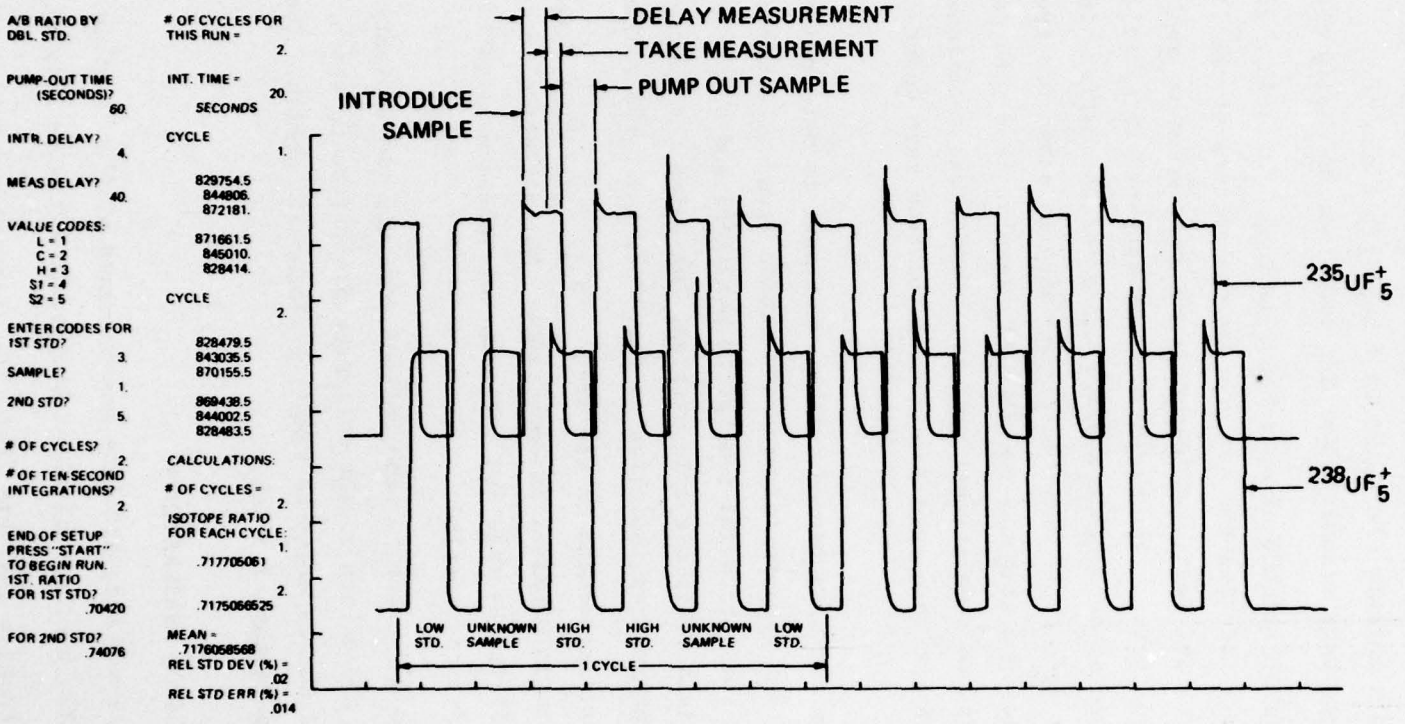

Figure 7-1. Measurement of $^{235}U/^{238}U$ Isotopic Ratio Using the Double Standard Interpolative Method

- Memory is not a significant factor in this measurement (based on our observations and those in Ref. 22)
- The resolution and abundance sensitivity that can be achieved in this mass range with the Nuclide spectrometer reduced cross talk between the peaks to a negligible amount
- Reference standards for SF_6 could not be easily obtained.

In the peak stepping mode of operation, isotopic ratio in a sample is determined by successively focusing the analyzer on the centers of the flat-topped peaks of each species of interest, and measuring the corresponding amplitude with an integrating voltmeter. The measurement is repeated in a cyclic fashion enough times to obtain an acceptable average value for the ratio. In the example shown in Fig. 7-2 a five cycle measurement sequence is shown for the determination of the isotopic ratio in a slightly enriched SF_6 sample. For each peak measured, zero value readings are made automatically at symmetrical locations on both sides of the peak which are then used to estimate the true zero underneath the measured peak.

The separation factor achieved in any experiment is determined from a series of measurements that compare measured ion ratios from collected samples that were obtained with the jet on (at some probe position) and with the jet off. A typical sequence consists of five sample entries, for which the average ion ratio in each sample is determined as indicated in Fig. 7-2; i.e., the collected jet-on and jet-off samples are introduced in the order: S_{on}, S_{off}, S_{on}, S_{off}, S_{on}. From the measured ion ratio obtained in each sample the separation factor α is calculated as the ratio of the average ion ratio in the jet-on samples to the average ion ratio in the jet-off samples.

The separation measurements made reflect not only the separating properties of the jet, but also the effect of the collector probe itself, which, as stated earlier, is for most of our experiments simply a diagnostic device. This effect will be discussed in paragraph 7.3 below.

7.2 TRANSMISSION MEASUREMENTS

Because we have not made absolute measurements of flux (upflow), we cannot normalize the flux directly by the equivalent background effusive flux ($n_b \bar{c}_b A_c/4$) as was done in the economics analysis (Ref. 2). Instead, we have normalized the process gas flux (i.e., ion current) by the process gas flux (ion current) taken with the

```
A/B RATIO BY
    PEAK STEPPING

MASS A = ?
          127.

MASS B = ?
          129.

ADJ U TO CNT OF
          127.

? IS CNT OK ON
          129.

SET ELCTRM ZERO
 10 MV UPSCALE
# OF CYCLES?
          5.

PRESS "START" TO
    BEGIN RUN

          5.
   CYCLES.

RATIOS:
          1.
22.95152271

          2.
23.0011436

          3.
22.96837387

          4.
22.94377934

          5.
22.9553457

MEAN =
22.96403304

REL STD DEV (%) =
          .098
```

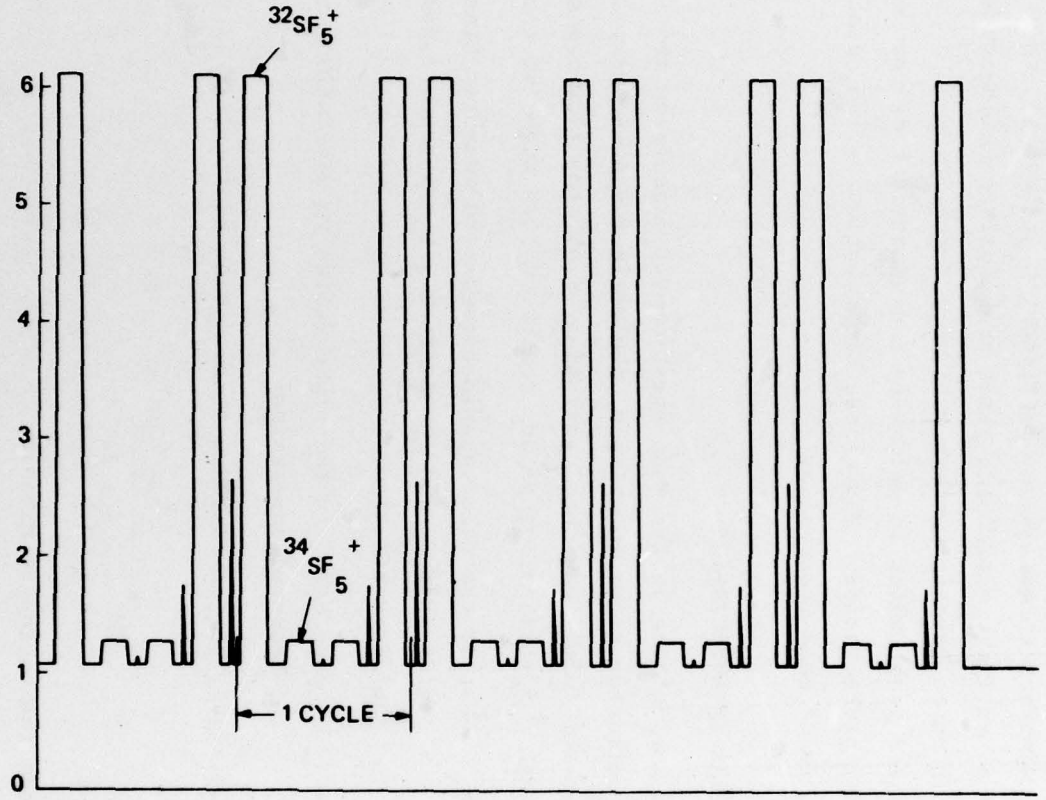

Figure 7-2. Measurement of $^{32}S/^{34}S$ Isotopic Ratio Using the Peak Stepping Method

jet off. The ratio $L_{PG}/(L_{PG})_{JO}$ is denoted as the measured transmission coefficient t_m. The jet membrane transmission coefficient t_{JM} is defined as $L_{PG}/(n_b \bar{c}_b A_c/4)$ as in Ref. 2. Under rarefied conditions (Refs. 18 and 20) the two transmission coefficients are virtually the same.

The jet membrane transmission coefficient t_{JM}, however, refers to the flux through a realistic enrichment plant probe/orifice geometry which will have small collector probe losses, whereas most of our measurements of transmission employed a collector probe which is primarily a diagnostic tool that can have large collector probe losses. Therefore, the question of the relationship between t_m and t_{JM} is of some importance.

7.3 DATA INTERPRETATION

The gas composition in the mass spectrometer depends on the local gas composition at the collector probe inlet face, the collector probe dimensions, and the spectrometer inlet leak characteristics, i.e., the flow regime in the probe and inlet leak. Specifically, we are concerned here with two questions:

- What is the relationship between the measured transmission coefficient t_m and the defined jet membrane transmission coefficient t_{JM}?
- Is enrichment in the probe (effusive separation) contributing to the measured separation?

By definition, the jet membrane transmission coefficient is

$$t_{JM} = \frac{L_{PG}}{n_b \bar{c}_b A_c/4} \tag{7-2}$$

We assume the upflow is given by

$$L_{PG} = v_{eff}\, n_{eff}\, A_c \tag{7-3}$$

where the subscript eff refers to effective conditions at the face of the collector probe; v_{eff} is the effective velocity of collection, defined by

$$v_{eff} = c_{eff} \sqrt{kT_{eff}/m_b} \tag{7-4}$$

where c_{eff} is a constant. Therefore, t_{JM} can be written

$$t_{JM} = 4c_{eff} \sqrt{\frac{\pi}{8}} \left(\frac{p_{eff}}{p_b}\right) \sqrt{\frac{T_b}{T_{eff}}} \tag{7-5}$$

The measured transmission coefficient t_m is defined by

$$t_m = L_{PG}/(L_{PG})_{JO} \tag{7-6}$$

In order to illustrate possible collector probe effects, we consider purely viscous flow.

For viscous flow of a mixture

$$L_{PG} \sim \frac{1}{\bar{\eta}} \; p_{eff} \; (p_T)_{eff} \tag{7-7}$$

where $\bar{\eta}$ is the viscosity of the mixture (process gas plus jet gas) entering the probe and $(p_T)_{eff}$ is the total static pressure of the mixture at the probe face. Similarly, for jet-off conditions

$$(L_{PG})_{JO} \sim \frac{1}{\eta_b} \; p_b^2 \tag{7-8}$$

Hence, t_m can be written

$$t_m \sim \frac{\eta_b}{\bar{\eta}} \; \frac{p_{eff}}{p_b} \; \frac{(p_T)_{eff}}{p_b} \tag{7-9}$$

Therefore, from Eqs. (7-5) and (7-9)

$$t_{JM} \cong 4c_{eff} \sqrt{\frac{\pi}{8}} \sqrt{\frac{T_b}{T_{eff}}} \; \frac{\bar{\eta}}{\eta_b} \; \frac{(p_T)_{eff}}{p_b} \; t_m \tag{7-10}$$

The total pressure at the probe face is related to the total flux (process gas and jet gas) into the collector probe

$$(L_T)_{eff} \sim \frac{1}{\bar{\eta}} \; (p_T)^2_{eff} \tag{7-11}$$

Hence

$$t_{JM} \sim 4c_{eff} \sqrt{\frac{\pi}{8}} \sqrt{\frac{T_b}{T_{eff}}} \sqrt{\frac{\bar{\eta}}{\eta_b}} \; \sqrt{\frac{(L_T)_b}{(L_T)_{eff}}} \; t_m \tag{7-12}$$

The total flux ratio $(L_T)_{eff}/(L_T)_b$ has been estimated by observing the rate of rise of pressure in the collector chamber when the valve connecting the collector chamber to the mass spectrometer is closed. The initial rate of rise of pressure when the valve is closed, is proportional to the flux. Figure 7-3 shows the results

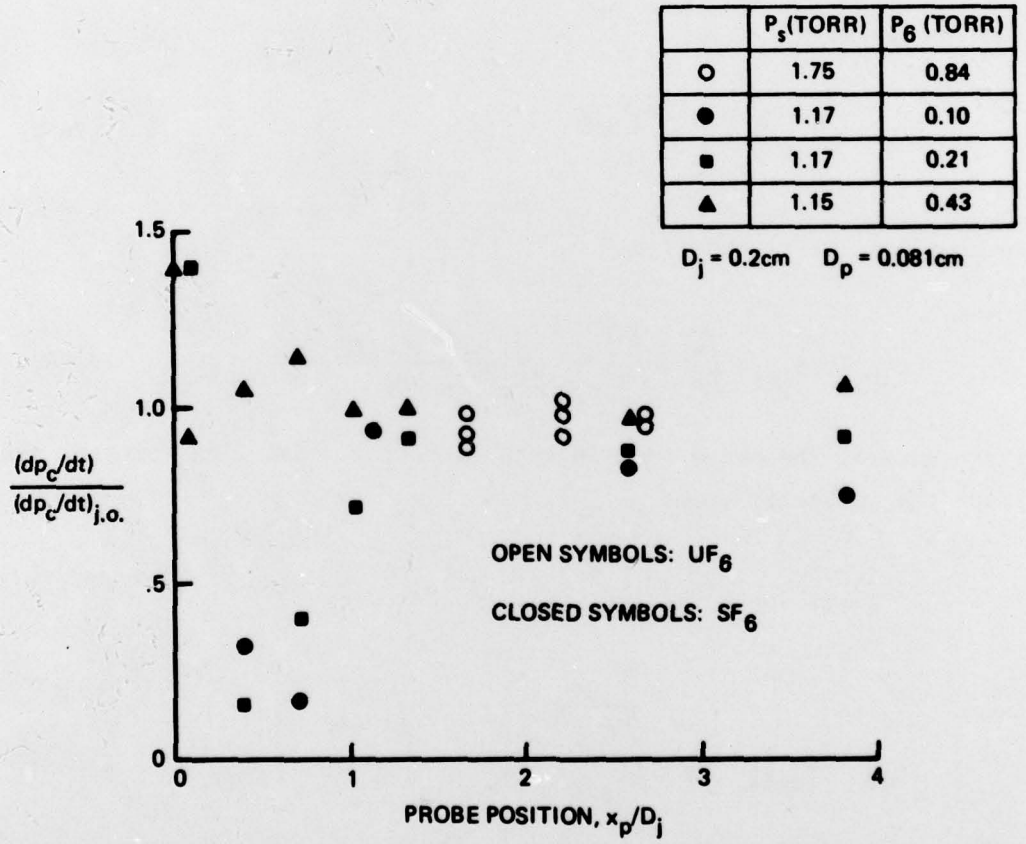

Figure 7-3. Rate of Rise of Collector Chamber Pressure: UF_6 and SF_6: FC-43 Jet: Small Cylindrical Collector Probe

for both SF_6 and UF_6 for the small probe configuration. As can be seen, over the range ($.8 \leq x_p/D_j \leq 4$), over which our enrichment measurements were made, $(L_T)_{eff}/(L_T)_b$ is essentially equal to one. Similar results for SF_6 in the large probe configuration are shown in Fig. 4-8. Hence, from Eq. (7-12), t_{JM} is proportioned to t_M. Since the other quantities in Eq. (7-12) were not measured, the constant of proportionality is not known. However, our best estimates place it equal to one within experimental scatter. Therefore, we conclude that $t_{JM} \approx t_M$. Again, in order to resolve this difficulty in interpretation, direct measurements of the collected flux using the proper geometry and flow regime should be made.

It should be noted that if the entire collected flux were process gas, then $(L_T)_{eff}/(L_T)_b \sim t_m$ and $t_{JM} \sim \sqrt{t_m}$. This alone would require a large correction of the performance curves in the direction of improved performance.

The separation factor may be written (Ref. 7)

$$\alpha = \frac{y/(1-y)}{x/(1-x)} \tag{7-13}$$

where y is the mole fraction of the light species in the upflow (heads) and x is the mole fraction of the light species in the downflow (tails). Recalling that we have referred separation to the feed, or background concentration, and that the molar density is proportional to the ion current in the mass spectrometer, Eq. (7-13) becomes

$$\alpha = \frac{(i^+_L)/(i^+_H)}{(i^+_L)_b/(i^+_H)_b} \tag{7-14}$$

The measured separation α_m at any probe position x_p includes, however, the separative effect of the jet plus any separation that occurs within the collector probe itself. Thus from Eq. (7-14) we may write

$$\alpha_m = \alpha_j \, \alpha_p \tag{7-15}$$

where α_p refers to the probe separation relative to conditions at the <u>entrance</u> to the collector probe. Similarly, with the jet off, the entire separative effect, if any, occurs within the collector probe itself. Hence,

$$(\alpha_m)_{JO} = (\alpha_p)_{JO} \tag{7-16}$$

Therefore, the separative effect of the jet itself can be written

$$\alpha_j = \frac{\alpha_m}{(\alpha_m)_{JO}} \frac{(\alpha_p)_{JO}}{\alpha_p} \tag{7-17}$$

Since the rate of rise of pressure data indicate that the total flux into the probe is relatively independent of probe position (including jet off), we conclude that the effective total pressure at the collector probe face is essentially constant. Hence, for both jet on and jet off the Knudsen number at the probe face can be assumed to be the same, and therefore $(\alpha_p) \simeq (\alpha_p)_{JO}$

Thus,

$$\alpha_j \simeq \frac{\alpha_m}{(\alpha_m)_{JO}} = \frac{(i^+_L/i^+_H)}{(i^+_L/i^+_H)_{JO}} \tag{7-18}$$

and to within the same accuracy as the transmission measurements requires no further correction. Again, any ambiguities in the separation factor can only be resolved by performing experiments using the correct geometry and in the proper flow region.

SECTION 8

CONCLUSIONS AND RECOMMENDATIONS

Based upon the results presented in this report we conclude the following relative to our program objectives.

- We have succeeded in separating uranium isotopes experimentally using the jet membrane concept
- We have not covered a wide enough range of process parameters to allow economic predicitons to be made directly from the UF_6 measurements alone
- Supporting experimental and theoretical tasks have been carried out which provide a rational basis for extrapolating the UF_6 results to full scale process conditions; e.g., we have found that
  - the same measured separation performance is obtained for SF_6 and UF_6 isotopes using small cylindrical collector probes and a condensible jet
  - the same measured separation performance is obtained for SF_6 isotopes using both small and large cylindrical collector probes and a condensible jet
  - separation performance in the N_2/He-A experiments is essentially invariant with collector probe geometry. These experiments were performed using small and large cylindrical collector probes as well as two-dimensional and conical configurations.

Thus we conclude that

- FC-43/SF_6 separation performance is transferable to FC-43/UF_6 for cylindrical collector probes
- FC-43/UF_6 separation performance for two-dimensional or conical collector probes will be essentially the same as that obtained in FC-43/UF_6 for small cylindrical collector probes.

That is, we have transferred the available UF_6 experimental separation data to a viable enrichment plant unit process geometry. Similarly, based on data in other gas systems, we have drawn conclusions concerning pressure levels, pressure

ratios, jet mass flows, etc. as they would apply to a UF_6 enrichment plant. Furthermore, we have assumed that all of these conclusions would also be valid using FC-75 as the jet fluid.

Based upon the above technical considerations and our economics program it has been shown that the jet membrane process continues to have attractive economics compared to competing enrichment technologies. Two plant sizes, 3×10^6 SWU/yr and 3×10^5 SWU/yr, were evaluated. The results indicate that

- For a 3×10^6 SWU/yr plant, the cost of enriched uranium using the jet membrane is approximatley 30% of the gaseous diffusion cost and 43% of the centrifuge cost, while the total capital investiment required is about 23% of gaseous diffusion and 34% of centrifuge
- For jet membrane plants larger than 3×10^6 SWU/yr the size of available thermal sources is likely to be a limiting factor
- For a small (3×10^5 SWU/yr) plant the capital investment for a jet membrane plant is projected to be 29% of gaseous diffusion and 62% of centrifuge capital investments. The relative costs of enriched uranium are 35% and 42%, respectively. The cost of enriched uranium for a 3×10^5 SWU/yr jet membrane plant is comparable (91%) to the cost for an 8.75×10^6 gaseous diffusion plant whereas the capital investment required is only 4.5%. Compared to a 3×10^6 SWU/yr centrifuge plant, the equivalent percentages are 103% and 13%, respectively.

Thus, the jet membrane holds promise as a load follower, i.e., the cost of enriched uranium for a 3×10^5 SWU/yr jet membrane plant is projected to be similar to present day (i.e., 1974) costs but the capital investment required is projected to be significantly lower than for present day processes. Therefore, changes in demand for enrichment services can be financed more readily using small jet membrane plants.

The results of this report indicate that continued development of the jet membrane process is clearly warranted. Further work should consider, in detail, the availability and cost of low grade thermal energy. In addition, engineering details of a multi-stage demonstration unit or pilot plant should be initiated. At the same time a parallel experimental program designed to expand the present data base and investigate other technical details should be carried out. This is necessary because many of the measurements presented in this report are unconnected in the sense that they were not performed simultaneously. The experiments whould be conducted in a fluorocarbon/SF_6 system using

- Conical and diverging 2-D collector probes
- Jet to background pressure ratios between 1.5 and 2
- Single and multiple probes
- At least two jet fluids, such as FC-43 and FC-75

- Simultaneous measurements should be made of
  - Separation factor
  - Absolute value of upflow
  - Absolute values of jet mass flow and jet backflow
- Condensation pumping should be used to control the suction pressure
- Pressure limit (p_s) should be studied systematically.

We have recommended the use of SF_6 rather than UF_6 because of the greater ease in handling and the much shorter times that will be required to make any configuration changes, and because we believe that the data we have obtained to date justify the transferability of results.

SECTION 9

REFERENCES

1. The Physical Basis of the Jet Membrane Enrichment Process. Bethpage, New York: J.W. Brook, Grumman Aerospace Corporation, June 1976. Research Department Memorandum RM-619.

2. Jet Membrane Process for Uranium Enrichment - Econometric Analysis. Bethpage, New York: J.W. Brook and B.B. Hamel, Grumman Aerospace Corporation, January 1976. Research Department Memorandum RM-611.

3. U.S. Atomic Energy Commission. Oak Ridge Operations Office. Data on New Gaseous Diffusion Plants, ORO-685. Oak Ridge, Tennessee: April 1972.

4. Garrett Corporation, Private Communication.

5. C. Frejacques, O. Bilous, J. Dizmier, D. Massignon, and P. Plurien. "Principal Results Obtained in France in Studies of the Separation of the Uranium Isotopes by Gaseous Diffusion." Proceedings of UN International Conference on Peaceful Uses of Atomic Energy, 2nd Geneva, p. 1262, 1968.

6. U.S. Atomic Energy Commission. Oak Ridge Operations Office. Gaseous Diffusion Plant Operations, ORO-684. Oak Ridge, Tennessee: January 1972.

7. J. Schacter, E. Von Halle, and R.L. Hoglund. Encyclopedia of Chemical Technology. New York: John Wiley, vol. 7, pp. 91-175, 1965.

8. M. Benedict and T.H. Pigford. Nuclear Chemical Engineering. New York: McGraw-Hill, Chapter 12, 1957.

9. Fluorinert Brand Electronic Liquids, Minnesota Mining and Manufacturing Co., 3M Center, Building 236-3B, St. Paul, Minnesota 55101.

10. Liquid-Vapor and Solid-Liquid Equilibria of the System Uranium Hexafluoride - Perfluorotributylamine. G.S. Jorden, J.C. Posey, and G.P. Rutledge; Carbide and Carbon Chemical Co., K-1073, October 28, 1953.

11. W. Ehrfeld. "The Separation Nozzle Process," in Von Karman Institute for Fluid Dynamics - 1976 Lecture Series 1. Aerodynamic Separation of Gases and Isotopes.

12. A Feasibility Study of Gas Centrifuge Enrichment Facilities/Executive Summary. Electro Nucleonics, Inc., Tennessee Valley Authority, Burns and Roe Industrial Services Corp., September 1975.

13. "Enrichment Plants - A Survey of Major New Uranium Enriching Projects" ed. D. Kovan. Nuclear Engineering International, vol. 21, no. 250, pp. 49-51, November 1976.

14. T.L. Deglow, Private Communication.

15. E.P. Muntz, B.B. Hamel, and B.L. Maguire, "Some Characteristics of Exhaust Plume Rarefaction," AIAA J., vol. 8, p. 1651, 1970.

16. J.W. Brook and B.B. Hamel, "Spherical Source Flow with Finite Back Pressure," Phys. Fluids, vol. 15, p. 1898,1972.

17. J.W. Brook, B.B. Hamel, and E.P. Muntz, "Theoretical and Experimental Study of Background Gas Penetration in Underexpanded Free Jets," Phys. Fluids, vol. 18, p. 517, 1975.

18. Deglow, T.L., "Background Gas Mixture Penetration of Underexpanded Jets with Application to Isotope Separation." Doctoral dissertation, University of Sourthern California, June 1977.

19. Product Bulletin, Pub. 1321-0373. Nuclide Corporation, 642 East College Avenue, State College, Pennsylvania.

20. R.E. Halsted and A.O. Nier, "Gas Flow Through the Mass Spectrometer Viscous Leak," Rev. Sci. Instrum., vol. 21, no. 12, pp. 1019-1021, December 1950.

21. Uranium Hexafluoride Isotopic Measurements Using an Interpolative Method. G.F. Kauffman and N.F. Christopher; Goodyear Atomic Corporation, Portsmouth, Ohio, GAT-291 (Chemistry), November 1960.

22. Sulphur Isotope Relative Ratios Determined by Mass Spectrometer. O.H. Howard; Oak Ridge Gaseous Diffusion Plant, Union Carbide Corporation., Oak Ridge, Tennessee, K1848, December 1973.

23. Energy Industrial Center Study. The Dow Chemical Company, Environmental Research Institute of Michigan, Townsend-Greenspan and Co., Inc., and Cravath, Swaine, and Moore, June 1975.

APPENDICES A AND B

Refer to Page vi in Table of Contents

APPENDIX C

ESTIMATE OF THERMAL ENERGY COSTS FROM A DUAL PURPOSE POWER PLANT

The cost of thermal energy obtained from a dual purpose nuclear power plant can be estimated from information compiled in Ref. 23. The specific case we consider here is that of a nuclear plant sized to generate 1200 MW (net) electrical energy and 2×10^6 lbs/hr of 150 psi steam. In the table below a comparison of operating costs for a 1200 MW electrical power only plant and a 1200 MW electrical power plant plus 2×10^6 lbs/hr steam is presented (from Table 29, Ref. 23).

BEFORE-TAX COST OF OPERATING NUCLEAR UNITS IN 1980 ($M) (REF. 23)

	Power Only	Dual Purpose
Investment	649,050	690,080
Depreciation of Fixed Charges	61,063	23,003
Operating & Maintenance	5,000	5,600
Miscellaneous	--	13,802
Fuel	26,873	31,643
Interest (9%)	--	31,054
Total Costs	92,936	105,102
Standard Return (BT)	47,978	
Value	140,914	

From this table we can see that

- A real cost of $12,000,000.yr for thermal energy (105M - 93M = 12M)
- If the plant operates at an 85% load factor, e.g., 7500 hrs/yr, 15×10^9 lbs/yr of steam would be available. At 10^3 BTU/lbs steam, this quantity of steam would represent 15×10^6 M BTU - $0.80/M BTU
- Since the above estimate is based on 1980 costs we use 31.26 mills/Kwh (pg. 94, Ref. 23) as the base industrial cost of electricity in 1980 or $9.16/M BTU. Then, the ratio of thermal to electrical cost is

$$\frac{\text{Thermal Cost}}{\text{Electrical Cost}} = \frac{0.8}{9.16} = 0.087$$

which is the value we have used in our economic analysis.